

**Tailing-dependent trimming of RISC-associated miRNAs
by the HuR protein**

Inauguraldissertation

zur

Erlangung der Würde eines Doktors der Philosophie
vorgelegt der
Philosophisch-Naturwissenschaftlichen Fakultät
der Universität Basel

von

Sokol Lena

aus Serbien, Novi Sad

Basel, 2014

Genehmigt von der Philosophisch-Naturwissenschaftlichen Fakultät auf Antrag von
Prof. Dr. Witold Filipowicz and Dr. Javier Martinez
(Referent) (Koreferent)

Basel, den 18. Februar 2014

Prof. Dr. Jörg Schibler
(Dekan)

The experimental part of this thesis has been done in the laboratory of Dr. Nicole Meisner-Kober, under the supervision of Dr. Nicole Meisner-Kober of DMP, NIBR Novartis and Prof. Dr. Witold Filipowicz of the Friedrich Miescher Institute of Biomedical Research.

The experimental data are presented in the form of a manuscript in preparation. 90% of the experiments have been performed by myself. The thesis also contains a general introduction and discussion.

Aknowledgements

First of all, I would like to thank my supervisors Prof. Witold Filipowicz and Dr. Nicole Meisner-Kober for giving me an opportunity to work on this exciting project. I would like to thank them for their dedication and support, as well as valuable discussions where I could learn to see scientific data critically and from multiple points of view.

I would especially like to thank Nicole for always being there, guiding me daily and keeping me enthusiastic in moments of doubt.

I wish to thank Dr. Javier Martinez for agreeing to act as coreferee for my dissertation, and for critically reviewing my work.

I also wish to thank my thesis committee members, Dr. Helge Grosshans and Prof. Dr. Susan Gasser for their support in decision making at crucial junctions in my thesis.

I wish to thank the members of the Meisner lab, Anja, Anne, Cornelia, Dominik, Justin, Lukas, and Wolf for their special help and support. A special gratitude goes to Nina for supporting me in the project and contributing to my thesis.

Finally, and importantly, I would like to thank my family and friends who have been there for me during good and frustrating times, my mother, Marijana, who could not be there for my defense but fiersly wanted to come, the man who raised me and her husband, Nikola for his sense of humor, my great sisters Bojana and Gaca, my best friend Joja, my brothers, my aunt Suzi and my grandfather Ferenc, a wonderfull man. And, of course, the man who gets all the good and bad of me, on a daily basis no less, and is still here - for which I am very thankfull, Bora.

And finally:



WWW.PHDCOMICS.COM

Table of Contents

1. Summary	9
2. Introduction	10
2.1. RNA metabolism	10
2.1.1. RNA stability	10
2.1.2. Nucleases	13
2.2. microRNAs.....	16
2.2.1. microRNA biogenesis	16
2.2.2. Mechanism of repression.....	19
2.2.3. miRNA regulation	20
2.2.4. Stability of miRNAs.....	21
2.2.5. miRNases.....	21
2.2.6. Factors that affect miRNA levels	23
2.2.7. Target mRNA effect on miRNA levels.....	24
2.2.8. Modifications of mature miRNAs	25
2.3. RNA binding domains.....	27
2.4. AU-rich element containing mRNAs.....	29
2.5. HuR.....	30
2.5.1. HuR and the stability of ARE-containing mRNA	32
2.5.2. HuR interaction with the miRNA pathway	33
2.5.3. HuR enzymatic activity	35
3. Background and objectives	36
4. Manuscript in preparation	38
4.1. Abstract.....	38
4.2. Introduction	38
4.3. Results.....	41
4.3.1. HuR binds and 3' adenylates miRNAs	41
4.3.2. HuR tails and trims miRNA.	44
4.3.3. The miRNA poly(A) polymerase and 3'→5' exonuclease activities map to the first two RRM of HuR.....	46

4.3.4.	Tailing dependent trimming of free and Ago-loaded miRNAs associated with a target	53
4.3.5.	HuR modulates miRNA isoforms and levels in HCT116 cells.....	57
4.4.	Discussion.....	61
4.5.	Materials and methods.....	65
4.5.1.	Recombinant protein preparation.....	65
4.5.2.	SDS-PAGE, western blotting, RP-HPLC and LC-MS proteomics.....	73
4.5.3.	miRNA 5' labeling.....	75
4.5.4.	Preparation of miRNA-HuR targets by <i>in vitro</i> transcription.....	76
4.5.5.	HuR-RNA binding experiments.....	77
4.5.6.	[α - ³² P]-ATP incorporation assay.....	79
4.5.7.	Tailing and trimming.....	79
4.5.8.	Size exclusion chromatography.....	80
4.5.9.	HuR refolding.....	81
4.5.10.	Motif search.....	81
4.5.11.	Ago2 Immunoprecipitation (IP).....	82
4.5.12.	Fluorescence microscopy.....	83
4.5.13.	CAT reporter experiments.....	83
4.5.14.	RT-qPCR for miRNA and mRNA.....	84
4.5.15.	Deep sequencing.....	86
4.6.	Appendix I. Reaction buffers and solutions.....	87
4.7.	Supplementary figures.....	90
5.	Discussion.....	104
5.1.	Relation to initial data on HuR terminal transferase activity.....	104
5.2.	The HuR-associated enzymatic activities.....	105
5.3.	Characterization of transferase and nuclease preferences and specificities.....	106
5.4.	HuR tailing and trimming on a target.....	106
5.5.	Ago-miRNA complex stability and accessibility.....	107
5.6.	HuR tails and trims Ago-loaded miRNA.....	107
5.7.	HuR ₁₂ cannot process target-bound miRNA.....	108
5.8.	Contribution of HuR enzymatic activity to Ago displacement.....	108
5.9.	HuR effect on miRNA bound to perfect target site.....	109

5.10.	Proximity of HuR and miRNA binding sites and competitive versus cooperative effects	109
5.11.	HuR knockdown modulates levels of miRNAs and iso-miRs with 3' non-templated A additions.....	110
5.12.	Mechanistic model for enzymatic turnover of RISC-loaded miRNAs by HuR on the 3'UTR	111
5.13.	Nuclease diversity	112
5.14.	Catalytic activity – a novel function of the RRM domain?	112
5.15.	Summary and outlook.....	113
6.	References	115
7.	Curriculum vitae.....	139

1. Summary

HuR is a ubiquitously expressed AU-rich element (ARE) binding protein. AREs are regulatory, typically destabilizing sequences found in the 3' UTR of many mRNAs in eukaryotes. However, binding of HuR acts to stabilize these messages. Another type of regulatory elements, miRNA-binding sequences are also found on the mRNA 3'UTR. miRNAs are short, (~22 nt) non-coding RNAs which guide the RISC complex to regulate the expression of proteins involved in the regulation of numerous biological processes.

HuR and miRNA sites have been shown to often co-localize on target mRNAs, and several studies have shown that there is a cross-talk between HuR and miRNAs. For example, HuR can counteract miR-122-mediated repression of CAT-1 mRNA, a process which is accompanied by Ago displacement from mRNA.

It was previously shown that HuR possesses an RNA 3'-terminal adenosyl transferase activity; however, the physiological substrates were not determined. In this thesis, we report that miRNAs are bound by HuR and act as substrates for the HuR-mediated transferase activity and that HuR can polyadenylate miRNAs. We further describe different type of evidence strongly suggesting that HuR also has a 3'-5' exonuclease activity acting on miRNAs, and describe and test *in vitro* a model of how HuR antagonizes the Ago-bound miRNA associated with mRNA. To access the miRNA-Ago complex associated *in cis* with the same target RNA, HuR recognizes the miRNA 3' end and adds to it a poly(A) tail, thus potentially weakening the Ago-miRNA interaction and creating a landing pad for the nuclease, which in turn leads to exonucleolytic degradation of miRNA turnover and displacement of Ago from RNA.

We further show that HuR knockdown in HCT116 colon carcinoma cells has a differential effect on mature miRNAs as compared to miRNA isoforms containing 3'-terminal non-templated additions of A residues. The levels of these isoforms are reduced upon HuR depletion, suggesting that HuR promotes miRNA tailing and degradation also *in vivo*.

2. Introduction

2.1. RNA metabolism

Ribonucleic acid, or RNA, is, next to DNA and proteins, one of three pivotal macromolecules essential for all known forms of life. With its ability to store genetic information like DNA, and catalyze enzymatic reactions like proteins, it may have played an important role in the evolution of life. mRNA is the direct messenger molecule, carrying genetic information to encode a protein amino-acid sequence. mRNA levels have the potential to directly influence gene expression, and are therefore tightly regulated. Until recently, RNA was thought to play mere passive roles in the cell, as the aforementioned copy of DNA to be read for protein synthesis, a structural component of the ribosomes reading this mRNA template, and an adaptor molecule carrying amino acids used by the ribosome to decode the genetic code and synthesize peptide chains. Now, important roles of various non-coding RNA species play in the regulation of RNA expression and stability are emerging, and the impact this tight regulation has on processes as varied as cell division, differentiation, stress response cell aging and death. Misregulation of the mRNA metabolism can lead to a number of diseases, including heart disease, cancer and neurodegenerative disorders.

2.1.1. RNA stability

mRNA has first been identified as a molecule that is rapidly synthesized and rapidly degraded. This was based on an observation that a gene can be both induced and repressed within minutes (Jacob & Monod 1961). Instability is one of the most significant features of mRNA, allowing for an adaptable pattern of gene expression, as well as a rapid reaction to the changing environment of a cell.

mRNA steady state levels are product of the balance between synthesis and degradation. In mammalian cells, the half-life of an mRNA ranges from 15 minutes for c-fos to over 24 hours for β -globin (Shyu et al. 1989). mRNAs are modified in the nucleus by the addition of a 5' cap structure, as well as a 3' poly(A) tail. In eukaryotes, degradation of mRNA is largely mediated by

exonucleases, thus the removal of these two terminal modifications is a rate-limiting step in mRNA decay. Pulse-chase experiments in which degradation of a homogenous population of mRNA is monitored after a brief activation of their promoter (Dellavalle et al. 1994) have revealed that the first step in mRNA degradation is a gradual shortening of the poly(A) tail, followed thereafter by a decrease in total RNA levels through either 3'→5' or 5'→3' exonucleolytic decay. In the major decay pathways, the step following deadenylation is the hydrolysis of the 5' cap leaving an mRNA with a 5' monophosphate, which can then be degraded in a 5'→3' direction (reaction order and mammalian enzymes summarized in Figure I1).

The main mRNA decay mechanism in eukaryotes is thus the deadenylation dependent degradation pathway, initiated by the removal of the 3' poly(A) tail, followed by decapping, and exonucleolytic decay from both ends. Another important pathway is the nonsense mediated decay, during which a premature stop codon is recognized, triggering 5'→3' exonucleolytic decay (NMD) (Wilusz et al. 2001). The exosome is a multiprotein complex catalyzing the 3'→5' turnover of mRNA in the cytoplasm. Together with the aforementioned mechanisms, it participates in mRNA quality control pathways such as NMD pathway or nonstop decay (mRNAs lacking translation termination codons)(Houseley et al. 2006).

Reaction		Enzymes
I	deadenylation	<ul style="list-style-type: none"> • Pan2/Pan3 • CCR4-NOT complex • PARN
IIa	decapping	• Dcp1/Dcp2
IIb	cap hydrolysis	• DcpS
III	5'-3' exonucleolytic decay	• Xrn1
IV	3'-5' exonucleolytic decay	• exosome

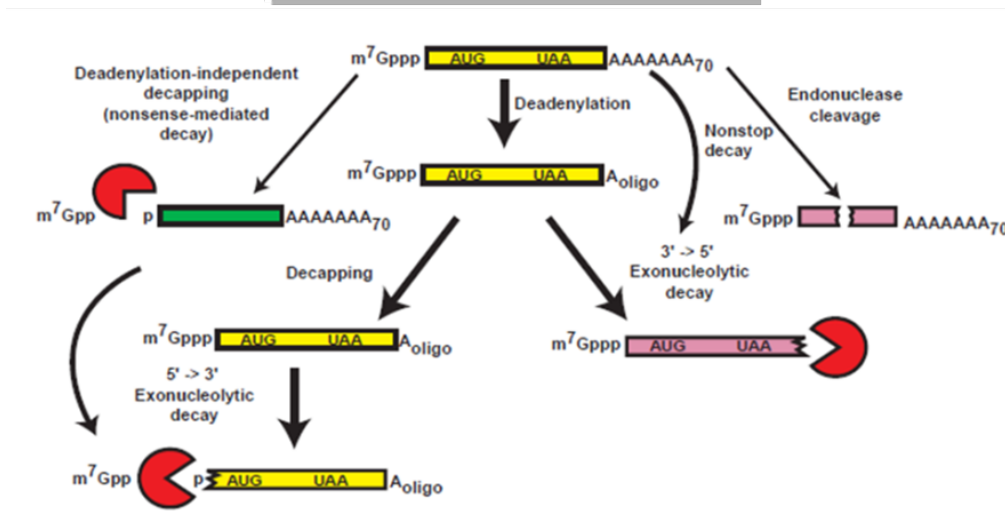


Figure 11. Pathways and enzymes of eukaryotic mRNA turnover, modified from (Parker & Song 2004) and (Meyer et al. 2004)

If the mRNA were a stable molecule in the cell, the only way to dilute its concentration and regulate protein expression in this manner would be by cell division, an inefficient way to respond to environmental and intracellular cues. With that in mind, as well as the omnipresence of RNases in the cell, and the intrinsic chemical liability of mRNA as a molecule, it is very surprising that the default state of a translatable mRNA in the cell is one of relative stability, and that specific cues are necessary to promote decay of a given mRNA (Meyer et al. 2004). In fact, mRNAs coding for housekeeping, constitutively expressed proteins can have a half-life of over 24h. β -globin mRNA, for example, is protected from degradation partially by constant ribosome occupancy and translation, which prevents decapping and degradation (von der Haar et al. 2000).

In most cases however, the RNA sequence itself can determine the differences in the decay rate of a stable mRNA compared to other, unstable messages. Many sequence elements can regulate the stability of a given mRNA. Stabilizer and destabilizer *cis* elements are found throughout the transcript. For instance, the α -globin has a cytosine-rich element in the 3' untranslated region (3'UTR) of its mRNA, which forms a stabilizing α -complex that protects the RNA from decay. On the other hand, short lived mRNAs, prevalently coding for proto-oncogenes, cytokines or growth factors generally possess destabilizing elements, such as AU-rich sequences in their 3' UTR which promote deadenylation and subsequent degradation (Chen & Shyu 1996).

2.1.2. Nucleases

Nucleases are indispensable molecules involved in every facet of the nucleic acid life-cycle, such as DNA replication, RNA splicing, processing, and maturation, RNA interference (RNAi) and microbial defense response (Kao & Bambara 2003; Shen et al. 2005; Reha-Krantz 2010; Patel & Steitz 2003; Abelson et al. 1998; Chu & Rana 2007; Moore & Proudfoot 2009; Nowotny & Yang 2009). The fundamental chemistry of the cleavage is a bimolecular nucleophilic substitution (S_N2). Nucleases cleave the phosphodiester bond of nucleic acids 3' or 5' of the scissile phosphate. This is a general acid-base catalysis, with the general base activating the nucleophile by deprotonation, and the general acid facilitating the product formation by protonating the leaving group (Yang 2011). Nucleophiles used vary strongly, and include water, desoxyribose, inorganic phosphate, or protein amino acid side chains, such as those of serine, tyrosine and histidine. The enzymatic reaction may or may not require one or two divalent cations. The substrate can be single stranded or double stranded DNA or RNA, although many nucleases are sugar non-specific and can cleave both (Hsia et al. 2005; Rangarajan & Shankar 2001). The cleavage product may be a single nucleotide or an oligonucleotide. For a cleavage reaction yielding single nucleotides, the directionality of the nuclease can be either 3'→5' or 5'→3'.

Based on the above listed catalytic mechanisms, and the substrate preference, nucleases can be categorized into several main classes. It is worth mentioning however, that there is little to no correlation between the catalytic mechanism and biological function, and that the same biological reaction can be performed by a wide range of nucleases, with different structures and

catalytic mechanisms. On the other side, a conserved structural fold as well as sequence motifs may function in divergent manners and pathways (Yang 2011).

Mg^{2+} is the most abundant divalent cation inside living cells (Maguire & Cowan 2002). Ca^{2+} is found in high concentration in life forms, and other ions, Cu^{2+} , Fe^{2+} , Zn^{2+} , Mn^{2+} and Ni^{2+} not as abundant, but are essential in the living organism. In cells, these ions never exist without water or ligand. Mg^{2+} for instance is surrounded by multiple shells of ligated water molecules (Maguire & Cowan 2002). Many divalent cations are involved in enzymatic catalysis. The Mg^{2+} ion is most often associated with nucleic acid enzymes (Cowan 2002).

The two-metal ion dependent nucleases are a class of nucleases containing the largest number of tertiary folds, and are involved in the most diverse biological functions. All DNA and RNA polymerases use two-metal ion-dependent catalysis, as do many nucleases (Yang et al. 2006). The reaction product of this catalysis is a 5'phosphate and a 3'OH group. The two metal ions are coordinated between one non-bridging oxygen of the scissile phosphate, and a conserved aspartic acid, with one metal ion on the 5' nucleophile side, and one on the 3'O leaving group side.

The one-metal-ion catalysis is used by two major classes of endonucleases, $\beta\beta\alpha$ -Me and HUH (Friedhoff et al. 1999; Koonin & Ilyina 1993; Kühmann et al. 1999; Monzingo et al. 2007). The two classes are dissimilar structurally, but both use a single positively charged histidine side chain, which replaces the second metal ion in the previous mechanism. Histidine may be used as the general base to deprotonate, and turn water into the nucleophile, or, alternatively, a tyrosine may be used as the nucleophile itself (Yang 2008).

Metal-independent RNases all use the 2'OH as the nucleophile to generate a 2'-3' cyclic phosphodiester as the intermediate product in a transphosphorylation reaction. After hydrolysis, the products of the reaction are a 3' phosphate (or 2' phosphate) and a 5'OH group (Yang 2011) (metal independent DNases form 3' phosphor-protein intermediates (Grindley et al. 2006; Schoeffler & Berger 2008)).

The two-ion-dependent nucleases include a subclass of DnaQ-like 3'→5' exonucleases with a DEDD motif, in which the nucleophilic water coordinated through either a histidine or a tyrosine (DEDDh or DEDDy). Poly(A)-specific ribonuclease PARN, as well as Pop2, a component of the Ccr4-NOT complex involved in mRNA degradation are both DEDDh nucleases (Parker & Song

2004). ERI-1, an enzyme recently implicated in the turnover of miRNA, an established function in histone mRNA degradation and 5.8S rRNA processing (Thomas et al. 2012), also has the same fold.

RNaseH-like nucleases are likewise two-ion dependent, and possess the same topology, however, unlike the former subclass, they are endonucleolytically active. However, their catalytic residues are more varied, and include aspartic acid, glutamic acid and histidines. Argonaute and PIWI, key players in the RNAi pathway are members of this subclass. (Nowotny & Yang 2009; Song et al. 2003). Four residues, DEDX (X is histidine or aspartic acid) form the catalytic tetrad in these proteins.

Additional players in the RNAi pathway belong to this subclass. Dicer and Drosha, the two endonucleases that excise the miRNA from the primary transcript are either dimers or pseudodimers with two active sites for simultaneous symmetrical cleavage (MacRae et al. 2007; Nowotny & Yang 2009). Their active sites are composed of two aspartic and glutamic acid pairs.

The major mammalian exoribonuclease Xrn1 belongs to the FEN1-like 5' exo- and endonucleases. Here, the catalytic residues are almost exclusively aspartic acids and glutamic acid (Szankasi & Smith 1996).

The RNase PH, PNPase, as well as the exosome belong to a distinct group of two-metal-ion dependent nucleases. Unlike other nucleases, that cleave the phosphodiester bond through a hydrolytic mechanism, these, and only these nucleases require an inorganic phosphate as a nucleophile (Deutscher et al. 1988). The released product is thus a 3'OH and a 5' diphosphate. Interestingly, PNPase can function both as a polymerase (synthesizing heteropolymeric tails (Slomovic et al. 2008; Portnoy et al. 2005; Mohanty & Kushner 2000)), as well as a 3' exoribonuclease *in vitro* (Régnier & Hajnsdorf 2009). In bacteria, PNPase can function to cleave RNAs with a complex secondary structure through an interesting mechanism – it cooperates with the PAP1 poly(A)-polymerase, which adds short adenosine tails to the inaccessible RNA 3' end. This provides the PNPase with a “landing pad”, to which it can bind, and force its way through the secondary structure in multiple rounds.

Nucleases are therefore a heterogeneous group, with new nucleases, novel sequence motifs and structures being discovered constantly. The catalytic motifs may be as small as to be contained within a sequence no larger than 20 amino acids. The $\beta\beta\alpha$ -Me motif, for instance, can be

incorporated into various tertiary structures and are extremely tolerant to amino acid substitutions. It is thus clear that there is much more to be added to our current knowledge on nucleases (Yang 2011).

2.2. microRNAs

2.2.1. microRNA biogenesis

microRNAs (miRNA)s are recently discovered class of small non coding RNA (ncRNA) molecules that regulate the expression of their target genes. The first miRNA, lin-4 was discovered in 1993 in *C.elegans* (Lee et al. 1994; Wightman et al. 1994). Lin-4 was described to be 22 nt long and had the ability to repress the lin-14 gene by imperfectly hybridizing to the 3'UTR of the lin-14 mRNA. In addition, lin-4 also existed as a longer, 61 nucleotide form, that could fold into a hairpin. However, as the 22 nt form possessed all sequence determinants necessary for lin-14 mRNA repression, it was concluded that the 61 nt RNA is the precursor (pre-miRNA) to the shorter, mature form.

7 years later, an analogous miRNA, let-7 was found to regulate lin-14, as well as other genes in *C.elegans* (Reinhart et al. 2000). However, unlike lin-4, let-7 was conserved in animals with a bilateral symmetry (Pasquinelli et al. 2000). Therefore, in 2001, many other miRNAs were identified that had features similar to let-7 and revealed this type of regulation to be more widespread than previously imagined (Lagos-Quintana et al. 2001). In fact, we know today that over 50% of human genes are regulated by miRNAs (Rajewsky 2006; Friedman et al. 2009; Brodersen & Voinnet 2009).

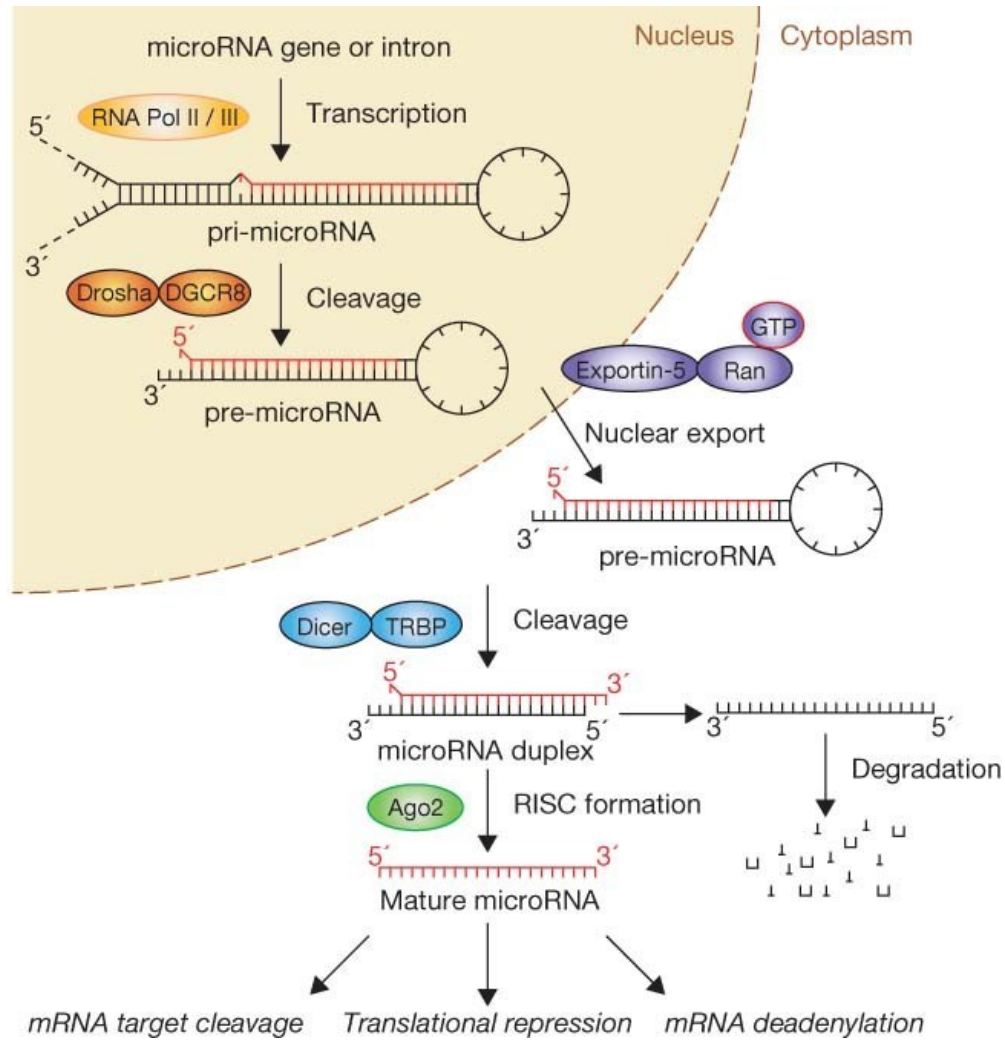


Figure 12. Canonical pathway of miRNA biogenesis. Reproduced from (Winter et al. 2009)

In the genome, several miRNA genes have been found in close vicinity to one another. As the expression profile of these miRNAs was similar, they were proposed to be generated as one, polycistronic transcript (Lee et al. 2002). Indeed, the primary miRNA (pri-miRNA) precursor can be synthesized by polymerase II as a polycistronic transcript, modified in a canonical pathway, polyadenylated and capped before being processed by the nuclear RNase III Drosha to pre-miRNA (Figure 12) (Cai et al. 2004; Lee et al. 2003). These ~70 nucleotides long pre-miRNA hairpins are transported into the cytoplasm by a Ran-GTP dependent nucleo-cytoplasmic transporter Exportin-5 (Yi et al. 2003). In the cytoplasm, pre-mRNAs are processed by the RNase III nuclease Dicer (Ketting et al. 2001) to mature ~22 nucleotide long duplexes with 3' dinucleotide overhangs, the mature miRNA and its star strand (miR/miR*).

Argonaute (Ago) proteins are recruited to small RNAs bound by Dicer through TRBP (the human immunodeficiency virus transactivating response RNA binding protein) (Chendrimada et al. 2005). These proteins together form the RISC loading complex (RLC) (Maniataki & Mourelatos 2005). The miRNA duplex is loaded into Argonaute proteins as a double stranded miRNA, in an ATP-dependent process that requires the chaperone machinery Hsc70/Hsp90 to accommodate the bulky double stranded RNA duplexes into Ago. In contrast to the loading, unwinding of the miRNA-miRNA* duplexes, and strand selection is a passive process, and does not require ATP. The strand typically selected to form the mature miRISC is the one with lower thermodynamic stability at its 5' end, and is called the mature (guide) miRNA, whereas the other is referred to as the star (passenger) strand (Schwarz et al. 2003; Khvorova et al. 2003).

Ago binds both ends of the miRNA, with the 5' nucleotide lodged in the MID domain (Ma et al. 2005), and the 3' end bound by the PAZ domain (P-element induced wimpy testes [PIWI], Argonaute and Zwiille) (Ma et al. 2005; Song et al. 2003). The 5' nucleotide is anchored in Ago, and does not participate in target mRNA recognition and binding. Nucleotides 2-6 are solvent-exposed in such a way that they can nucleate the initial binding to the target mRNA. They constitute the "seed", a stretch of nucleotides functionally determined to encompass positions 2-8 (Lai 2002). The seed is a major determinant of the targeting specificity (Lewis et al. 2003), and the strength of Watson-Crick base pairing within the seed region influences the strength of repression.

In catalytically active Ago proteins, the RNase-H like PIWI domain cleaves the phosphodiester bond in the target mRNA opposite the paired miRNA nucleotides 10 and 11 (Ma et al. 2005). Perfect binding of the guide RNA (like in the case of small interfering RNA, siRNA) is necessary for the cleavage. In miRNAs, bulges and mismatches generally exist to prevent RISC cleavage of mRNA.

The contribution of the pairing of the 3' miRNA region to the mRNA target is typically minimal and only ~5 % of miRNAs have conserved binding sequences in that region. In those cases, base pairing with the mRNA can contribute to silencing efficiency. Overall, the first nucleotide, as well as terminal 3' nucleotides are unlikely to base-pair with their target even if complementary, and instead facilitate Ago loading and contribute to tighter binding (Wee et al. 2012; Brennecke et al. 2005; Doench & Sharp 2004). Interestingly, CLASH (crosslinking, ligation, and sequencing of hybrids, a technique involving purification of Ago complexes and ligation of base-paired RNAs

for miRNA-target site co-identification) analysis has shown that a substantial number of miRNAs is bound to non-canonical sites, with either incomplete seed sequence complementarity or even with 3' complementarity only (Helwak et al. 2013).

Interestingly, Ago tethering to the mRNA 3'UTR has proven sufficient to induce silencing, suggesting that the miRNA really merely acts as a guide to recruit the RISC and associated proteins to the specific mRNA (Pillai et al. 2004).

2.2.2. Mechanism of repression

In most cases, multiple miRNA sites on an mRNA are required for efficient silencing. In other cases, one target site is sufficient, which is why it was proposed that sequences flanking the miRNA site, the "context" in which the sequences are found, may have an influence on inhibition proficiency (Didiano & Hobert 2006).

The mechanism of silencing by miRNAs is hotly debated, and includes translational repression at the initiation and post-initiation checkpoints, degradation of the nascent polypeptide chain, as well as the target mRNA deadenylation and decay. The two main, seemingly disparate theories for mRNA silencing favor mRNA degradation (Baek et al. 2008; Selbach et al. 2008; Hendrickson et al. 2009; Guo et al. 2010), while others describe situations in which the mRNA is translationally reversibly repressed (Bhattacharyya et al. 2006; Muddashetty et al. 2011; Krol et al. 2010; Schratt et al. 2006). Another possible mechanism, reconciling both proposed modes of regulation suggested that, in sequential steps, the initial effect of target silencing may be the inhibition of translation at the initiation step, followed by increased deadenylation through the RISC mediated recruitment of the PAN2-PAN3 and CCR4-NOT deadenylating complexes. The loss of the protecting poly(A) tail would make the 5' end (through preventing the functional mRNA circularization) of the mRNA more accessible, and could eventually lead to recruitment of the decapping machinery and degradation of the target mRNA (Chen et al. 2009; Behm-Ansmant et al. 2006).

This theory is strengthened by the fact that miRNA-repressed mRNA is found in processing bodies (P-bodies), cytoplasmic foci which are enriched in proteins involved in translational repression as well as mRNA decay (Kedersha & Anderson 2002; Coller & Parker 2005).

Translation inhibitors, deadenylases, decapping enzymes, as well as exonucleases reside in the P-bodies (Pauley et al. 2006). Most of the cell's repressed mRNA fraction is present in these foci, and global inhibition of miRNA repression greatly represses their formation (Pauley et al. 2006). In addition, miRNA-repressed mRNA can be stored in the foci, for future utilization (Brenques et al. 2005; Pillai et al. 2007), seen in the case of the CAT1 mRNA. Upon stress, this RNA can leave the foci and be translated again. Crucial for this regulation is an AU-rich element binding protein, HuR. In this and other cases, miRNA-mediated repression can be reversed (Bhattacharyya, et al. 2006).

2.2.3. miRNA regulation

There are over 1,000 miRNAs coded by the mammalian genome. Some miRNAs in turn have been predicted to have hundreds of targets, partially due to the short recognition sequence of the seed needed for target recognition (Lim et al. 2005). The need for tight regulation of this posttranscriptional checkpoint is therefore obvious.

The first and most obvious node of regulation of miRNA silencing is the transcription of the primary miRNAs and their processing by the two RNase III family nucleases Drosha and Dicer. Indeed, the two endonucleolytic cleavage steps can be influenced by their partner proteins, or, alternatively, the precursor molecules can be modified to affect their maturation (Viswanathan et al. 2008; Piskounova et al. 2011; Fukuda et al. 2007; Guil & Cáceres 2007).

For instance, DDX5 and DDX17, two DEAD-box RNA helicases serve as coactivators of processing of a set of miRNAs by Drosha (Fukuda et al. 2007). In addition, they may serve as a scaffold for the recruitment of additional co-regulators, like p53, which has been shown to act in a similar manner. Also SMAD proteins can interact with DDX5 and promote processing of the pri-miR-21. Negative regulators can likewise bind Drosha in a DDX5/DDX17 dependent manner. The estradiol-bound estrogen receptor blocks processing of pri-miRNA by Drosha, and induces dissociation of the complex (Yamagata et al. 2009).

Other factors are able to interact with the miRNA precursors themselves. KSRP (KH-type splicing regulatory protein) and hnRNP A1 can bind the loop of several miRNA precursors and promote

miRNA maturation (Guil & Cáceres 2007; Trabucchi et al. 2009; Ruggiero et al. 2009). In addition, KSRP has a role in the cytoplasmic maturation of pre-miRNAs.

miRNA biogenesis can also be inhibited by modifying the pre-miRNA itself. In *C. elegans*, Lin-28 binds the let-7 pre-miRNA and recruits the uridylyase TUT4 which polyuridylylates let-7 and thus suppress its processing, as Dicer cannot cleave the hairpin RNA with such a long tail (Heo et al. 2009). In addition, uridyl tails are known to recruit 3'→5' exonucleases, and it is possible the pre-miRNA is degraded by as yet to be identified nuclease (Kim et al. 2010)

2.2.4. Stability of miRNAs

miRNAs have been thought to be exceptionally stable for many years (Haase et al. 2005). However the fact that multiple mature miRNAs are expressed in a tissue- or development-specific manner, without much variation in the expression of the precursor molecules was an indication of a regulated turnover.

The first solid evidence of an active miRNA degradation pathway came from *A. thaliana* (Yan et al. 2012), where a family of RNA degrading nucleases was shown to degrade miRNAs in vitro. The confirmation of a physiological relevance came from the joint knockdown of several family members, which increased the steady-state level of mature miRNAs *in vivo*.

2.2.5. miRNases

In *C. elegans*, XRN-2 has been identified as the enzyme mediating miRNA degradation (Chatterjee & Grosshans 2009). It is a 5'→3' exonuclease, conserved in eukaryotes. In *C. elegans*, XRN-2 is capable of processing free miRNA as well as miRNA loaded into the *C. elegans* Ago paralogue (ALG-1 and ALG-2- in round worms), however, the mechanism of release from Ago is still unknown (Chatterjee & Grosshans 2009). Not all miRNAs accumulate to the same extent upon XRN-2 knockdown, suggesting that some degree of miRNA specificity may be involved (Miki et al. 2014). In mammalian cells, XRN-2 plays only a small role, and another general miRNA nuclease has not been identified to date.

In human and other animal cells, miRNAs have been found that show accelerated decay in multiple systems, including neurons, retina, epithelial and embryonic kidney-derived immortalized cell lines, as well as breast cancer, glioma, melanoma and cervical cancer cells (Rüegger & Großhans 2012; Hwang et al. 2007; Bail et al. 2010; Das et al. 2010; Avraham et al. 2010; Zhang et al. 2011; Sethi & Lukiw 2009; Rajasethupathy et al. 2009; Rissland et al. 2011)). The causes for the decay vary from specific extracellular signals and cell cycle state, to exogenous factors like virus infection.

In neurons, miRNA turnover seems to be invariably fast, as shown by the decay rate in differentiated pyramidal neurons from mouse ES cells (Krol et al. 2010). In contrast, undifferentiated ES cells did not rapidly turnover the same miRNAs. The turnover in pyramidal neurons was dependent on neuronal activity, therefore blocking action potentials prevented the fast turnover.

Stimulation of breast epithelial cells by the epidermal growth factor (EGF) likewise rapidly reduced the levels of several miRNAs. These miRNA were either shown or predicted to target several genes that are rapidly upregulated in response to EGF, consequently the miRNA degradation favors the cellular response to the EGF (Avraham et al. 2010).

Although regulated miRNA turnover is well documented, a general miRNA degrading enzyme (miRNase) has yet to be identified in mammals. Knockdown of RRP4, the catalytic exosome subunit, and to a lesser extent Xrn1, the main 3'→5' and 5'→3' RNases in the cell, respectively, was sufficient to increase the steady-state levels of the unstable miR-382, without affecting the levels of the more stable miR-378. XRN2 depletion did not have any effect on either miRNA levels (Bail et al. 2010).

In mouse lymphocytes knock-out of ERI-1, a DEDDh family 3'→5' exoribonuclease, resulted in approximately twofold increase in levels of several miRNAs. However, precise understanding of how ERI-1 modifies miRNA levels, whether it is by direct degradation, is still unknown (Thomas et al. 2012).

In human melanoma cells, PNPase (polyribonucleotide nucleotidyltransferase), a 3'→5' exonuclease degrades certain mature miRNAs, without affecting their respective pri- or pre-miRNA levels (Das et al. 2010).

In several reports, the miRNA sequence has been shown to influence its stability. In miR-29a for instance, the 6 nucleotides at 3' end of the miRNA were responsible for its cellular localization and stability (Hwang et al. 2007).

Other factors can stabilize mature miRNAs. Translin, a DNA and RNA binding protein binds to and stabilizes miR-122 levels *in vivo* (Yu & Hecht 2008)

2.2.6. Factors that affect miRNA levels

As previously described, miRNAs base-pair to their target mRNA, and through RISC and associated complexes, affect the levels and/or the translation of this mRNA. However, can the targets affect the miRNAs themselves?

In *C. elegans*, base-pairing of a miRNA to its target prevented its degradation by XRN-2, an exonuclease with a preference for single-stranded substrates (Chatterjee et al. 2011). Addition of an *in vitro* synthesized RNA containing the natural let-7 target site, but not a RNA containing a mutated site or an unrelated sequence led to an accumulation of that miRNA in cleared worm lysates (Chatterjee & Grosshans 2009). The target may either prevent processing of the miRNA-mRNA duplex by XRN-, or otherwise perhaps prevent the release of the miRNA from Ago, necessary for the digestion.

miRNAs are loaded into Ago such that both ends are bound and secured within the protein. Typically, a miRNA loaded in Ago is stable for long periods of time, and the dissociation rate is very slow (up to 24h, unpublished data) (Martinez & Tuschl 2004). In line with that, overexpression of Ago2 has been shown to stabilize mature miRNA levels, whereas depletion of Ago reduces them (O'Carroll et al. 2007; Diederichs & Haber 2007). This effect of Ago overexpression might be explained in two ways – either the miRNA and Ago go through cycles of association and dissociation, and the miRNA stabilized through the increased chance of binding the now more abundant Ago protein upon dissociation, or otherwise the steady-state number of miRNA molecules in the cell exceeds the number of Ago proteins, and the overexpression served to stabilize the previously unbound, vulnerable miRNA. In accordance with the second theory, it has been shown that, in HeLa cells, only a fraction of a given miRNA is loaded into Ago, suggesting that the protein is the limiting factor (Stalder et al. 2013).

2.2.7. Target mRNA effect on miRNA levels

Transfection of duplex siRNA or miRNA molecules in HeLa cells perturbs the gene expression on a global level, counteracts the miRNA-mediated downregulation by competing with natural miRNA occupancy of Ago (Khan et al. 2009), suggesting that Ago loading is not irreversible, and that Ago can be recycled and reprogramed (loaded with a new guide). Several mechanisms have been proposed in the last couple of years as possibly mediating this step of Ago recycling, and most of them center on the target-mediated effect on Ago-loaded miRNA.

The interaction of a programmed Ago with a target site exhibiting high complementarity destabilized the interaction of Ago with the guide miRNA, unloading the miRNA from Ago2 in minutes (De et al. 2013), (Unpublished data, Meisner lab). A typical miRNA binding site with little complementarity at the 3' end or an unrelated sequence had no effect on stability of a miRNA-Ago complex. This may point to a mechanism of how the miRNA-Ago complex is turned over, with the miRNA eventually being displaced from Ago, leaving Ago available for miRNA re-loading. Upon changes in the cellular environment, stress or signaling, certain miRNAs may be degraded or their processing inhibited/enhanced, providing Ago with a modified miRNA pool to choose from.

Highly complementary miRNA targets likewise resulted in a downregulation of miRNA levels in *D. melanogaster*, mice and human HeLa and HEK293T cells (Ameres et al. 2010; Xie et al. 2012; Baccarini et al. 2011; Rügger & Großhans 2012). The downregulation was associated with an observed nucleotide extension and degradation of the target miRNAs. This process, termed tailing (incorporation of mainly Us and As) and trimming, was not abolished in *Drosophila* by up to 8 miss-matches between the 3' of the miRNA and the target site, unlike unloading (described above), which is already affected by a single mismatch in the 3' end (Ameres et al. 2010; De et al. 2013).

Similarly, certain viruses can destabilize miRNAs by using miRNA-target containing RNA molecules. *H.saimiri* virus uses the viral transcript HSUR to downregulate miR-27a. miR-16 and miR-142-3p, which also bind the viral RNA, are not destabilized by this interaction, perhaps due to a less extensive pairing (Cook et al. 2004; Cazalla & Steitz 2010). HCMV, the human cytomegalovirus, induces downregulation of several miRNAs from the miR-17-92 cluster through

base-pairing to the so-called intergenic miRNA decay element (miRDE). Abrogating the interaction between the miRNAs and the miRDE delayed virus production, pointing to a relevant physiological role of this interaction (Lee et al. 2013).

The murine cytomegalovirus MCMV induces downregulation of miR-27a through the viral transcript m169, which likewise contains a miR-27a binding site (Marcinowski et al. 2012). The degradation of miR-27a is accompanied by tailing (and, presumably, trimming), which persists even when the seed region is mutated to affect miR-27a binding. The authors were unable to detect modified miRNAs in Ago immunoprecipitated samples, which suggested that the tailing either happens upon release of the miRNA from Ago, or that the process is too quick to detect. Theoretically, the miRNA 3' end would be accessible to enzymatic modification even in Ago, as the miRNA 3' end is not as tightly anchored in Ago as is the 5' end (Wang et al. 2009). Indeed, in *Drosophila* the tailed and trimmed products could be immunoprecipitated with Ago (Ameres et al. 2010).

The consequence of such modifications of the Ago-loaded miRNA can be twofold. On one hand, the added tail could destabilize the binding of Ago to the miRNA. The importance of a standard miRNA length is visible in the conform size of miRNA sequenced to date, with both ends of a standard-sized miRNA bound by Ago. The addition of a long tail would certainly affect this interaction, perhaps resulting in miRNA unloading. However, Tan et al demonstrated that Ago can also bind long, unstructured RNA, and use it as a guide to cleave the target mRNA (Wang et al. 2009). Alternatively, given that the tailing is accompanied by trimming, i.e. degradation of the miRNA, the tail of the miRNA could serve as a "landing pad" for nucleases, a way to access the miRNA 3' end. Precedents for this mechanism are known (Bühler et al. 2008; Houseley et al. 2006; Gallouzi & Wilusz 2013; Régnier & Hajnsdorf 2009; Iost & Dreyfus 2006; Condon 2007), with polynucleotide tails being added to a highly structured RNA, to help initiate degradation.

2.2.8. Modifications of mature miRNAs

The 5' ends of mature miRNAs define the crucial seed sequence, and are relatively invariable, and 5' isoforms are present in only 10% of miRNAs. In contrast, next generation sequencing has determined that a substantial percentage of mature miRNAs possesses highly heterogeneous

3' ends. The miRNA 3' end often contains 1-3 untemplated nucleotide additions (3' NTAs), most often A and U residues. Interestingly, the 3' NTA do not occur indiscriminately across miRNA species, but in a pattern, with specific 3' NTAs being enriched in certain miRNAs (Wyman et al. 2011).

Non-templated uridylation of mature miRNA was first seen in *hen1* mutant of *Arabidopsis*. In these mutants, miRNA lack the 2'-O-methyl group at the 3' end of the miRNA. The global levels of miRNAs were decreased in this system, and U-tail additions of various lengths were detected in the miRNA population. It was suggested that the methyl group protects the miRNA from uridylation and subsequent degradation (Li et al. 2005). Consistent with this, a nucleotidyl transferase MUT68 was identified in *Chlamydomonas* that uridylates small RNA, leading to their degradation via the exosome subunit RRP6 (Ibrahim et al. 2010). For most known cases of tailing and trimming, the nuclease responsible has not been identified.

In animals, *let-7* maturation is suppressed by *Lin28* which 3' uridylates pre-*let7* through *TUT4* (*ZCCHC11*) (Hagan et al. 2009). The oligo-U tail acts again as a degradation signal, and promotes degradation of the pre-miRNA. In *C. elegans*, *PUP-2* acts on pre-*let7* through a similar mechanism (Lehrbach et al. 2009). Uridylation of the mature miR-26 by *ZCCHC11* abrogated miR-26-mediated downregulation of its target mRNA. Thus, it seems that uridylation is either a destabilization signal for miRNAs, or an inhibitory modification preventing their function.

In human monocytic cells, *PAPD4* (*GLD-2*) was identified as the primary miRNA adenylating enzyme (Burroughs et al. 2010). *PAPD4* was previously described to adenylate and stabilize miR-122 levels in mouse liver cells (Kato et al. 2009). However, in human monocytes the knockdown of *PAPD4* did not globally affect the stability of miRNA, but rather restored the repression of the mRNAs targeted by miRNAs which are adenylated by *PAPD4*. The same authors noted a slight effect of miRNA adenylation on loading into *Ago2* and *Ago3*, whereas the *Ago1* loading was unaffected. Other nucleotidyl transferases responsible for 3' miRNA adenylation were identified in human prostate samples, in addition to *PAPD4*: *PAPD5*, *MTPAP* and *Z11* (Wyman et al. 2011). Knockdown of each of these individual enzymes was sufficient to abrogate a significant percentage of individual mature miRNA adenylation. However, additional enzymes responsible for miRNA modifications have yet to be identified, as all to date performed knockdown experiments still do not fully account for all detected modification. In plants, adenylation of miRNA was associated with slower miRNA degradation (Lu et al. 2009).

The interesting question to answer will be what defines specific miRNAs as a target for modification, and to determine the exact effect of uridylation and adenylation. In particular, the same modification can have different effects on miRNA stability, and Ago loading and targeting, and it will be important to differentiate the context under which one modification may have different effects. To date, no motif or sequence characteristic has been identified that can explain why a subset of miRNA is modified. It is possible therefore, that the distribution between different Ago proteins, or interaction with a subset of miRNA-binding proteins on the target message might play a role in this process.

Additional effort in the field is directed toward into the identification of miRNA-modifying enzymes, the yet undetected nucleotidyl transferases, and, more importantly, the nucleases mediating the trimming reaction.

2.3. RNA binding domains

RNA binding proteins are involved in every facet of the RNA lifecycle. These proteins bind the RNA through RNA binding domains or RBDs, in a manner ranging from unspecific to highly sequence specific.

The Zinc finger domain (ZnF) can be found alone, or in a combination with other RNA binding domains. It is approximately 30 amino-acid long, with a $\beta\beta\alpha$ topology, with the β -hairpin and α -helix joined by a Zn^{2+} ion (Wolfe et al. 2000). Originally thought to bind DNA only, recently it was discovered that zinc fingers bind RNA as well (Amarasinghe et al. 2000), using hydrogen bonds and aromatic-base stacking interactions (Cléry & Allain 2012). The Lin-28 and TUT4 both possess such domains (Hagan et al. 2009).

The KH domain (hnRNP K homology) is a larger domain of about 70 amino acids. It has a $\beta\alpha\beta\beta\alpha$ topology, and forms a cleft that typically accommodates four bases (Valverde et al. 2008; Grishin 2001). One famous example of a KH-domain containing protein is the AU-rich element binding protein KSRP (Gherzi et al. 2004).

Double-stranded RNA binding motifs or dsRBM, were interestingly the first ones described to recognize the RNA shape, instead of its sequence (Stefl et al. 2005). Like the KH domain, dsRBMs

are composed of roughly 70 amino-acids; however the topology is a conserved $\alpha\beta\beta\beta\alpha$ fold. As is the majority of RNA binding domains, dsRBM are also found in multiple copies. Preferentially, as the name states, they interact with double stranded RNA.

The most common RBDs are the RNA recognition domains (RRMs), present in over 1% of human genes (Venter et al. 2001). These most studied RNA binding domains can bind both RNA and DNA with sequence specificity (Cléry et al. 2008). On a primary sequence level, RRM consists of approximately 90 amino-acids. It adopts a $\beta_1\alpha_1\beta_2\beta_3\alpha_2\beta_4$ topology, a four-stranded β -sheet packet between two α -helices. Two conserved sequences of 6-8 amino-acids, the RNP1 and RNP2, can be found in the two central β -sheets, and in the three dimensional domain fold they expose several aromatic residues on the surface of the β -sheets that form the primary RNA binding surface (Maris et al. 2005). Variants of the RRM domain, the quasi-RRM, pseudo-RRM and the U2AF homology domains (UHD) differ from the “true” RRM, by lacking several or all of these residues (Cléry & Allain 2012). The RNA nucleotides are accommodated within the RRM as the 5' and the 3' nucleotides stack on the two aromatic rings on two β -sheets, whereas the third aromatic ring is inserted between the two sugar rings of the nucleotides. Additional nucleotides can be accommodated through additional aromatic rings and planar side chains. Additionally, multiple RRM domains can work in tandem to bind a longer continuous RNA sequence, and thus potentially increase affinity and binding specificity. A large portion of RRM proteins contain more than one RRM. Interestingly, protein loops connecting the secondary structure elements, typically unstructured, can likewise be used for sequence as well as RNA secondary structure recognition (Cléry & Allain 2012).

Palm domains are RRM-like folds with a $\beta_2\alpha_1\beta_3\beta_1\alpha_2\beta_4$ topology. Interestingly, this domain contains catalytic activity, centered around a strongly conserved aspartate at the end of the first β -sheet, and two additional acidic residues in the hairpin between β -sheets 2 and 3. These residues coordinate two Mg^{2+} ions, and are responsible for the polymerase function of these domains (Anantharaman et al. 2010).

In HuR, an RNA binding protein which contains three RRM domains, the crystal structure shows a large conformational change in the tertiary structure necessary for converting the protein into the closed conformation and forming the RNA-binding cleft (Wang et al. 2013). The authors suggest an initial recognition of the RNA by RRM1, and subsequent binding of RRM2 and the interdomain linker to the RNA upon conformational change.

2.4. AU-rich element containing mRNAs

AU-rich elements (AREs) were first discovered to confer instability to mRNAs in a seminal paper from Shaw and Kamen (Shaw & Kamen 1986). Starting from an observation that the deletion of a 67 nt AU-rich stretch from the c-fos gene converted it into a transforming gene (Meijlink et al. 1985), they hypothesized that this might lead to a stabilization of the message, and an increase in its oncogenicity. Deducing similar highly conserved motives in many unstable mRNAs, they inserted a 51 nt AU-rich stretch from the human lymphokine gene mRNA GM-CSF sequence into the 3'-UTR of a stable β -globin gene. This caused the mRNA to become highly unstable and undergo degradation within minutes. They subsequently detected the same long runs of AU-rich sequences in 3'UTRs from numerous unstable cytokine, lymphokine and proto-oncogene mRNAs, and thus concluded that AU-rich sequences are a recognition signal for an mRNA degradation pathway. It was later determined that ARE sequences can promote rapid deadenylation and decay of the transcript (Bakheet et al. 2006; Chen & Shyu 1996; Wilusz et al. 2001). Over 4,000 genes (8% of all genes) were found to be regulated by AREs (Bakheet et al. 2003).

In 1995, Ying and Shyu proposed that ARE range in size from 50 to 150 nt, and roughly classified them into three classes: (1) Class I, with 1-3 copies of the pentameric motif scattered within a U-region; (2) class II, with two overlapping copies of a nonamer UUAUUUUA(U/A)(U/A) in a U-rich region, and (3) class III, a mostly U-rich sequence. They have determined the decay of ARE-bearing mRNAs to be biphasic, with synchronous (Class I and III) or asynchronous (class II) deadenylation preceding the decay of the RNA body. Since then, the nonameric sequence was determined to be the minimal ARE sequence (Lagnado et al. 1994; Lewis et al. 1998).

ARE-containing mRNAs are rapidly downregulated once they have fulfilled their purpose. Regulation of such transiently expressed genes is important in cell growth and differentiation, signal transduction, hematopoiesis, the immune response, inflammation, malignant cell transformation external stress mediated pathways and apoptosis (Bakheet et al. 2001). The regulation via ARE depends on a wide array of ARE-binding proteins (AUBPs), such as tristetraproline (TTP), KH-type splicing regulatory protein (KSRP), AUF1, Hu antigen R (HuR) and others. Most ARE sequences are bound by more than one AUBP (Barreau et al. 2005). The

majority of AUBPs recruit mRNA decay machineries to promote ARE-mediated decay or AMD (Barreau et al. 2005; von Roretz & Gallouzi 2008). For instance, in yeast, Puf3p binds to an ARE in the COX-17 3'-UTR and mediates rapid deadenylation of the message by recruiting the CCR4-NOT complex (Tucker et al. 2002). In addition, some evidence suggests that Puf3p binding to ARE may also accelerate capping. Tristetraprolin, or TTP binds to the 3' of the TNF- α message and promotes deadenylation (Carballo et al. 2000).

There are some exceptions to the destabilization mediated by AREs - under certain conditions, ARE sequences have been shown to confer stability (Ford et al. 1999). In response to various external stresses, some messages are stabilized by trans-acting AUBPs, such as HuR. For instance, by competing for the same binding sites as the negative regulators of ARE mRNAs, TTP or KSRP, HuR can stabilize the RNA upon binding.

2.5. HuR

The mammalian genome codes for four closely related RNA binding proteins, which are a part of the ELAV family (Good 1995). The prototype member of the family, ELAV (embryonic lethal, abnormal visual system), was discovered in 1985 in *Drosophila* as an essential factor for neural development (Campos et al. 1985). In humans, the ELAV orthologue HuR was identified as a nucleoprotein in material from patients with paraneoplastic syndrome and small cell lung carcinoma (Budde-Steffen et al. 1988; Dalmau et al. 1990; Dalmau et al. 1991). HuR is ubiquitously expressed; while its three paralogues, HuB, HuC and HuD are expressed in neurons (HuB is additionally present in the gonads). In 1995, HuR was reported to bind AU-rich elements (Liu et al. 1995). Four years later, this binding was found to have a stabilizing effect on a reporter gene with an ARE sequence from TNF- α (Ford et al. 1999).



Figure 13. HuR domain organization, modified from (Meisner & Filipowicz 2010)

On a molecular level, HuR is a 36 kDa mRNA-binding protein, with three classical RNA Recognition Motifs (RRMs, Figure 13). In HuR, the N-terminal RRM (RRM1, amino acids 19-100) has been proposed to initiate contact with the mRNA, whereupon the interdomain region as well as the second RRM (RRM2, amino acids 103-189) would bind, increasing the affinity substantially (Wang et al. 2013) (structure of HuR RRM1 and RRM2 shown in Figure 14). A 56 amino acid hinge region between the second and third RRM encompasses a nuclear localization signal, termed HNS (HuR Nucleoplasmatic Shuttling), narrowed down to the amino acids 205-237 (Fan & Steitz 1998). The exact function of RRM3 (amino acids 245-326) had not yet been elucidated, although RRM3 of HuD had been implicated in poly(A) tail binding (Ma et al. 1997). In addition, RRM3 has been identified as the site of protein-protein interaction with HuR ligands, such as pp32, APRIL, Set α and Set β (Brennan et al. 2000). However, a RNA ligand for this RRM domain has not yet been identified.

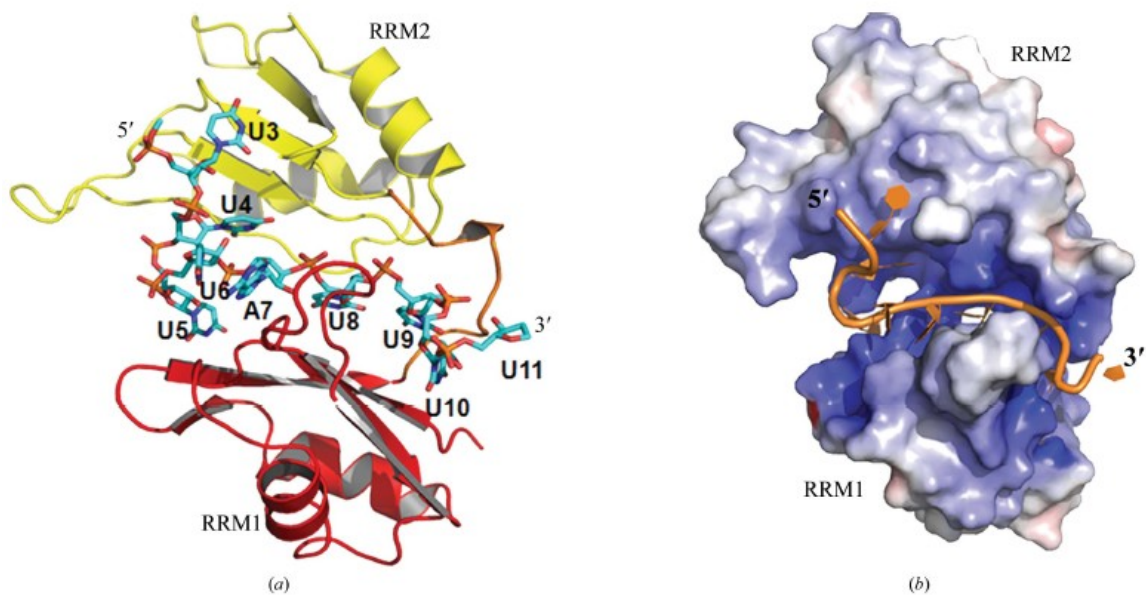


Figure 14. Crystal structure of HuR RRM1 and RRM2 (HuR₁₂), in complex with RNA reproduced from (Wang et al. 2013). A) All RNA bases are labeled. RRM1 is shown in red, RRM2 in yellow, B) Positive charges are shown in blue, negative in red. The RNA is represented in orange (11 nt 5'-AUUUUUUUUUU-3' of c-fos mRNA)

HuR is predominantly nuclear, however, certain stimuli may cause it to translocate into the cytoplasm where it can bind and stabilize its target mRNAs. These stimuli includes stress – UV radiation, amino-acid starvation, oxidative stress, transcription block - as well as the activation

of certain receptors by growth factors and immune cell activation (Wang et al. 2000; Westmark et al. 2005; Yaman et al. 2002; Abdelmohsen et al. 2008; Fan & Steitz 1998; Meisner & Filipowicz 2010). Crucial for the cytoplasmic translocation are two pathways, a CRM1-independent, and a CRM-dependent pathway which does not need the HNS sequence, and is based on the interaction of HuR with pp32 and APRIL, and thus indirectly with CRM. Transportin-2 (and later transportin-1) was identified as the receptor for the nuclear shuttling of HuR (Guttinger et al. 2004; Rebane et al. 2004). In addition, HuR function, localization and binding affinity to ARE can be affected by various posttranslational modifications, including phosphorylation, methylation and caspase cleavage (reviewed in (Meisner & Filipowicz 2010)).

2.5.1. HuR and the stability of ARE-containing mRNA

Since 1999, when the first report of the HuR stabilizing effect on mRNA appeared, many HuR target genes have been identified. Initially, HuR binding to a U-rich sequence has been reported, however evidence for a more defined consensus binding motif for Hu proteins emerged only when HuD was crystalized with a 11-mer AUUUUUAUUUU sequence (Wang & Tanaka Hall 2001). The two N-terminal RRM domains are strongly conserved within the Hu family, and have been proposed to bind to mRNA in the same manner. Therefore, in a systematic *in vitro* approach, this proposed recognition sequence was further dissected for HuR binding using synthetic oligonucleotides, and a refined nonamer NNUUNUUU (N = any nucleotide) sequence was determined as the minimal binding requirement. This suggested HuR can bind to both class I and II AREs (Meisner et al. 2004). Another study identified a more flexible, uracil rich motif of up to 20 nucleotides, which formed a stem loop structure (De Silanes et al. 2004).

In one study, HuD was shown to bind to poly(A) tails and thus protect them from degradation (Beckel-Mitchener et al. 2002). Although this would be a very elegant mechanism for HuR, further studies showed that this protein rather protects the body of the message from degradation. In addition, it can also increase protein production from its target mRNA by activating translation. In other cases, HuR has even been reported to promote ARE-mediated

translational repression (Lafon et al. 1998; Millard et al. 2000; Kullmann et al. 2002). Whatever the outcome, good understanding as to the molecular mechanism of how HuR mediates its effects is missing. Of course, competition with other AUBPs, which generally have a negative effect on mRNA stability, is a strong possibility (Sureban et al. 2007). In addition, the interplay between miRNA and HuR has been reported, and recently, a proximity bias was described for ARE and miRNA sites which further suggests that an interaction of the two posttranscriptional regulation pathways might be a possibility (Lebedeva et al. 2011; Mukherjee et al. 2011).

2.5.2. HuR interaction with the miRNA pathway

Evidence has been accumulating in the past couple of years for an active interplay between the miRNA and the ARE pathway. Both competitive and cooperative interactions have been reported for HuR and other RBPs (Tominaga et al. 2011; Srikantan et al. 2012; Jing et al. 2005; Kim et al. 2009; Bhattacharyya et al 2006; Young et al. 2012; Mukherjee et al. 2011; Kedde et al. 2007; Kedde 2008; Jafarifar et al. 2011; Ashraf & Kunes 2006). HuR and miRNAs seem to influence the activity of each other in multiple ways. Several miRNAs, including miR-16, miR-34a, miR-125a and miR-519 (Abdelmohsen et al. 2008; Guo et al. 2009; Kojima et al. 2010; Xu et al. 2010), target the HuR message, and, conversely, HuR influences the levels and activity of several pre- and mature miRNAs (Young et al. 2012; Chang et al. 2013).

In a first such report, Bhattacharyya et al (Bhattacharyya et al. 2006) discovered that repression of mRNA by a miRNA can be reversed under stress conditions. Upon amino acid starvation in Huh7 hepatoma cell line, HuR translocated from the nucleus into the cytoplasm, resulting in CAT1 mRNA release from processing bodies (PB) and relief of miR-122 repression. Other reports followed the same pattern: HuR competes with miR-16 repression of COX-2, miR-331-3p with repression of ERBB2 and others. The opposite was also true, as seen in synergistic HuR and miRNA regulation of other targets (summarized in Figure I5).

miRNA	Target shared with HuR	Type of interaction
miR-122	<i>CAT1</i> mRNA	Competitive
miR-548c	<i>TOP2A</i> mRNA	Competitive
miR-494	<i>NCL</i> mRNA	Competitive
miR-16	<i>COX2</i> mRNA	Competitive
miR-331	<i>ERBB2</i> mRNA	Competitive
let-7	<i>MYC</i> mRNA	Cooperative
miR-19	<i>RhoB</i> mRNA	Cooperative
(RISC)	<i>p16</i> mRNA	Cooperative

Figure 15. Coordinate control of a mutual target mRNA by miRNAs and HuR. Adapted from(Srikantan et al. 2012). References for examples listed, from the top: (Bhattacharyya, et al. 2006; Srikantan et al. 2011; Tominaga et al. 2011; Young et al. 2012; M R Epis et al. 2011; Kim et al. 2009; Glorian et al. 2011; Chang et al. 2010)

Recently, two papers (Lebedeva et al. 2011; Mukherjee et al. 2011) reported PAR-CLIP (Photoactivatable-Ribonucleoside-Enhanced Crosslinking and Immunoprecipitation) data showing that miRNA sites were preferentially found in the vicinity of but not overlapping with HuR binding sites on an mRNA. This excludes the possibility of direct competition as a mechanism of antagonistic regulation, although steric (including secondary structure conformation change) or nonsteric inhibition is still a possibility. Specifically, the derepression of the *CAT1* mRNA by HuR discovered by Bhattacharya et al. involved miRNA and HuR sites which were several hundred nucleotides apart. In a follow-up paper, the ability of HuR to displace Ago2-RISC and alleviate repression of such an mRNA was attributed to its ability to oligomerize on the mRNA, an activity mediated via the C-terminal segment of HuR (Toba & White 2008; Soller & White 2005; Kasashima et al. 2002; Devaux et al. 2006; Fialcowitz-White et al. 2007). Needed for both the derepression and for oligomerization was the mRNA target containing both miRNA and HuR sites, as well as a full-length protein including the hinge and RRM3.

HuR was found to bind miRNA directly *in vitro*, and miR-16 has been detected in HuR immunoprecipitations (Srikantan et al. 2012; Young et al. 2012). In a study from Young et al (Young et al. 2012), this interaction resulted in the derepression of the *COX-2* mRNA, which has binding sites for both miRNA and HuR, and promoted the *degradation* of miR-16. This suggests that in the cases where HuR and miRNA sites co-localize on the same mRNA, the stabilization of

the message could be due to HuR sequestering the miRNA, perhaps making it accessible to nucleases, thus inhibiting its repressive effect on the mRNA.

2.5.3. HuR enzymatic activity

In 2009, Meisner et al. reported that HuR possesses a RNA terminal adenosyl transferase activity located in the C-terminal RRM of HuR, RRM3 (Meisner et al. 2009). This novel activity was Mg^{2+} dependent, and was inhibited by the HuR-targeted small molecular inhibitor MS-444, a compound which also inhibited binding of HuR to ARE elements by interfering with HuR dimerization. Although a classical RRM domain has never been implicated in enzymatic activity, a RRM-like palm domain fold was shown before to possess 3' →5' polymerase activity (Anantharaman et al. 2010).

In the study, total RNA was used as a substrate for modification by HuR, and incorporation of radiolabeled ATP was assayed in a thin layer chromatography format, which showed the label incorporation. The exact RNA substrate was therefore not defined. The previously established rules for ARE-RNA binding by RRMs 1 and 2 were not predictive as to whether an RNA oligonucleotide could serve as a substrate for the transferase activity. This suggested that transferase substrates were bound in a different mode than ARE RNAs, possibly even by the orphan RRM3.

3. Background and objectives

HuR is an AU-rich (ARE) element binding protein. However, unlike the majority of ARE-binding proteins, it typically acts to rather stabilize than destabilize its target mRNAs. Bhattacharyya et al. reported that, under stress, HuR can counteract the miR-122-mediated downregulation of CAT-1 mRNA if bound to the same message (Bhattacharyya et al. 2006). The de-repression was shown to be dependent on the miRNA since HuR was unable to counteract repression mediated by Ago2 protein directly tethered to mRNA (Kundu 2011). This indicated that HuR in some manner interferes with either miRNA binding to the target mRNA or miRNA binding to Ago2.

HuR and miRNA sites are enriched in the vicinity of one another, pointing to a potential interaction as well as mutual regulation of their target mRNAs (Lebedeva et al. 2011; Mukherjee et al. 2011). Indeed, the HuR/miR-122 co-regulation of CAT-1 mRNA is not an isolated case, and eight examples have been reported to date where HuR and miRNA act either in a competitive or in a cooperative manner to control mRNA expression (Srikantan et al. 2011; Tominaga et al. 2011; Young et al. 2012; Epis et al. 2011; Kim et al. 2009; Glorian et al. 2011; Chang et al. 2010)

Previous data from our laboratory have uncovered that HuR possesses enzymatic activity catalyzing transfer of adenosine nucleotide to the 3' terminus of RNA. However, the physiological substrates and biological context of this activity were not determined (Meisner et al. 2009). It was since demonstrated that HuR binds miR-16 directly *in vitro* (Young et al. 2012). In addition, siRNA-mediated knockdown of HuR led to an increase in miR-16 levels, suggesting that HuR can contribute to miRNA removal from a target mRNA (Young et al. 2012).

Given that single nucleotide additions/deletions at the miRNA 3' terminus have recently been shown to influence miRNA stability (Kato et al. 2009) as well as Ago loading (Burroughs et al. 2010), the present study was aimed at characterizing the adenylyating enzymatic activity further, uncovering the physiological context it is active in, and finally determining whether the HuR transferase activity might play a role in the cross-talk of HuR and miRNA on a target mRNA (Figure B1)

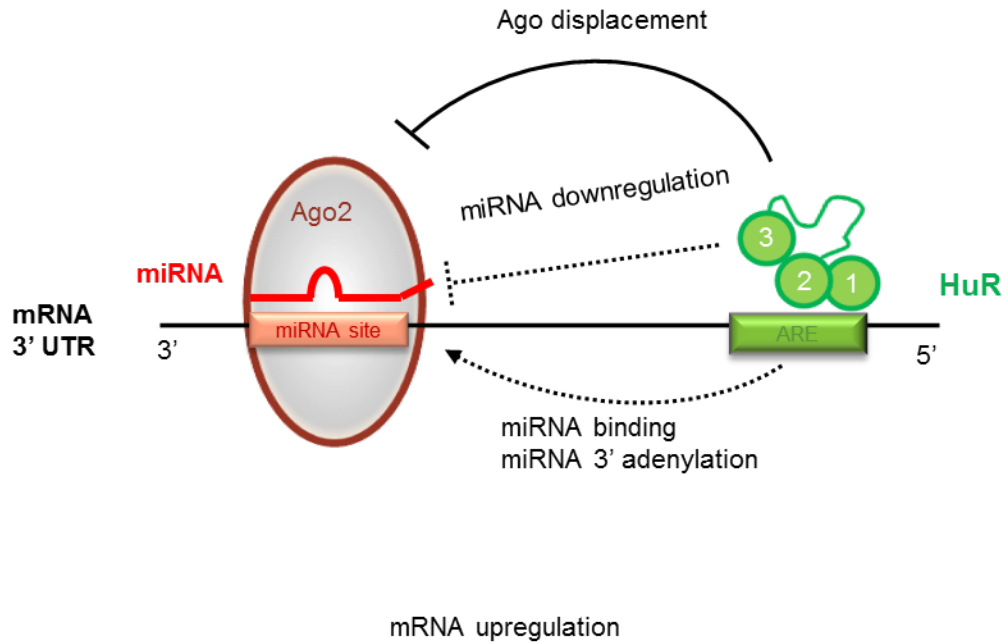


Figure B1. Summary of potential HuR interactions with Ago and miRNA. Continuous line: HuR displaces Ago and relieves mRNA repression in a miRNA-dependent manner. Dotted lines: HuR-mediated miRNA binding, 3' adenylation and downregulation.

4. Manuscript in preparation

4.1. Abstract

HuR is an AU-rich element (ARE) - binding protein important for the stabilization of short-lived mRNAs, including those encoding many cytokines and proto-oncogenes. microRNAs (miRNAs) are short ~22 nt non-coding RNAs that, when loaded into an Ago effector molecule, act to regulate the expression of over half of human genes. Together, HuR and miRNA co-regulate > 1000 mRNAs in either an antagonistic or cooperative manner. Specifically, HuR has been shown to counteract miR-122-mediated repression of the CAT-1 mRNA. Here we describe the dual enzymatic activity mediated by HuR, a poly(A)polymerase and a novel, 3'→5' exonuclease acting on the 3' end of many miRNAs. Our results demonstrate that HuR can access Ago2-loaded miR-122 when bound *in cis* to the same RNA. Initially, by adding a poly(A) tail to the miRNA, HuR generates a landing pad for the tailing-dependent exonuclease activity, which then degrades the miRNA. The tailing- and trimming-dependent antagonization of the Ago-loaded miRNA by HuR represents a possible mechanism of how HuR, together with RISC, can co-regulate common target mRNAs.

4.2. Introduction

Eukaryotic gene expression is controlled to a significant extent at the posttranscriptional level. In particular the fast on- and off-responses essential in transient and early response expression are most effectively achieved downstream of transcription. Regulation at the level of mRNA represents a cellular compromise between increasing energetic expense with decreasing delays in the protein responses. A complex interplay of *trans* acting factors binding to *cis* acting regulatory elements in mRNAs, mostly within the 3' untranslated region (3'UTR), mediates the fate of mRNAs from nuclear export through translation and storage to nucleolytic turnover (Chen & Shyu 1996; Silanes et al. 2007; Pesole et al. 2000). While our understanding of

individual posttranscriptional pathways has been growing extensively over the past decade, it is becoming increasingly clear that these processes are not acting in isolation but are rather being orchestrated in a coordinated manner, with the 3'UTR as a master control unit. In particular, recent work has provided increasing evidence for a close interrelation between two of the main posttranscriptional pathways – AU-rich element (ARE) control and microRNA (miRNA) mediated RNA silencing (Srikantan et al. 2011; Tominaga et al. 2011; Kedde et al. 2007; Bhattacharyya et al. 2006)

miRNAs are a class of small RNAs essential for posttranscriptional fine tuning of gene expression. By imperfect base-pairing to their target sites they guide the RNA induced silencing complex (RISC) to target mRNAs, thereby inducing target mRNA degradation and/or translational repression (Tabara et al. 1999; Lee et al. 1994; Baek et al. 2008; Selbach et al. 2008; Hendrickson et al. 2009; Guo et al. 2010). The molecular processes of how miRNAs regulate mRNAs have been studied in great detail but the mechanisms for control of miRNA themselves only start to be unraveled (MacRae et al. 2008; Behm-Ansmant et al. 2006; Zdanowicz et al. 2009; Eulalio et al. 2008; Chen et al. 2009). Recent work provided insights to regulation of miRNA expression and biogenesis (Viswanathan et al. 2008; Piskounova et al. 2011; Fukuda et al. 2007; Guil & Cáceres 2007), miRNA turnover (Rüegger & Großhans 2012; Chatterjee & Grosshans 2009; Cerutti & Ibrahim 2010; Krol et al. 2010), and fine-tuning of miRNA repressive activity (Yates et al. 2013; Jones et al. 2009; Kai & Pasquinelli 2010). Some of these mechanisms involve direct enzymatic modifications of miRNAs themselves (Li et al. 2005; Wyman et al. 2011; Burroughs et al. 2010; Jones-Rhoades et al. 2006; Jones et al. 2009); In particular, non-templated nucleotide additions to miRNA were reported to modulate miRNA activity and stability (reviewed in (Kim et al. 2010)).

AREs are a class of regulatory *cis* elements for posttranscriptional regulation of a wide variety of early response genes. By interaction with specific RNA binding proteins (RBPs) they mediate tight control of mRNA half-lives, localization and translation (refs). The ubiquitously expressed ELAV (embryonic lethal, abnormal vision) family protein HuR (also known as HuA or ELAVL1) is one of the key effector proteins acting as predominantly positive regulator of short lived ARE mRNAs. Upon binding to the ARE it protects the mRNA from rapid decay and/or relieves the translational block (Dean et al. 2001; Ford et al. 1999; Cherry et al. 2006). HuR is primarily localized in the nucleus in resting cells but redistributes rapidly into the cytoplasm

under stress or in response to specific cellular stimuli (Atasoy et al. 1999). It has therefore been proposed that HuR might bind to its target mRNAs already in the nucleus and actively promote their nuclear export, possibly using two alternative nucleocytoplasmic shuttling pathways (Fan & Steitz 2001; Fan & Steitz 1998; Gallouzi et al. 2001). Despite over 20 years of research on HuR (Myer et al. 1997), our understanding of its mode of action in antagonizing posttranscriptional downregulation by AREs is still incomplete. While a simple competitive displacement of destabilizing factors such as Tristetraproline (TTP), AU-rich element binding factor-1 (AUF1, hnRNP D) or K-homology splicing protein (KSRP) from the ARE might be involved, there is also accumulating evidence for more complex mechanisms. For example, artificial recruitment of HuR to non-ARE sites by computationally designed “mRNA Openers” oligonucleotides was sufficient for stabilization of IL-2 and TNF- α mRNAs (Meisner et al. 2004).

More recently, many examples of functional interrelation of HuR with miRNAs, both antagonistic and agonistic, have been reported (Kedde & Agami 2008; Bhattacharyya et al. 2006) found that HuR relieves the miR122-mediated translational repression of the cationic amino acid transporter-1 (CAT-1) mRNA in Huh7 hepatocytes upon amino acid starvation (Bhattacharyya et al. 2006). Since elimination or mutation of the CAT-1 ARE phenocopied the effect of HuR knockdown by siRNAs, the authors concluded that binding of HuR to the miR122 repressed mRNA *in cis* was required to mediate the repression relief. A follow up study demonstrated that binding of HuR to chimeric ARE - miRNA target reporter RNAs *in vitro* resulted in the displacement of the Argonaute 2 (Ago2) RISC and thereby protected the target RNA from slicing (Kundu et al. 2012).

Following this work, further evidence has been published demonstrating that HuR can antagonize repression of Cox-2 mRNA by miR-16 (Young et al. 2012), TOP2A mRNA by miR548c-3p (Srikantan et al. 2011), nucleolin mRNA by miR-494 (Tominaga et al. 2011), ERBB2 mRNA by miR-331-3p (Epis et al. 2011), stim1 mRNA by miR-195 (Zhuang et al. 2013), and HMGB1 mRNA by miR1192 (Dormoy-Raclet et al. 2013). In addition, there are also several examples of the potentiating effect of HuR on miRNA-mediated repression (Kim et al. 2009; Glorian et al. 2011; Chang et al. 2010). However, the molecular mechanism of cross talk between HuR and miRISC on the 3'UTR still remains enigmatic. As supported by *in vitro* data (Kundu et al. 2012), the most plausible mode of action would involve an active displacement of miRISC from mRNA by HuR. A direct competition for overlapping binding sites or steric hindrance do not appear as plausible

general mechanisms since in some of the studied mRNAs (CAT-1, TOP2A, and nucleolin) and also reporters, the HuR binding site was located up to several hundred nucleotides away from the affected miRNA sites (Bhattacharyya et al. 2006; Srikantan et al. 2011; Tominaga et al. 2011). Consistent with this long-distance effect, it has been proposed that spreading of HuR along RNA, supported by its oligomerization, might be involved (Kundu et al. 2012). Recent PAR-CLIP studies have shown that HuR binding sites are enriched in immediate proximity to rather than overlapping with miRNA sites (Lebedeva et al. 2011; Mukherjee et al. 2011), which also speaks for a more complex cross-talk between the two factors rather than competition for the same or overlapping binding sites. It has also been speculated that HuR might indirectly inhibit RISC binding through modulation of RNA folding (Srikantan et al. 2012); for a long distance cross-talk this would however imply rather complex conformational rearrangements in the 3'UTR, which are hard to predict computationally and investigate experimentally. Interestingly, derepression of Cox-2 mRNA was shown to involve direct binding of HuR to mature miR-16 and an HuR-dependent downregulation of miR-16 levels (Young et al. 2012), thereby pointing to yet another mechanistic possibility.

In this work we investigate the role of the recently discovered enzymatic activity of HuR to 3'-terminally adenylate RNA (Meisner et al., 2009) in the cross-talk of HuR with the miRNA-mediated repression. We show that HuR, when bound to target RNA associated with Ago-loaded miRNA, is able to exonucleolytically degrade the miRNA, in a process facilitated by its initial 3' polyadenylation.

4.3. Results

4.3.1. HuR binds and 3' adenylates miRNAs

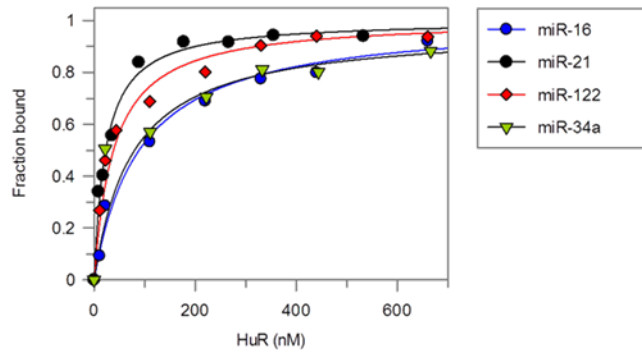
We have recently reported that HuR directly binds miR-16 (Young et al. 2012). Using purified recombinant protein and synthetic miRNAs 5'-terminally-labeled with 5'carboxymethyl tetrahydroamine (TMR), we now found that in addition to miR-16, HuR also binds to miR-122, miR-34a, and miR-21 as measured by 2D-FIDA (2-dimensional Fluorescence Intensity Distribution Analysis) anisotropy (Meisner et al. 2004). These miRNAs, selected due to their

established role in regulation of expression of ARE-containing target mRNAs (Cok et al. 2003) were bound by HuR with nanomolar (20-100 nM) affinities (Figure 1A). A truncated variant of HuR comprising only the two N-terminal RNA recognition motifs (RRM1 and 2; residues 2-189; referred to as HuR₁₂) also bound these miRNAs, however with a ca. 70-fold reduced affinity (Figure S1A, Supplementary Figures shown at the end of the manuscript, chapter 4.7, page 87). This indicates either a major energetic contribution of the C-terminal region of HuR to the interaction or a different organization of RRM1 and 2 in the absence of the C-terminal domains. In a systematic *in vitro* study, we had previously demonstrated that HuR has a strong preference for single stranded NNUUNUUU (where N is any nucleotide) (Meisner et al. 2004), which is consistent with the HuR consensus sites in target mRNAs derived from recent CLIP studies (De Silanes et al. 2004).

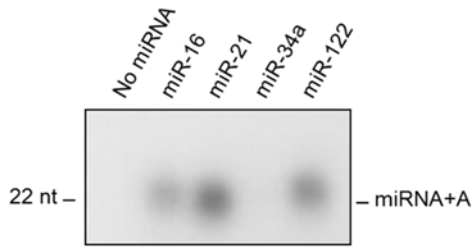
Since none of the interacting miRNAs comprised sequences resembling HuR-specific AREs we hypothesized that miRNAs might be bound in a different mode than AREs and potentially act as substrates for the previously reported RNA adenylation activity of HuR (Meisner et al. 2009). Upon incubation with recombinant HuR and [α -³²P]-ATP, we observed labeling of miR-16, miR-21, and miR-122, revealing that HuR can adenylate miRNAs (Figure 1B). No adenylation of miR-34a was observed, indicating that not all miRNAs are good substrates, even if they are bound by HuR. In the experiment shown in Figure 1B, only monoadenylated products were generated according to the mobility in PAGE. However, synthetic miR-122 variants with 3'-terminal extensions of one to four adenosyl residues underwent further mono-adenylation (Figure 1C), suggesting that HuR has a poly(A) tailing activity. Titrating concentrations of HuR, miRNA, and [α -³²P]-ATP showed that ATP (at 33 nM) was highly limiting in mono-adenylation reactions (Figure S1B). Adding an excess of cold ATP into the reaction containing [α -³²P]-ATP (to final ATP concentration of 10 μ M) resulted in generation of miR-122 bearing long radiolabeled poly(A) tails (Figure 1D), revealing that HuR has miRNA poly(A) polymerase activity.

Figure 1

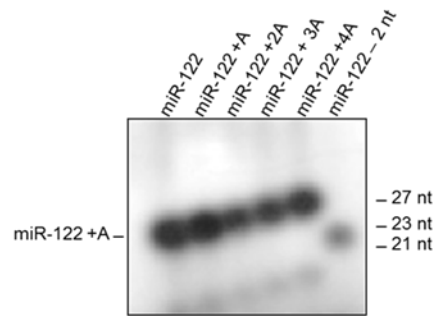
A



B



C



D

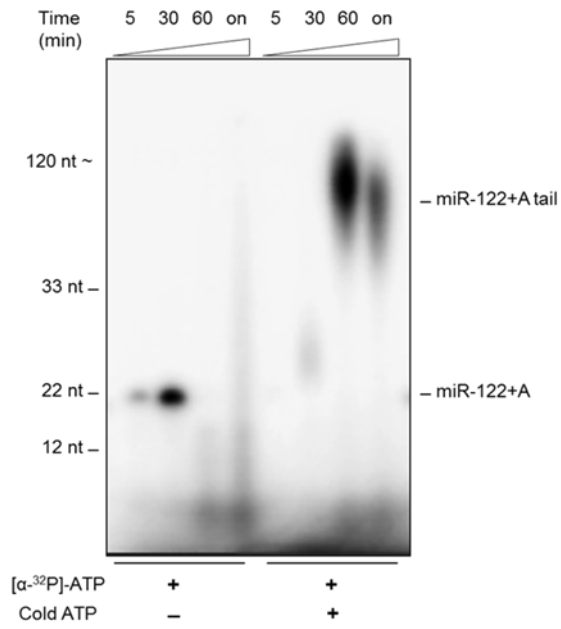


Figure 1. HuR binds and oligo adenylates miRNA. (A) Binding of full length HuR to 5'-TMR labeled miRNA measured by 2D-FIDA anisotropy (Kask et al. 2000). 5 mM EDTA was used in the assay buffer to monitor the interaction under steady state conditions (HuR affinities: miR-122: $K_d = 38 \pm 7$ nM; miR-16: $K_d = 90 \pm 15$ nM; miR-21: $K_d = 23 \pm 2$ nM; miR-34a: $K_d = 75 \pm 11$ nM;) (B) Adenosyl incorporation ($[\alpha\text{-}^{32}\text{P}]\text{-ATP}$, at 33 nM) into miR-16, miR-21, miR-34a and miR-122 (all miRNAs at 5 μM , HuR at 1.5 μM , MgCl_2 at 5 mM), monitored on a 10 cm 15 % TBE-urea PAGE with autoradiographic detection. (C) Incorporation of $[\alpha\text{-}^{32}\text{P}]\text{-ATP}$ into miR-122 variants with up to four 3'-terminal synthetic A extensions, as well as a miR-122 variant with a 2 nt 3'-terminal truncation. (D) Time course of $[\alpha\text{-}^{32}\text{P}]\text{-ATP}$ reaction of miR-122 with HuR without and with addition of an excess of cold ATP (10 μM) monitored on a 20 cm 12 % TBE-urea PAGE and autoradiographic detection. Size determination using TMR-labeled synthetic miRNA as indicated.

4.3.2. HuR tails and trims miRNA.

To monitor the substrate as well as the products of the reaction we used synthetic 5'- ^{32}P -labeled miR-122 as a substrate. Under conditions with an excess of HuR over RNA and 1 mM ATP, the miR-122 substrate was quantitatively turned over by HuR resulting in poly(A) tails up to ca. 100-200 nt tail length (Figure 2A, left part). Surprisingly, we noted that miR-122 underwent in parallel a nucleolytic processing when incubated with HuR but not in its absence (Figure 2A, right part), pointing towards a potential second catalytic activity of HuR. The nuclease was also active in the absence of ATP (Figure 2A, middle part), but not in the absence of HuR or in purifications from untransformed, mock-induced *E.Coli* cultures (data not shown). The same tailing and trimming activity was also detected for miR-16, miR-21, and miR-27a (Figure S2A). Tailing of another tested miRNA, miR-192, was less pronounced whereas its trimming was very effective. We also noted that titration of ATP from the low concentrations used in the ATP incorporation assay to more physiological concentrations (1 mM) resulted in the increase in length of the poly(A) tails, and a general shift from trimming to tailing at early time-points (Figure S2B).

We used several approaches to eliminate or minimize the possibility that either polyadenylation or nucleolytic activity of recombinant HuR is due to contaminating proteins. We first tested susceptibility of miRNA turnover to a small-molecule HuR inhibitor, MS-444. This compound prevents HuR homo-dimerization, inhibits HuR binding to ARE-containing mRNA and ATP, and affects HuR nucleo-cytoplasmic distribution (Meisner et al. 2009); it also inhibits mono-adenosyl transferase activity investigated before (Meisner et al. 2007), as well as miRNA binding in a dose-dependent manner (Figure S2C). In the presence of increasing amount of MS-444, not

only tailing but also trimming of miR-122 was progressively inhibited, consistent with both enzymatic activities being dependent on HuR (Figure 2B). Both enzymatic activities were also strongly inhibited by addition of an oligodeoxynucleotide bearing an HuR-specific ARE sequence but not one with an inverted ARE sequence, indicating that binding to the ARE *in trans* prevents miRNA turnover, possibly by interfering with miRNA binding (Figure S2D). Notably, none of the tested general RNase inhibitors had an effect on miRNA polyadenylation or degradation (Figure S2E). In addition, HuR₁₂ also catalyzed the nucleolytic digestion as well as poly(A) tailing of miRNA, but generated shorter tails than the full-length protein.

Although the recombinant HuR proteins used in this work were of high (>99 %) purity as based on SDS-PAGE and RP-HPLC analysis (Figure S2F), we additionally subjected protein preparations to high sensitivity liquid chromatography - mass spectrometry (LC-MS). Among very few non-HuR peptides detected at trace levels, there were no peptides mapping to known nucleases (Figure S2G). Given the attomolar detection sensitivity, this implies that there would be at most 5 molecules of such a non-detectable trace contaminant in the typical enzymatic reactions used in this study. Since titrating HuR concentrations down maintained trimming activity to at least 100-fold dilution (Figure S2H) this would imply activity of such contaminants at below 0.05 molecules per reaction. However, we cannot unequivocally rule out that another, as yet unidentified *E.coli* enzyme, could be co-purifying with HuR in our protein preparations. Interestingly, each 10-fold dilution resulted in a slightly different degradation pattern, however this may reflect the change in the ratio of the two counteracting activities, the poly-A tailing and nucleolytic activity.

We next tested for co-fractionation of HuR and HuR₁₂ with their enzymatic activities by size exclusion chromatography. As shown in Figures 2C and S3A, for both proteins the transferase and nuclease activities co-fractionated with optical density peaks of the proteins eluting at the respective molecular weights expected for monomeric proteins, making it unlikely that a larger complex of HuR with putative contaminants is responsible for observed activities. The peak of maximal enzymatic activity shifted together with the shift in retention time between HuR and HuR₁₂, arguing also against a possibility that the enzymatic activities, co-fractionating with HuR peaks, are due to contaminants having the same size as HuR. Furthermore, the nuclease activity was partially retained upon subjecting HuR₁₂ to denaturing reverse phase (RP)-HPLC purification, lyophilization and refolding of the protein by ion exchange

chromatography, where it co-eluted with the HuR₁₂ peak (Figure S3B). Notably, much of the nuclease activity was lost during the renaturation process. The transferase activity was also lost upon this harsh procedure, most likely due to its generally high biochemical sensitivity also observed during purification (see Materials and Methods).

Finally, to rule out co-purifying contaminations from *E.coli*, we purified HuR_{fl} and HuR₁₂ in a different system. HuR proteins obtained from Baculovirus-infected insect cells were of a good purity, but did not reach the high purity levels of *E.coli* expressed proteins. Baculovirus HuR showed comparable nuclease activity on miRNA to *E.coli*-purified proteins (see Figures 2D, lower panel, and S3C for degradation patterns). *Baculo*-purified HuR_{fl} in addition showed transferase activity, although we did not observe tailing on a high resolution gel (Figure 2C, upper panel). Both the nuclease and transferase were, again, inhibited by MS-444. Due to reasons unknown, the same intein fusion constructs that we purify routinely from *E.coli* is significantly less stable in *Baculo* purifications. As mentioned above, the transferase activity was highly unstable and sensitive to the purification procedure. We therefore believe that either the conditions in the *Baculo* purification process leading to this instability or a possible protein modification in the *Baculo*-infected cells could explain this discrepancy in transferase efficiency.

We conclude from the data presented above that HuR can carry out both 3'-terminal poly(A) tailing as well as nucleolytic processing of miRNA substrates *in vitro*.

4.3.3. The miRNA poly(A) polymerase and 3'→5' exonuclease activities map to the first two RRM of HuR

miR-122 was both trimmed and tailed by the C-terminally truncated HuR₁₂ variant thereby mapping both catalytic activities to within the N-terminal domains of HuR (Figure 2A). Yet, previous data indicated that the HuR transferase activity might involve a conserved DxD₂₅₄₋₂₅₆ motif within RRM3, with D254 contributing to ATP binding (Meisner et al. 2009). While impaired in transferase activity, none of the RRM3 point mutants, including D254S, D256S, and D312S, was however catalytically dead (Meisner et al. 2009). We now mutated D254 to alanine to eliminate hydrogen bonding potential of the serine mutations we had previously used and investigated these mutants for their miRNA tailing and trimming activity. The D254A mutant bound ARE RNA with almost identical affinity to the wild type protein (Figure S4A), indicating

that the mutant protein was folded, but showed no incorporation of [α - 32 P]-ATP into miR-122 in the ATP incorporation assay (Figure S4B). However D254A, similarly as D254S, retained the miR-122 tailing activity albeit weaker than the wild type protein (Figure S4C and S4D), which is consistent with a contribution of D254 to ATP binding rather than its essential role in the catalysis. Of note, the effect of the D254A mutation on tailing activity was comparable to the effect of deleting the C-terminal part of the protein (HuR₁₂; Figure 2A). Also, the ATP affinity of HuR₁₂, which is ca. 15-fold weaker ($230 \pm 40 \mu\text{M}$; Figure S4E) than the ATP affinity of the full length protein, was similar to the reduced affinity previously observed for the D254S mutant (Meisner et al. 2009). To identify amino acids within RRM1/2 involved in catalysis we performed a small scale alanine mutation screen, including selected candidate aspartates and glutamates, and identified D105A to have significantly reduced transferase activity (Figure S4F). In addition, the nuclease activity of D105A was increased – possibly reflecting the altered balance of the two activities upon tailing inhibition (See Figures S2A, S2B). Of note, D105A bound ARE RNA with a reduced affinity which could possibly account for the reduced transferase activity (Figure S4A). These data show that both catalytic sites are contained within the N-terminal peptide and/or RRM1/2 of HuR, and indicate that amino acids in RRM3 may additionally contribute to ATP binding (see also thesis discussion).

Figure 2

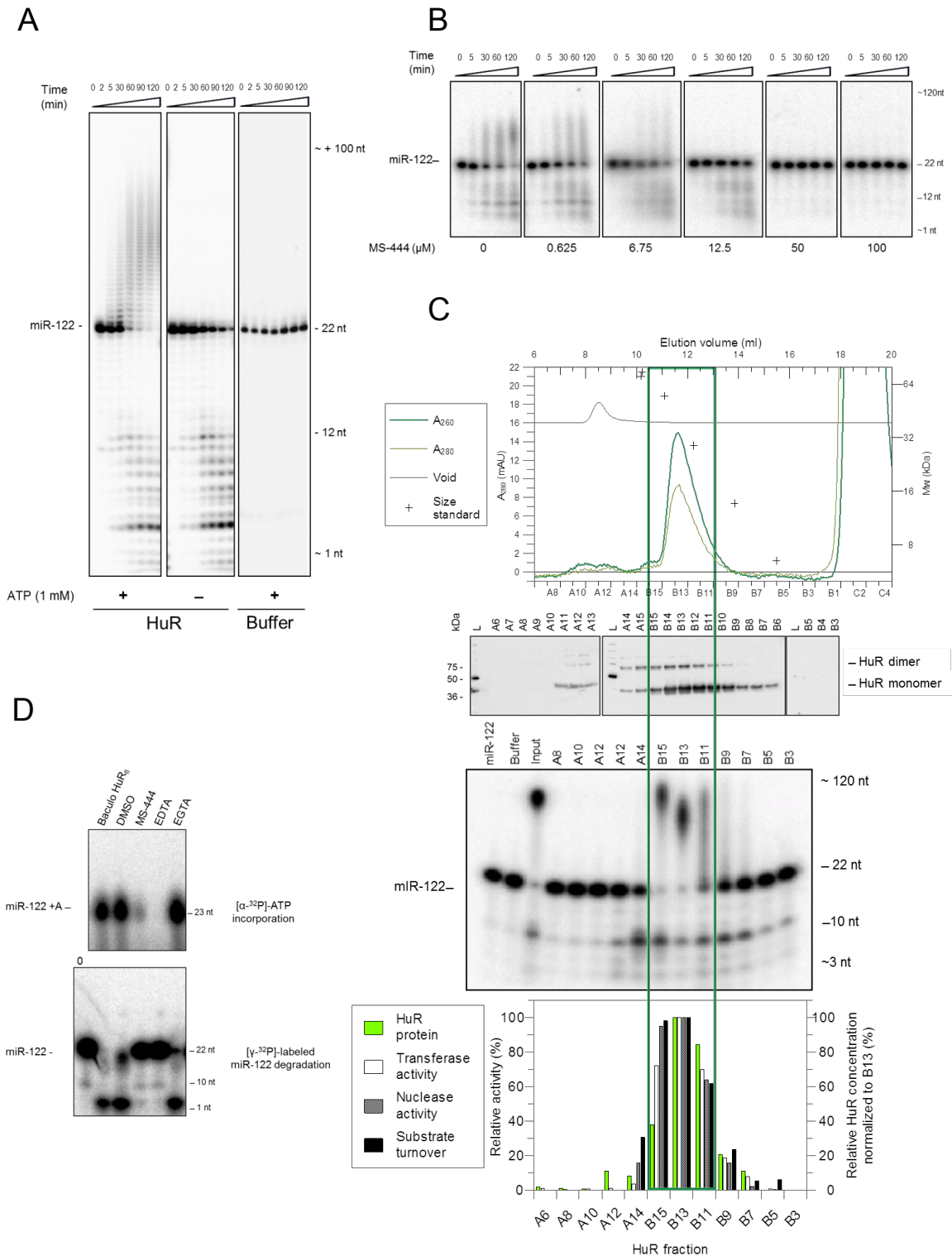


Figure 2. HuR tails and trims miRNAs (A) Reaction time course of 5'- 32 P-labeled miR-122 with HuR in the presence or absence of ATP, monitored by high resolution TBE-urea PAGE (52x20 cm, 0.4 mm, 12 % PAA

1xTBE 6 M urea PAGE) and autoradiographic detection. The third panel shows a control reaction without HuR. (B) Tailing and trimming of 5'-³²P-labeled miR-122 by HuR in presence of DMSO (0.1% v/v) or increasing amount of MS-444 (10 cm 15% TBE-urea PAGE). (C) Co-fractionation of tailing and trimming activities with HuR in size exclusion chromatography on a Superdex-75 10/300 GL column. First panel from the top: Superdex-75 size-exclusion chromatogram are shown for HuR (dark green: 280 nm absorbance, light green: 260 nm absorbance) and Dextran (grey, void). Retention volumes of the size standard are labeled in the chromatogram (black cross) with the corresponding molecular weight scale plotted on the right y-axis. 500 µl fractions were collected as indicated (fraction number bottom x-axis, elution volume top x-axis). Second panel from the top: HuR Western blot of collected fractions as indicated. Both, HuR monomer and dimer are detected in all fractions, possibly including re-dimerization following chromatography. Size standard: Precision plus western C (Biorad). Third panel from the top: tailing and trimming of 5'-³²P-miR-122 by collected fractions as indicated in the chromatogram with HuR input sample as reference (10 cm 15% TBE-urea gel and autoradiography detection). Lower panel: densitometric quantification of HuR protein in each fraction by western blot analysis overlaid with transferase and nuclease activities based on densitometric quantification of either the products or overall substrate consumption (fraction B13 set to 100%). (D) Upper panel: Single timepoint (30 min) adenosyl incorporation of [α -³²P]-ATP, at 33 nM into cold miR-122 by Baculo-purified HuR. (Lower panel): degradation of 5'-³²P-labeled miR-122 by Baculo-purified HuR in the presence of DMSO (0.1% v/v), MS-444 (100 µM), EDTA and EGTA (both 20 mM). Incubation for 30 min.

We proceeded to biochemically characterize both enzymatic activities associated with HuR (summarized in Figure 3A). HuR requires Mg²⁺ for both enzymatic activities. It cannot use Ca²⁺, Co²⁺, Mn²⁺ or Zn²⁺ as a cofactor (S5A, left panel). Even in the presence of Mg²⁺, addition of Co²⁺ and Zn²⁺ induces protein precipitation. This is accompanied, as expected, by an inhibition of both tailing and trimming (Figure S5A, right panel). Ca²⁺ ions present in the reaction medium do not induce protein precipitation; however they do inhibit both enzymatic reactions. In the presence of Mn²⁺ at 1 mM, the reaction is unperturbed. However, at 5 mM, tailing is completely, and the nuclease partially inhibited.

The nuclease activity did not require ATP (Figure S5B), and replacing ATP with α -S-ATP at identical concentrations maintained transferase activity though yielded shortened tails, but did not affect trimming (Figure S5C). Furthermore, transferase activity was impaired upon capping of the 3'-terminal 3'OH group by alkylation (3'-O-C3) as well as by modification in the 3'-terminal ribose (2'H 3'OH, 2'OH 3'H, or 2'H 3'H), indicating that the transferase requires both the 2' and 3' hydroxyl groups (Figure S5D and E). None of these 3' nucleotide modifications affected the nuclease activity (Figure S5E, 4C, and data not shown). HuR enzymatic activity was also affected by different miRNA 5' chemistries. A miRNA with a 5' phosphate was, in most cases, the best substrate for the HuR transferase. However, this was not due to changes in the binding affinities of HuR to a 5' phosphate or 5' OH RNA as HuR bound them with near identical affinities (Figure S5F). A miR-122 in either DNA form or fully phosphorothiorate modified form was not a

substrate for either the transferase or nuclease activity of HuR (Supplementary Figures S5G and S5H). Likewise, perfect blunt-ended duplexes of miR-122 or miR-27a with their antisense strands did not act as substrates (Figure 4A), suggesting that HuR acts preferentially on (at least partially) single stranded RNA.

Next we asked whether the HuR enzyme(s) have any sequence preferences. As we had observed that not all miRNAs were substrates for the transferase (Figure 1B), we tested a larger number of randomly selected synthetic miRNAs for *in vitro* 3'-adenylation by HuR. To allow for a simple readout in this small screen, we reverted to the "mono-adenylation" experimental setup used in Figure 1B and C and quantified incorporation of [α -³²P]-ATP as a single measure for the transferase efficiency. As we had no means to uncouple the transferase from the nuclease, we chose an early 15 min time point when the nuclease contribution is still minimal (see Figure 2A). As summarized in Figure 3C (data in Figures 3C and S6A), 19 out of the 45 tested miRNAs acted as HuR transferase substrates. Visual inspection of sequences of active miRNAs did not reveal any obvious common motif apart from a tendency for GU-rich 3' ends. An unbiased frequency analysis of nucleotides at each individual position (aligned from the 3' end; Figure 3D, upper panel) revealed enrichment in G and U in the 3'-terminal region of HuR substrates when compared to 500 randomly chosen miRNAs. In a further attempt to identify potential consensus motifs, we analyzed the substrate miRNA sequences by different Motif Search algorithms. GLAM2 (Frith et al. 2008), DREME (Bailey 2011) and MEME (Bailey & Elkan 1994) all delivered similar loosely defined GU-rich motifs at the very 3' end of miRNAs (GLAM2 motif shown in Figure 3D, middle panel). We next tested whether such a 3'-terminal sequence would be sufficient to convert a non-substrate miRNA into an HuR transferase substrate. Replacing the 3'-terminal nucleotides of the non-substrate miR-192 with GUUUG was sufficient to induce adenylation by HuR (Figure 3E, left panel), suggesting that a 3'-terminal GUUUG represents one variant of a minimal HuR transferase consensus motif (Figure 3E, middle panel; data from Figure S6B). Using the miR-192 backbone allowed us to further dissect the position and sequence requirements for the HuR transferase activity (Figure 3E, right panel). As summarized in Figure S6B (right panel), testing of 23 different synthetic chimeric miR-192 variants indicated that a 3'-proximal GU-rich pentamer with terminal guanosines represents one type of a consensus sequence preferred by the HuR transferase. Of note, we had also identified miRNAs which act as substrates but lack this motif (See Materials and methods, Chapter 4.5.10. Table M5), suggesting existence of alternative functional motifs.

We next tested for any potential preferences of the nuclease, using different 5'-labeled miRNAs. To effectively uncouple nuclease from transferase activity, we again used HuR₁₂ in the absence of ATP. In contrast to the transferase, we did not observe any obvious differences in nuclease activity for the tested miRNAs, including miR-192 which does not act as a transferase substrate (Figure S6C). Interestingly, also, oligo(A)₂₃ but not oligo(U)₂₃ was very effectively degraded by HuR₁₂. In distinction to miRNAs, the oligo(A)₂₃ degradation, in the absence of ATP, followed a uniform pattern with no intermediate stalling products accumulating. The differing degradation patterns of each individual miRNA indicates that not every nucleotide is cleaved with the same efficiency. The uniform pattern of oligo(A) or (U) degradation however suggest that the degradation occurs exonucleolytically in a 3'→5' direction (Figure S6C). Oligo(A)₂₃ was in addition a poor substrate for polyadenylation by either HuR or HuR₁₂ (Figure 3B). A trimming time course of synthetic oligoadenylated miR122 (miR-122-A₂₀) with HuR₁₂ in absence of ATP showed a biphasic reaction with rapid removal of the A-tail followed by the typical turnover kinetics of the miRNA body with the main intermediate stalling products in the center of the miRNA sequence (~8-10 nt, Figure S6D).

Figure 3

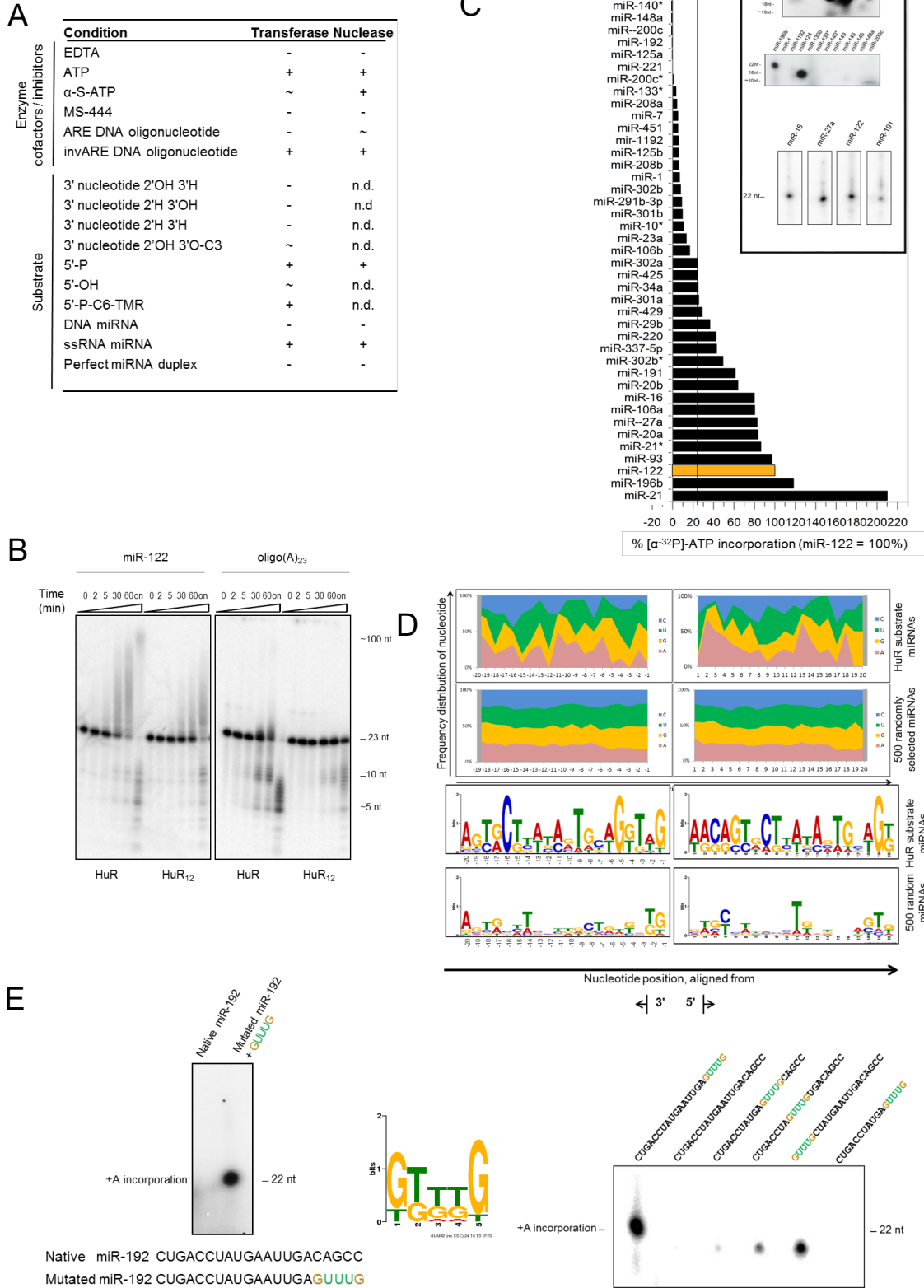


Figure 3. Biochemical characterization of the two HuR enzymatic activities (A) Summary of biochemical characterization of HuR nuclease and transferase enzymes (Data in Supplementary Figures S5A-H and Figures 4A and 4C). Legend: (+) reaction unaffected; (~) reduced reaction efficiency; (-) reaction inhibited; (n.d.) not determined. (B) Tailing and trimming time course of 5'-³²P-labeled miR-122 versus oligo(A)₂₃ by HuR and HuR₁₂ (20 cm 12 % TBE-urea PAGE). (C) Quantification of HuR [α -³²P]-ATP incorporation into 45 synthetic miRNAs (PAGE autoradiograms in inset, Figure S6A). miR-122 (set to 100 %) and/or miR-196b were included on all gels for cross comparison. A threshold to classify miRNAs as confirmed (*in vitro*) substrates was set based on the limit of quantification determined by densitometry. (D) Upper panel: Frequency of nucleotide distribution at each position for 3' and 5' aligned HuR transferase substrate miRNAs versus 500 randomly selected miRNA sequences. Lower panel: Web logo of GLAM2-derived consensus motif derived from 3' and 5' aligned HuR transferase substrate miRNAs versus a random selection of 500 miRNA sequences from miRBase. (E) Left panel: Reaction of HuR with the non-substrate miR-192 and a chimeric miR-192 variant comprising a 3'terminal sequence substitution by GUUUG. The PAGE analysis shows [α -³²P]-ATP incorporation into unlabeled miRNAs. Middle panel: 23 pentameric 3'-terminal sequence substitution variants of miR-192 were tested for turning the non-substrate miR-192 into an HuR transferase substrate. PAGE images and autoradiographic quantification of [α -³²P]-ATP incorporation are shown in Figure S6B. The motif derived from all sequences sufficient for HuR transferase activity on miR-192 chimeras is shown (GLAM2 (Frith et al. 2008)). Right panel: HuR transferase activity ([α -³²P]-ATP incorporation) for miR-192 variants with GUUUG motif substitution at various positions in the miRNA sequence.

4.3.4. Tailing dependent trimming of free and Ago-loaded miRNAs associated with a target

RRMs typically bind single stranded RNA (Manival et al. 2001). Since we observed that perfectly base-paired miRNA duplexes are inert to both tailing and trimming by HuR, we examined whether association of miRNAs with their natural target sites also affects their processing by HuR. Indeed, pre-hybridizing miR-122 or miR-27a to short RNAs corresponding to their natural sites, originating from the CAT-1 mRNA (Chang et al. 2004) and HSUR-1 RNA (Murthy et al. 1986) respectively, completely impaired tailing of the miRNA, and partially inhibited trimming. However, processing of both miRNAs was restored when the target RNAs also included an HuR-specific ARE (originating from the IL-1 β mRNA (Caput et al. 1986) and from HSUR-1 RNA) positioned 20 nt downstream of the miRNA target site (Figure 4A). No major differences were observed for chimeric miRNA-ARE targets bearing three different miR-122 target sites (CAT-1d, CAT-1e, and CAT-1f (Chang et al. 2004), Figure S7A), or between targets containing the ARE either downstream or upstream of the miR-122 site (Figure S7B). In contrast, miR-122 hybridized to a perfectly complementary target site remained resistant to modification

even when an ARE was present in the target (Figure S7A; sequences of all miRNA duplexes are shown in the lower panel). When the target RNA was extended by a scrambled, non-HuR binding sequence (Meisner 2005) the processing of miRNA by HuR was slightly less efficient (Figure 4B).

The data presented above suggested that HuR tails and trims miRNAs *in cis* when bound to the same target RNA, independent of the relative orientation of the binding sites for miRNA and HuR (Figure S7B). Interestingly, the poly(A) tail length of miRNAs bound to chimeric ARE-miRNA targets was significantly shorter than in the case of free miRNAs (Figures 4A-D and S7A-S7C); the tail length also appeared to be affected by the distance separating the two sites (Figure 4C). Furthermore, the time course experiments suggested that the tailing and trimming reactions of target bound miRNAs occur successively, with tailing preceding trimming (Figure 4C, left part). We thus hypothesized that when the miRNA substrate is sequestered at its binding site, the poly(A) tailing by HuR bound to the target *in cis* might facilitate nucleolytic degradation by bridging the distance separating the miRNA and HuR sites and/or generating a more optimal nuclease substrate by adding a single stranded poly(A) extension to miRNA. In addition, poly(A) tailing might be a means to access the miRNA deeply buried within RISC and thereby provide a “landing pad” for the HuR nuclease.

To address these questions we first tested whether tailing is required for HuR to trim a miRNA bound to the chimeric miRNA-ARE target. To uncouple nuclease activity from the transferase we used miR-122 bearing the 3'-terminal 3'-deoxy nucleotide to prevent its tailing. While trimmed efficiently by HuR in the absence of the target, trimming of this tailing deficient miRNA was lost when hybridized to a chimeric RNA (Figure 4D, middle part). In addition, when using HuR₁₂ in the absence of ATP to prevent tailing, the trimming of the (non-modified) miR-122 bound to the chimeric target was strongly impaired when compared to the reaction catalyzed by tailing proficient HuR (Figure 4D, right part). Notably, even in presence of ATP HuR₁₂ remained deficient in trimming a chimeric target bound miR-122 (Figure S7C), indicating that not only tailing activity but also RRM3 and/or the hinge region may be required for HuR to efficiently trim a miRNA hybridized to target RNA.

To test how the results obtained for free miRNA compare with miRNA which is associated with Argonaute protein, we used an *in vitro* system described by MacRae et al (De et al. 2013). Recombinant Ago2 was loaded with miR-122 to generate slicing proficient RISC (De et

al. 2013). The correct loading of the miRNA into Ago2 was verified by testing its ability to slice a target perfectly complementary to miR-122 (Figure S7D). When associated with the Argonaute protein and bound to a chimeric 1e-ARE target, miR-122 was resistant to micrococcal nuclease (MNase) digestion for at least 16 h, while non-Ago2 loaded miRNA was largely degraded by MNase within 60 min (Figure S7E). Importantly, in the presence of HuR Ago2 loaded miR-122 was quantitatively turned over within 60 min (Figure 4E). The nucleolytic turnover was dependent on the presence of the chimeric miRNA-ARE target (Figure 4E, compare conditions 3 and 4) as well as miRNA tailing proficiency (Figure S7F, compare conditions 3, 4 and 5), consistent with the results obtained with free miRNA hybridized to the chimeric target. Replacing ATP with α -S-ATP appeared to stall the reaction in the tailing phase, with the resulting short tailed Ago2-loaded miR-122 products being resistant to nucleolytic processing (Figure S7F, condition 5).

Figure 4

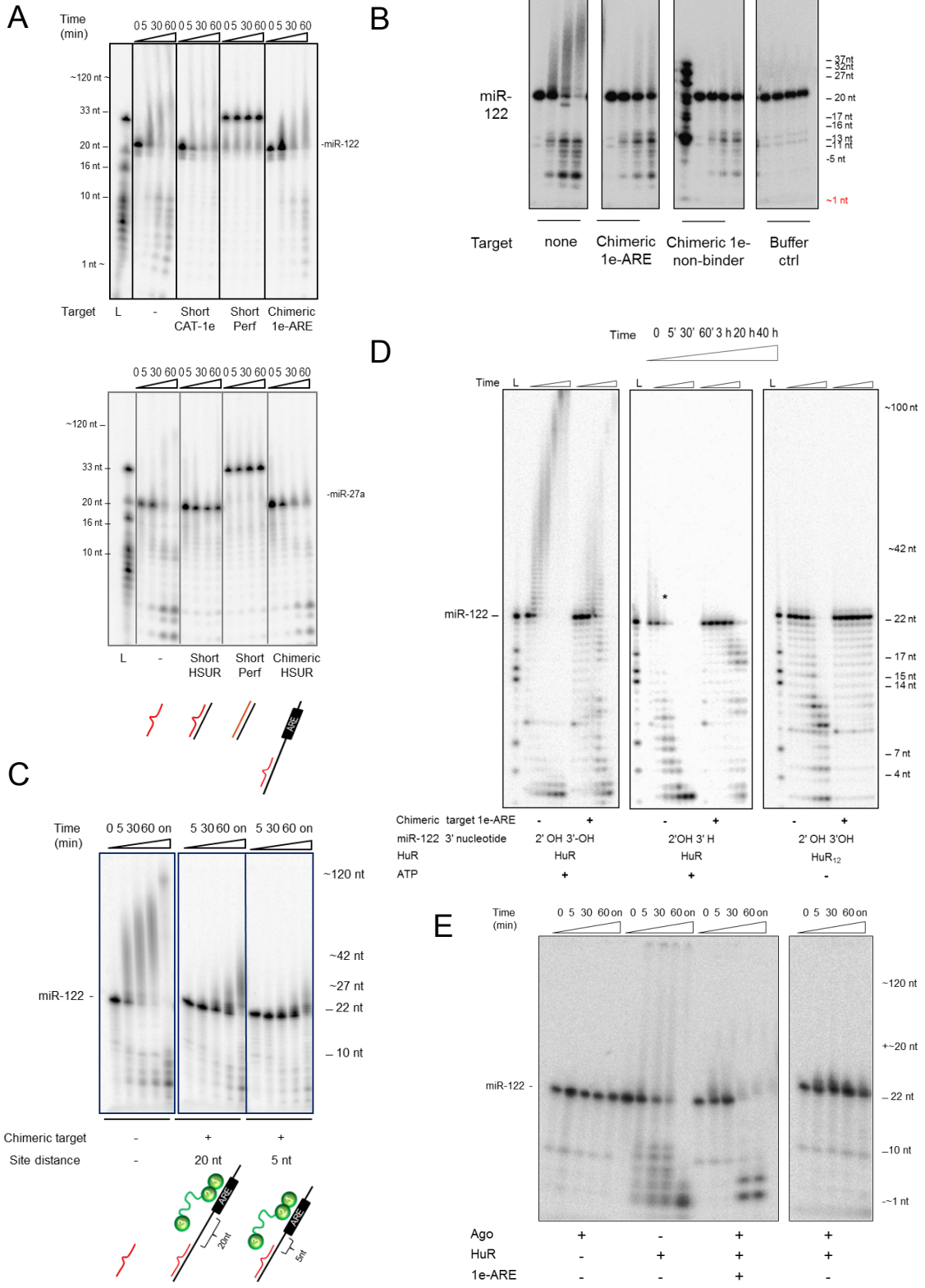


Figure 4. Tailing dependent trimming of free and Ago2 loaded miRNA on a target. (A) HuR reaction time course with 5'-³²P-labeled miR-122 (upper part) and miR-27a (lower part) either in free form or pre-hybridized to a short perfect or canonical target site, or a chimeric target containing a natural miRNA target site fused to an ARE (for miR-122: target site 1e from the CAT-1 mRNA alone or spaced 20 nt upstream of the IL-1 β ARE (1e-ARE); for miR-27a: both miRNA target sites and ARE according to the sequence in the HSUR1 viral transcript). Data for chimeric ARE-miRNA targets with other miR-122 target site variants as well as a perfect site are shown in Figure S7A. (B) (A) HuR reaction time course with 5'-³²P-labeled miR-122 (upper part) either in free form or pre-hybridized to a chimeric target containing a natural miRNA target site fused to an ARE or a scrambled, non-binder sequence. (C) HuR tailing and trimming time course of 5'-³²P-miR-122 as free miRNA or pre-hybridized to chimeric targets with a 20 nt or 5 nt spacing between the miRNA and HuR binding sites. (D) Comparison of HuR processing of miR-122 pre-hybridized to a target under conditions where it can/cannot be tailed. Tailing and trimming of 5'-³²P-labeled free miR 122 or miR-122 pre-hybridized to the chimeric 1e-ARE construct by HuR (left panel), using a tailing-protected miR-122 modification (3' nucleotide 3'desoxy 2'OH) (middle panel), or under tailing deficient conditions with HuR₁₂ in absence of ATP (right panel), or Data for HuR₁₂ with ATP are shown in Figure S7C. Of note, the asterisk in the left part denotes a gel artefact, present already at the zero time point (E) Tailing and trimming of 5'-³²P-labeled, Ago2-loaded miR-122 by HuR depending on a mutual HuR-miRNA chimeric target.

4.3.5. HuR modulates miRNA isoforms and levels in HCT116 cells.

To investigate the role of HuR enzymatic activities in cells we used GFP fusions of the wild type HuR, and its double D105A/D254A mutant, constructed by combining two transferase deficient point mutations (see Figures S4D and S4F). In transfected Huh7 cells grown in the presence of amino acids, both wild type and mutant proteins showed predominantly nuclear localization and, alike the endogenous protein (Bhattacharyya et al. 2006), relocalized to the cytoplasm upon amino acid starvation (Figure S8A). Using Renilla luciferase (RL) reporters bearing different region of the CAT1 3'UTR as described previously (Bhattacharyya, et al 2006) we tested effects of wild type and mutant HuR on the starvation-induced derepression of RL activity. Briefly, the RL-catA reporter (Bhattacharyya et al. 2006) contains a full length 3' UTR of CAT-1 with both miR-122 and ARE sites, while RL-catB comprises a truncated 3'UTR lacking the ARE. Each RL reporter is co-expressed with firefly luciferase (FL) reporter present on the same plasmid.

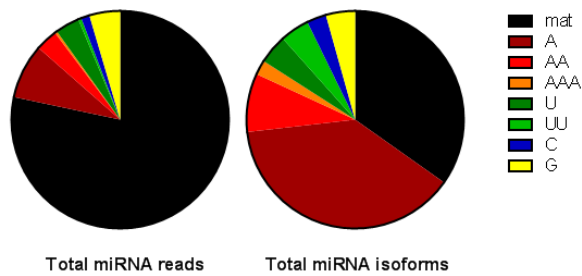
We measured an about 80% derepression of the RL-catA reporter in wild type-HuR-expressing cells upon starvation. This effect was counteracted by MS-444 treatment (Figure

S8B). No derepression was observed for the RL-catB reporter or a control RL reporter containing no CAT1 3'UTR. Overexpression of the tailing deficient HuR D254AD105A mutant strongly downregulated RL-catA expression but had little or no effect on activity of control reporters, consistent with a role of HuR enzymatic activity in antagonize miR-122 *in cis*. Of note, upon amino acid starvation, some degree of derepression of catA by HuR D105AD254A was maintained, possibly mediated by the activity of endogenous HuR..

To analyze the effect of endogenous HuR on miRNA isoforms and their metabolites in a more unbiased manner, we performed deep sequencing analysis of the small RNA population (ca 18-60 nt in length), isolated from control cells and cells in which HuR was knocked down by siRNA (Figure S8C). HCT116 cells were chosen due to their constitutive cytoplasmic localization of HuR (Derech-Haim et al. 2012). No major change was observed in total read numbers of genome-mapped miRNAs between control and HuR knockdown cells (4.35×10^5 vs 4.22×10^5 , respectively). After filtering for read thresholds and statistical criteria (Materials and Methods), relative expression changes were analyzed for all mature miRNAs and their isoforms containing non-genome-encoded extensions. In control cells, A and U extensions were the most common and abundant extensions of full-length mature miRNAs (Figure 5A). Single G and C extensions were less frequent (< 10 or 5 isoforms, respectively) and no longer homopolymeric G and C tails were detected. The scatter dot plots in Figure 5B show relative changes in mature miRNAs and their tailed isoforms in response to HuR knockdown. Subsets of mature miRNAs that increased, decreased or remained unchanged were observed. A specific and statistically significant overall decrease was detected in A-tailed isoforms upon HuR knockdown, which was not the case for any of the other extensions (A and U-extensions in Figure 5B, data not shown for other extensions). Strikingly, we could see an inverted correlation between the length of the A-tail and changes in iso-miR levels upon HuR knockdown (Figure 5B). Figure 5C, lower panel shows relative changes for all individual miRNAs and their isoforms for which we detected >1A extensions. In addition, we also performed Ago2 immunoprecipitations from the same experiment (Figure S8C) and performed an analogous analysis. The data obtained for Ago2-associated miRNAs were very similar to the data obtained for total miRNA (Figure S8D). Taken together, these results are consistent with HuR being responsible for A tailing and turnover of a subset of miRNAs in HCT116 cells.

Figure 5

A



B

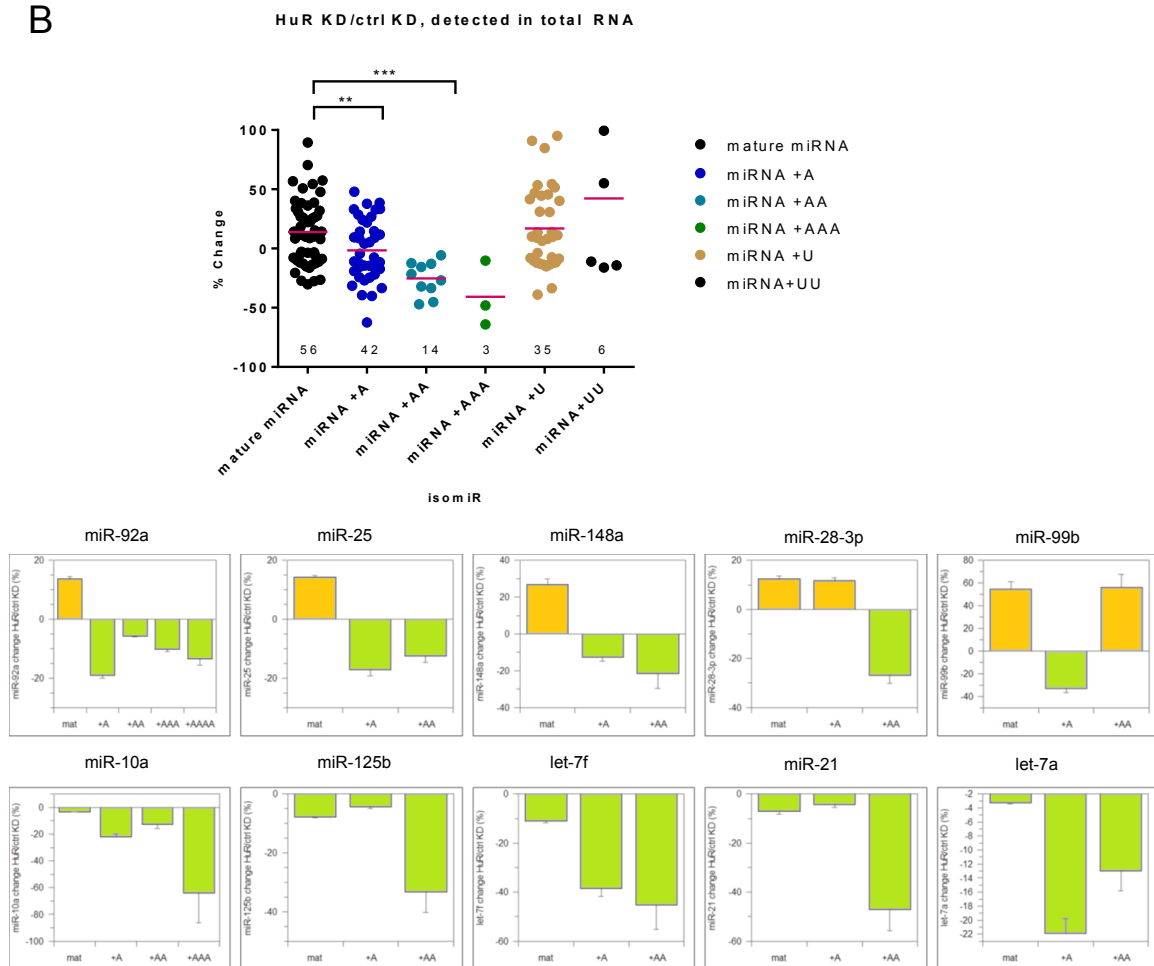


Figure 5. Modulation of microRNA levels and isoforms by enzymatically active HuR in Huh7 and HCT116 cells. (A) Frequency distribution of miRNA isoforms in total miRNA reads (left) and total miRNA isoform counts in HCT116 cells (right). (B) Deep sequencing analysis of mature miRNA and non-genomically-encoded 3'extended isoforms in HCT116 cells upon HuR or control knock down by siRNA (72 h, western blotting data shown in Figure S8C). Upper panel: relative change of mature miRNA levels with and without 3' terminal extensions upon HuR knockdown in the total miRNA population. The total isoform number in each category is indicated. The data is an average of 2 separate experiments, with 3 biological replicates each. Lower panel: relative changes of mature and A-tailed isoforms for the 10 miRNAs for which > 1 A extension was detected.

Figure 6

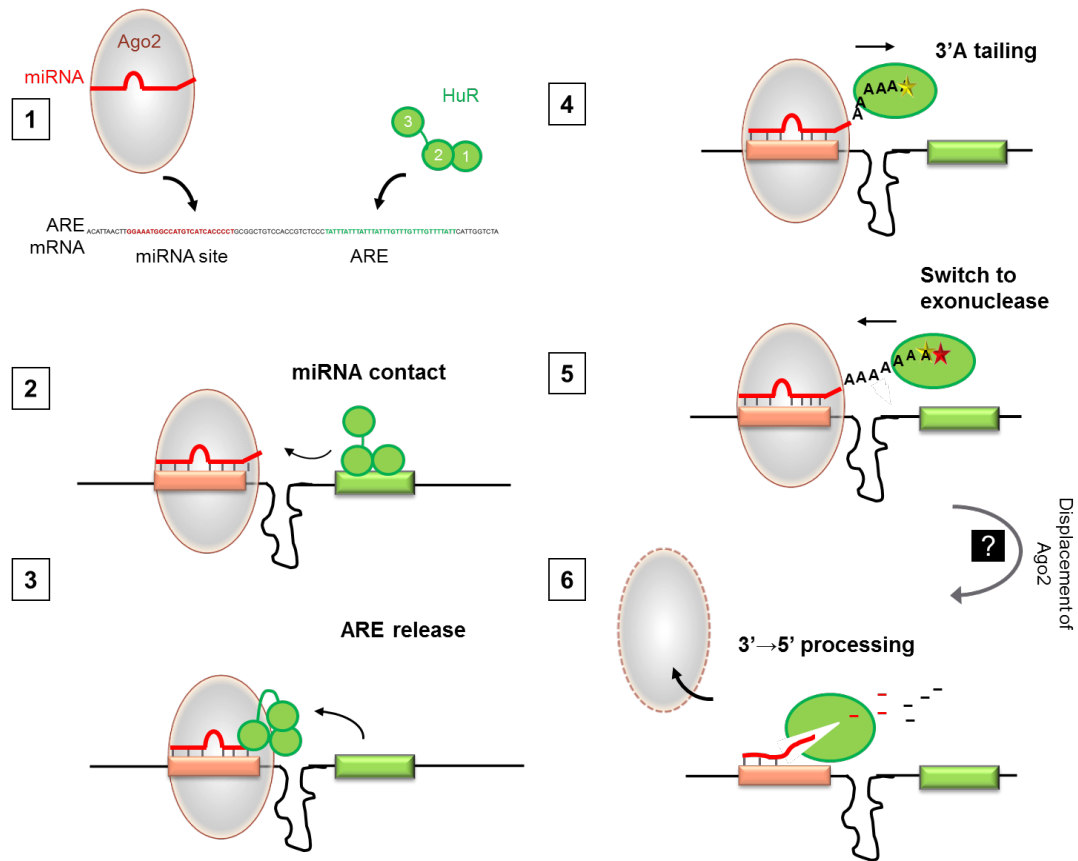


Figure 6. Model for miRNA processing and RISC displacement by HuR on an ARE mRNA. To access the deeply buried and well-shielded guide RNA within the Argonaute protein, sequestered *in cis* but possibly distant on the same message, HuR employs an elaborate mechanism with multiple successive and coordinated steps. Following initial contact of the miRNA 3' end most likely involving RRM3, HuR first adds an A-tail to extend the miRNA out of RISC. Thereby HuR generates itself a primer for its 3'→5' exonuclease activity. Upon release of the ARE and most likely Ago displacement, HuR proceeds to full exonucleolytic turnover of the miRNA thereby relieving the mRNA from repression.

4.4. Discussion

Multiple mechanisms have been proposed for the interplay of HuR with miRISC on a mutual target mRNA, including rearrangement of the mRNA secondary structure to influence miRISC binding (Srikantan et al. 2012), direct competition for overlapping binding sites (Mukherjee et al. 2011) and an HuR oligomerization mediated displacement of miRISC (Kundu et al. 2012). In this work, we discover and propose an alternative mechanism based on HuR-mediated direct enzymatic processing of RISC loaded miRNA.

Our group has previously shown that HuR possesses a 3' terminal adenosyl transferase activity, however neither the physiological RNA substrate nor the biological context was known. In this work, we describe that miRNAs act as a substrate for the HuR enzyme. Moreover, we uncover two HuR- associated, apparently opposing catalytic activities acting on miRNA substrates, a poly(A)-tailing activity cooperating with a second, first-in-class 3'→5' exonuclease activity (trimming). Both catalytic centers reside within the N-terminal part of HuR with the C-terminal RRM3 domain partially contributing to both, ATP and miRNA binding. Both enzymes are Mg²⁺ dependent, and have a preference for single stranded RNA. The transferase displays moderate sequence specificity for miRNA sequences with a GU-rich 3' end which is sufficient but not necessary for HuR to tail a miRNA substrate. An oligo(A)₂₃ was a surprisingly poor transferase but preferred nuclease substrate, suggesting that the exonuclease also possesses some degree of sequence preference.

Given the novelty of this discovery, we carefully tested that both poly(A)polymerase and exonuclease activities represent integral functions of HuR itself rather than being due to contaminating *E. coli* proteins co-purifying with recombinant HuR. In addition, we purified HuR proteins from Baculovirus-infected insect cells, and could verify nuclease and transferase activities of these proteins. High purity of *E.coli* HuR was verified by RP-HPLC and LC-MS/MS analysis where, at attomolar sensitivity, no peptides mapping to either known nucleases or transferases could be detected. Both enzymatic activities co-eluted with the HuR peak in size exclusion chromatography at the expected monomeric molecular weight. Importantly, the activity peaks shifted according to the size differences between HuR and HuR₁₂. After isolating HuR₁₂ under denaturing conditions by preparative RP-HPLC chromatography and refolding of the

denatured protein on a cation exchange column, a considerable fraction of the nuclease activity was recovered and cofractionated with the single peak after the successive chromatographies. Both HuR activities from proteins expressed in E.coli as well as Baculovirus-infected insect cells were inhibited by the HuR targeting inhibitor MS-444; likewise, both activities were inhibited *in trans* by an ARE deoxyoligonucleotide but not its inverse complementary variant. Furthermore, HuR binds directly to ATP as demonstrated by direct visualization of HuR associating to ATP-beads (Meisner et al. 2009) and point mutants of HuR with reduced ATP binding affinity (D254S, D254A) paralleled a reduction in tailing activity. HuR also binds to miRNAs as revealed by the 2D-FIDA-anisotropy data in this study as well as directly by NMR (data not shown). In consequence, should the activities come from a hypothetical contaminating enzyme, then miRNA binding by HuR should compete with the putative contamination and thereby rather have an adverse effect on enzymatic activity. Since inhibition of HuR by MS-444 or ARE however *inhibits* both enzymatic activities such a scenario is inconsistent with the current experimental data.

Interestingly, while ARE oligodeoxynucleotides *in trans* inhibited HuR to process free and target bound miRNA, an ARE sequence present *in cis* with a miRNA binding site allowed HuR to turn over the miRNA bound to a natural imperfect binding site. A miRNA binding site followed by a sequence which is not bound by HuR did not allow turnover of miRNA by HuR to the same extent. In addition, in the presence of such a mutual target, HuR but not micrococcal nuclease, was able to access Ago2-loaded miRNA and, in a tailing-dependent manner, degrade the normally highly protected miRNA which is bound to Argonaute. Very likely this is accompanied by the dissociation of HuR from the ARE prior to tailing and unloading of miRNA from Ago during the exonucleolytic degradation.

Although RISC-loaded miRNAs are deeply buried within Ago with both 5' and 3' ends being associated with specific binding pockets, and have therefore been generally thought to be protected from nuclease attacks, several studies have now shown that enzymatic turnover of miRNAs within miRISC does occur. While the most plausible mechanism is nuclease action following unloading from Argonaute as has been shown (Chatterjee & Grosshans 2009; De et al. 2013), there is evidence that miRNAs can also be accessed within Argonaute by the RNA 3' end modifying enzymes, including uridylases and adenylation (Ameres & Fukunaga 2010; Landgraf et al. 2007). In fact, adenylation and uridylation is being increasingly linked to regulation of

exonucleolytic attack on small RNAs and their precursors (Ibrahim et al. 2010), (Ameres & Fukunaga 2010; Marcinowski et al. 2012). However, “tailing and trimming” has to date been mostly linked to the modification of miRNAs bound to highly complementary artificial targets (Ameres et al. 2010; Marcinowski et al. 2012), (Xie et al. 2012). Here we describe a new mechanism of miRNA turnover within RISC, nucleated on their natural target mRNAs and with tailing facilitating trimming. We propose that initial poly-adenylation by HuR facilitates nuclease attack on miRISC by (i) generating a landing pad for the oligo(A)-philic HuR exonuclease and (ii) potentially also facilitates unloading the miRNA from Ago given that the extended miRNA 3' end may no longer be efficiently bound by the Ago PAZ domain (Han et al. 2011), eventually making the full miRNA body accessible for degradation. Co-existence of both catalytic activities within the same protein rather than in two separate enzymes may offer mechanistic or energetic benefits.

HuR relieves miR-122 mediated repression of the CAT-1 mRNA upon stress-induced translocation of HuR to the cytoplasm (Bhattacharyya, et al. 2006). The effect is thought to be caused by Ago displacement due to weakening of either mRNA-miRNA or Ago2-miRNA interactions (Kundu et al. 2012; Kundu 2011). However, in their system, Bhattacharyya et al do not see an effect on total miR-122 levels upon HuR upregulation of CAT-1 based on Northern blotting (Bhattacharyya et al. 2006). Whether this might be due to the small fraction of miRNA that HuR encounters within Argonaute on the same target message in relation to total levels of miR-122, and/or a more complicated response of balanced miRNA turnover and biogenesis upon stress remains to be addressed. Likewise, in a transcriptome-wide study Lebedeva et al (Lebedeva et al. 2011) reported that HuR knockdown did not have an effect on global miRNA levels in quiescent HeLa cells, hence under conditions where HuR is almost exclusively localized to the nucleus. In contrast, other studies have reported that HuR knockdown and knockout upregulated several miRNAs (Young et al. 2012; Chang et al. 2013). Consistent with this, we observed a moderate global increase (up to 2-fold) of mature miRNAs upon knockdown of HuR in HCT116 cells, which constitutively accumulate HuR in the cytosol. Interestingly, we also observed that miRNA isoforms with increasing number of non-templated A-additions are downregulated more strongly upon HuR knockdown, which was not observed for U additions. These data are consistent with HuR mediating tailing of a subset of miRNAs in HCT116 cells. In addition, we were able to reproduce HuR-mediated relief of repression of a *catA* reporter gene (containing both miRNA and HuR binding sites, (Bhattacharyya, et al. 2006), but not *catB* (lacking

the HuR site) upon overexpression of wild type HuR but not the tailing impaired D105AD254A mutant.

In summary, we reveal a novel mechanism for a cross-talk between miRNAs and HuR on the 3'UTR, which is based on the tailing- and trimming-dependent antagonization of Ago-loaded miRNA by HuR. This mechanism potentially represents a precedent for other factors promoting miRISC turnover. The finding of two novel, coupled enzymatic activities in RRM-domain-containing RNA binding protein raises a possibility that also other RRM proteins are enzymatically active and has thereby important implications for the interplay of post-transcriptional factors at the mRNA 3'UTR to fine tune gene expression. However we are aware of certain shortcomings of the work. Fully convincing demonstration that nuclease activity is indeed an intrinsic property of HuR will require mapping of the catalytic site and identification of a HuR mutant devoid of nuclease activity.

4.5. Materials and methods

The recipes for all buffers can be found in Appendix I

4.5.1. Recombinant protein preparation

4.5.1.1. HuR site directed mutagenesis and E.coli expression and protein purification

Coding sequence for human HuR (Genebank accession number NM_00141, ELAVL1, ELAV (embryonic lethal, abnormal vision, Drosophila)-like 1 (Hu antigen R) [Homo sapiens (human)])

```
ATGTCTAATGGTTATGAAGACCACATGGCCGAAGACTGCAGGGGTGACATCGGGAGAACGAATTTGATC
GTCAACTACCTCCCTCAGAACATGACCCAGGATGAGTTACGAAGCCTGTTTCAGCAGCATTGGTGAAGTTG
AATCTGCAAACTTATTCGGGATAAAGTAGCAGGACACAGCTTGGGCTATGGCTTTGTGAACTACGTGAC
CGCGAAGGATGCAGAGAGAGCGATCAACACGCTGAACGGCTTGAGGCTCCAGTCAAAAACCATTAAGG
TGTCGTATGCTCGCCGAGCTCAGAGGTGATCAAAGACGCCAACTTGACATCAGCGGGCTCCCGCGGA
CCATGACCCAGAAGGACGTAGAAGACATGTTCTCTCGGTTTGGGCGGATCATCAACTCGCGGGTCTCTGT
GGATCAGACTACAGTTTGTCCAGAGGGTTGCGTTTATCCGGTTTGACAAACGGTTCGGAGGCAGAAGA
GGCAATTACCAGTTTCAATGGTCATAAACCCCAAGTTCCCTCTGAGCCATCACAGTGAAGTTTGCAGCC
AACCCCAACCAGAACAAAACGTGGCACTCCTCTCGCAGCTGTACCACTCGCCAGCGCGACGGTTCGGA
GGCCCCGTTACCACCAGGCGCAGAGATTAGGTTCTCCCCATGGGCGTTCGATCACATGAGCGGGCTCT
CTGGCGTCAACGTGCCAGGAAACGCCTCCTCCGGCTGGTGCATTTTCATCTACAACCTGGGGCAGGATGC
CGACGAGGGGATCCTCTGGCAGATGTTTGGGCCGTTTGGCGCCGTCACCAATGTGAAAGTGATCCGCGA
CTTCAACACCAACAAGTGCAAAGGGTTTGGCTTTGTGACCATGACAAACTATGAAGAAGCCGCGATGGC
CATAGCCAGCCTGAACGGCTACCGCCTGGGGGACAAAATCTTACAGGTTTCCTTCAAAAACCAACAAGTCC
CACAAA
```

HuR amino acid sequence of the protein (Uniprot), sp|Q15717|aa2-326

```
SNGYEDHMAEDCRGDIGRTNLIVNYLPQNMNQDELRLSIFSSIGEVESAKLIRDKVAGHSLGYGFVNYVTAKDA
ERAINLNLRLQSKTIKVSYPSPSEVIKDANLYISGLPRTMTQKDVEDMFSRFGRIINSRVLVDQTTGLSRGV
```

AFIRFDKRSEAEAAITSFNGHKPPGSSEPITVKFAANPNQNKNVALLSPLYHSPARRFGGPVHHQAQRFRFSP
MGVDHMSGLSGVNVPGNASSGWCIFIYNLGQDADEGILWQMFGPFGAVTNVKVIRDFNTNKCKGFGFVT
MTNYEEAAMAIAASLNGYRLGDKILQVSFKTNKSHK

The HuR (HuR₁₂) CDS had been cloned into the pTXB1 (pTWIN, both from the IMPACT™-CN system, New England BioLabs) vector, at NdeI/SapI sites, to allow for C-terminal fusion with an intein-chitin binding domain (intein-CBD). This system has the advantage to generate fusion proteins in which the affinity tag can be self-cleaved to generate a native terminus without amino acid additions, mediated by thiol induced self-splicing of the intein protein tag (Figure M2A).

Site directed mutagenesis was used to introduce point mutations resulting in the following amino acid exchanges: D254 to A (Figure M1, via PCR-driven overlap extension with primer sequences in Table M1), D105 to A (QuikChange® Site-Directed Mutagenesis Kit, according to the manufacturer's protocol).

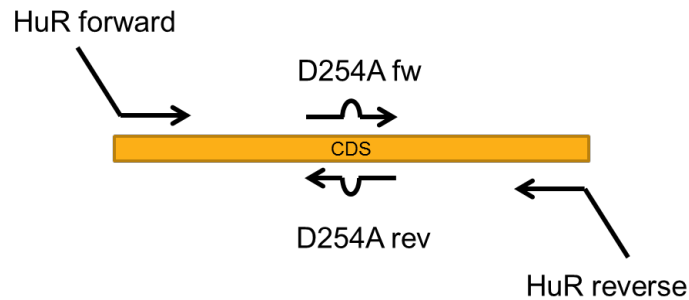


Figure M1. Site-directed mutagenesis performed by PCR-driven overlap extension

Primer	Sequence (5'-3')
HuR-forward	GGAGGAGGAGG CATATG TCTAATGGTTATGAAGACCACAT
HuR-reverse	AAATAAT GCTCTTCC GCAATTTGTGGGACTTGTGGTTTTG
D254A_fw	GCAG GCG GCCGACGAGGGGATCCTCTG
D254A_rev	GATCCCTCGTCGG C CGCTGCCCCAGGTTGTAGATGAAAATGC
Quikchange primer	
D105A_fw	GAGGTGATCAA GCG GCCAACCTGTAC
D105A_rev	GTACAAGTTGG C CGCTTTGATCACCTC

Table M1, PCR primers, Restriction enzyme sites used for cloning are shown bold. Point mutation sites are shown in red.

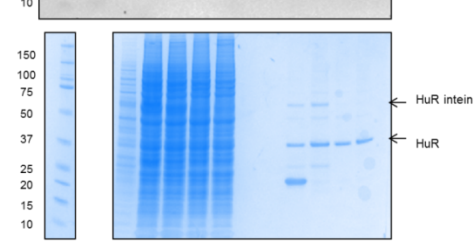
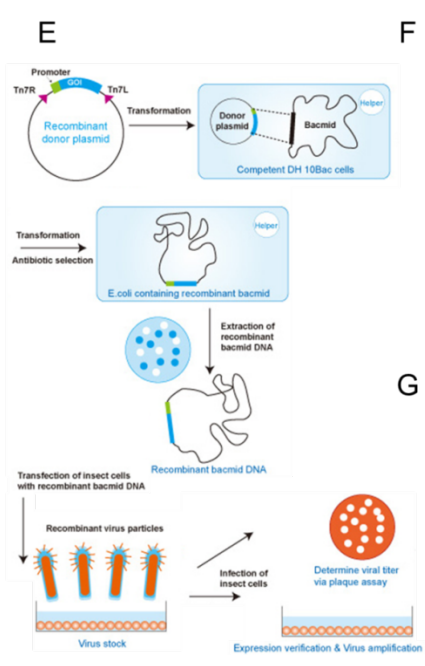
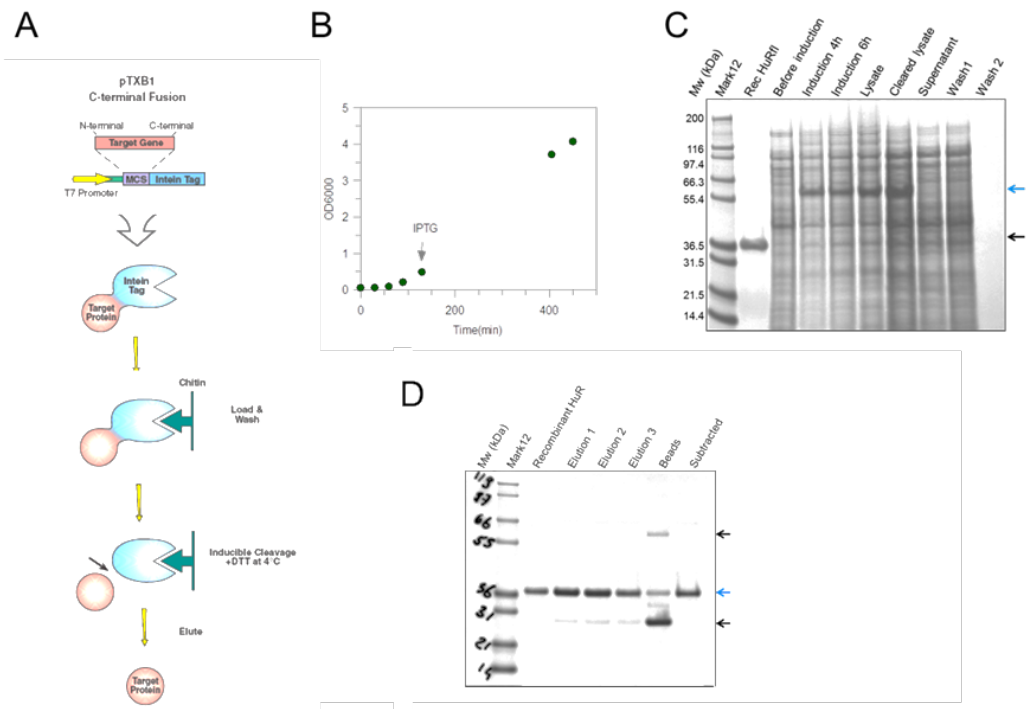
The PCR products were purified via the Qiaquick PCR purification kit (Qiagen). The second PCR reaction was performed with the outer forward and reverse primers (HuR-forward and HuR-reverse), and with the two annealed PCR products as templates. The PCR reaction setup was analogous to the previous one, and the PCR product was again purified with Qiaquick PCR purification kit. The product size and quality is monitored on a 1 % agarose gel.

400 ng of PCR product was then digested with SapI for 3 h at 37 °C before adding 25 U of NdeI for another 1 h. After each digestion the enzyme was inactivated for 20 min at 60 °C to minimize cross reactivity. Digestion with NdeI and SapI is performed sequentially to ensure optimal performance. As a control, the pTXBI-HuR vector was digested as well, and subsequently dephosphorylated by the addition of 3 units of Shrimp Alkaline Phosphatase (SAP) for 2 h at 37 °C. Both the vector backbone and the PCR products were column purified as previously described and ligated overnight at a 1:25 (backbone: insert) ratio at 16 °C.

The ligation was added to a frozen sample of chemically competent E.coli TOP10 cells (One Shot, Invitrogen) and the mixture was incubated on ice for 30 min to thaw and mix slowly. The bacteria were heat shocked for at 42 °C for 30 s, incubated on ice for 2 min, after which 250 µl of complete S.O.C. (all mediums defined in Appendix I) medium was added. The transformed cells were grown in suspension culture with 350 rpm shaking at 37 °C for 1 h. The entire volume was plated out on LB-agar plates containing 100 µg/ml Ampicilin (Sigma) and incubated overnight at 37 °C. The resulting colonies were inoculated into 5 ml LB medium (Luria-Bertani) containing 100 µg/ml ampicillin, and grown overnight (ON) at 37 °C with gentle shaking (150 rpm). In addition, a sample for colony PCR was taken (the tip of the inoculation loop that was used to inoculate the samples was placed in 30 µl DNase free water) for a preliminary PCR to test for the presence of the plasmid/insert.

DNA was isolated from 4 ml overnight culture using the Qiagen plasmid mini kit, and amplified using the HuR forward and HuR reverse primer to verify the presence of the insert. The DNA that tested positive for the insert was sequenced by Sanger-sequencing on Applied Biosystem 96-capillary array sequencers (ABI3730xl) and all sequences were analyzed using ContigExpress / Vector NTI.

For HuR, HuR₁₂, and point mutant protein expression, CaCl₂-competent ER2566 E.coli (protease deficient strain, New England BioLabs) were transformed with 250 ng either pTWIN-HuR₁₂-intein, or the pTXB1 vector carrying the Intein-fused wild type HuR, or the D254A and D105 point mutant, and plated on Amp-100 LB-agar plates. The fresh transformation was imperative to ensure high expression of the recombinant fusion protein. After the overnight incubation at 37 °C, a single colony from the transformation was inoculated into 5 ml LB medium containing 100 µg/ml ampicillin to grow an overnight culture, which was then further diluted to grow a 150 ml starter culture. The overnight OD₆₀₀ of the starter culture is expected to be 3-4 OD₆₀₀. The expression culture was inoculated to OD₆₀₀ = 0.05 in into pre-warmed LB medium containing 50 µg/ml ampicillin, and grown at 200 rpm, 37 °C. At OD₆₀₀ = 0.5, the temperature was lowered to 28°C, and the expression of the fusion proteins was induced with 1 mM IPTG for 6 h. 30 min after induction, 500 µl Glanapon was added per 500 ml culture to prevent foaming (Figure M2B). Protein expression was tested by a denaturing, non-reducing SDS-PAGE of aliquots taken immediately before induction, during expression, and immediately before harvesting (Figure M2C).



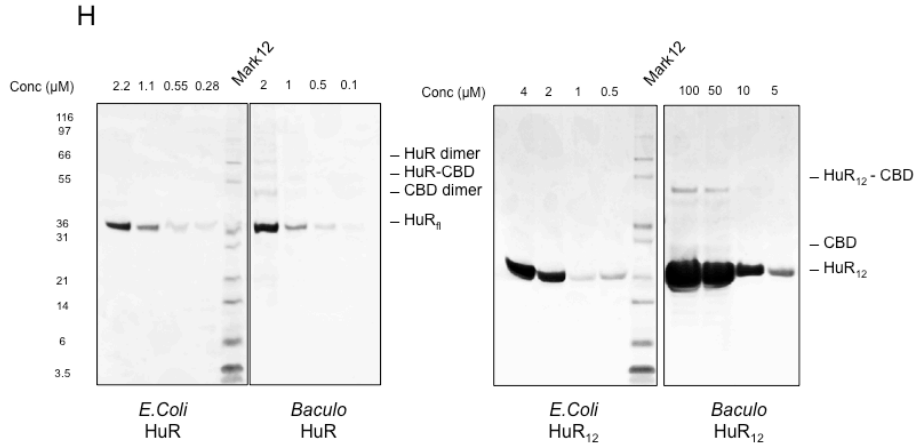


Figure M2. HuR expression and purification via the IMPACT system (New England BioLabs). (A) Modified schematic of protein expression and purification via the impact system (B) *E. coli* ER2566 growth curve during HuR protein expression. The overnight culture is inoculated into warm LB Ampicillin-50 medium at OD_{600} 0.05. Growth is monitored every 30 min until OD_{600} reaches 0.5, at which point the protein expression is induced by 1 mM IPTG for further 4-6 h. (C) Expression and purification of HuR was monitored at each step by analyzing the samples on a non-reducing SDS-PAGE with coomassie (C) or silver staining (D). 4 h and 6 h after induction with 1 mM IPTG, the HuR-intein-CBD band becomes visible at 63 kDa – black arrow (Mw HuR = 36k Da, Mw Intein-CBD tag = 27k Da,). Recombinant HuR is indicated by a blue arrow at 36 kDa. Equal cell amounts were loaded in each lane. The bacteria is collected by mild centrifugation and lysed in a triton-containing buffer (lysate), and the lysate is cleared by ultra-centrifugation (cleared lysate). HuR-intein was captured onto pre-equilibrated chitin beads during a 6 h incubation at 4 °C (supernatant), and the beads are extensively washed (wash 1 and wash 2). Black arrow – recombinant HuR. Blue arrow – HuR-intein CBD fusion protein (D) The protein is recovered from the chitin resin by thiol-induced Intein splicing with 50 mM 2-MESNA for 16 h at 4 °C (elution 1, HuR at 36k Da, blue arrow). To maximize protein recovery, the elution step can be repeated several times in a smaller volume for 1 h (elution 2 and 3). The elutions are pooled, and a subtractive step is performed by repeated incubation with chitin beads to eliminate uncleaved fusion protein, as well as the cleaved Intein-CBD tag (in lanes elution 1-3, beads, 63k Da and 27k Da, black arrows). The resulting HuR in the purified fraction (subtracted) is indicated by a blue arrow. (E) Modified schematic of the Baculo expression system. (F) Western blot analysis of purification of Baculo expressed HuR_{fi} . Abbreviations: CL- cleared lysate, NB- non-bound, W1- washing step 1, E- elution, S- after subtractive step. FF- flash frozen, D- dounce homogenized. See text for detailed purification protocol (G) Coomassie staining of the fractions in Figure M2F. (H) Coomassie staining of Baculo-purified compared to *E. coli* HuR_{fi} (right panel) and HuR_{12} (left panel) proteins. A dilution series of the *E. coli* proteins on the left of each gel is compared to the sequential concentration of the Baculo HuR proteins by centriprep centrifugal concentrators (Centriprep, 10 kDa cutoff) on the right. The concentrations of Baculo HuR protein are approximate, due to the high level of precipitation of HuR upon concentration.

The culture was harvested at 3,000 rpm for 30 -60 min at 4 °C. The pellet was then stored at -80 °C for a short time to preserve enzymatic activity.

The bacterial cells were resuspended in HuR lysis/washing buffer with Triton x-100 (120 ml per 3 L) bacterial culture and lysed by 3 successive cycles of shock freezing in liquid nitrogen and gentle thawing. 5 mM MgCl₂ was added for 30 min of DNase treatment (5 U) at room temperature, which was then stopped by the addition of EDTA to the final concentration of 6 mM. The lysates were cleared by centrifugation (10,000 g, 4 °C, 30 min), and the pellet disposed. All subsequent steps were done on ice, with pre-cooled buffers.

The fusion protein (HuR-Intein-CBD) was captured from the cleared lysate by incubation for 4 h with chitin agarose beads (New England Biolabs), pre-equilibrated with 500 ml lysis buffer containing 0.2 % (v/v) Triton X-100 on a size 2 filter-funnel, 50 ml slurry per 3 L fermentation. After extensive washing with the high salt HuR lysis/washing buffer (2 L with and 2 L without Triton x-100), the recombinant protein was recovered by thiol-induced self-splicing of the intein tag with MESNA (2-mercaptoethanesulfonic acid, sodium salt, 50 mM in HuR lysis/washing buffer without Triton-X-100) for 16 h at 4 °C (Figure M2D). In order to keep the protein soluble, 0.2 % (w/v) Pluronic-F-127 (Invitrogen) was added to the HuR full length preparation. Of note, HuR₁₂ was purified an analogous manner; however it does not tolerate Pluronic in the elution medium¹. Any co-eluted intein tag and uncleaved fusion protein was then captured and removed from the eluate in one to two subtractive affinity steps with 15 ml buffer equilibrated chitin agarose bead slurry (1 h, 4 °C). The full length protein was found to preserve its activity when stored for several days at 4 °C in the high salt buffer. Alternatively, the protein was shock-frozen and stored at -80 °C which retained activity for at least one year. HuR₁₂ was found to preserve full activity when stored for up to several weeks at 4 °C in the high-salt buffer as well as upon storage following shock-freezing.

4.5.1.2. Expression of HuR in the Baculo expression system and purification

HuR and HuR₁₂ Intein-CDB fusion genes were PCR amplified from the pTXB1 and pTWIN vectors, respectively (described in section 4.5.1.1.), and inserted into compatible HindIII/NotI restriction sites in the pFastBac1 plasmid. 200 ng of the plasmid is transformed into a DH10Bac competent *E.coli* strain (Invitrogen) where a homologous site-specific recombination takes place. The foreign genes are incorporated such as to disrupt the lacZ sequence in the bacmid, rendering the

positive colonies white in the presence of X-gal in the substrate. In addition, the positive colonies are selected for kanamycin, tetracycline and gentamycin resistance. Positive colonies are inoculated into 35 ml medium complemented with 50 µg/ml kanamycin, 10 µg/ml tetracycline and 7 µg/ml gentamycin, grown at 37°C, and the bacmid is isolated using the EPlmotion with the 5 Prime Perfectprep BAC 96 kit.

For bacmid transfection and generation of viral particles with the incorporated bacmid, 30 million Sf21 cells are resuspended in 10ml fresh Ex-cell420 medium supplemented with 1 % FCS and 1 % glutamine. The transfection mix, consisting of 200 µl Ex-CELL420 SFM and 4 µg purified bacmid is transfected into 3 million SF-21 insect cells using 15 µl Superfect (Qiagen). This leads to the generation of recombinant baculovirus particles that can be amplified and stored as BIIIC (Baculovirus Infected Insect Cell) stocks at -80°C. The BIIICs are used to infect SF-21 cells which will produce the recombinant protein when grown in SF-4 BaculoExpress ICM medium (Bioconcept) in the presence of IPTG and 10 µM E-64 proteinase inhibitor with shaking at 90 rpm. The recombinant proteins are visible in the cellular fraction (not secreted) after 48 h, with a peak of expression at 72 h.

500 ml of baculo cells expressing HuR_{fl}-Intein-CBD and HuR₁₂-Intein-CBD are centrifuged at 3000 g for 30 min. The pellet can be kept at -80°C for several days without a loss in activity of the purified protein. The pellet is resuspended in 40 ml HuR lysis/washing buffer with Triton x-100, and the cells are lysed either through 6 strokes with a dounce homogenizer, or by 3 freeze-thaw cycles in liquid nitrogen, and the purification is carried out analogous to the purification of HuR from *E.coli*.

4.5.1.3. Recombinant Ago2

Purified Ago2 was kindly provided by Andrea Gerber and Marion Mahnke (Novartis PPE/NBC), purified from Baculovirus transformed Sf9 cells as a His6-tagged protein with a TEV protease cleavage site (pFastBac-HTA-L21-hAgo2 (MacRae et al. 2008)) using the following protocol: The frozen Sf9 cell pellet was thawed in 500 ml Sf9 lysis. The cells were lysed by 7 strokes in a 40mL glass Dounce homogenizer, and the lysate was cleared by centrifugation at 10,000 g for 30 min at 4 °C. The supernatant was again cleared by filtration (Millipore Opticap 4; 0.22 µm) and applied to a freshly packed 5 ml Ni-NTA Superflow column at 1 ml/min overnight. After baseline washing with Sf9 buffer A, bound material was eluted with Sf9 buffer B at 4°C for 36 h). Dialyzed

material was cleared by sterile filtration and analyzed by RP-HPLC (for concentration determination) and SDS-PAGE. The purified protein was stored at -80 °C in 50 mM NaH₂PO₄/300 mM NaCl, pH 7.8, 0.5 mM TCEP.

4.5.1.4. HuR-GFP expression constructs

To generate the HuR-EGFP (as well as HuR₁₂-GFP, HuR D254A-GFP, HuR D105AD254A-GFP) mammalian expression constructs, a vector modified from pSecTagA (Life technologies) was used with the EGFP gene inserted into the BstBI-Xho sites. The respective HuR sequence was then PCR amplified using the pTXB1-HuR D254A, pTXB1-HuR D105AD254A) or pTWIN1-HuR₁₂ vectors as a template, and inserted upstream and in frame with the EGFP CDS into NheI-BstBI sites of pSecTag2-EGFP. Expression from this vector is driven from the CMV promoter and yields an HuR protein as a C-terminal fusion with EGFP, a myc and a His₆ solubility tag.

4.5.2. SDS-PAGE, western blotting, RP-HPLC and LC-MS proteomics.

SDS-PAGE analysis: Protein samples were denatured in 1 x NuPAGE LDS sample buffer (Invitrogen) for 5 min, at 95 °C under non-reducing conditions and run on a 4-12 % (w/v) Bis-Tris NuPAGE gel in MES buffer (or MOPS for proteins >50 kDa) for 35 (50) min at 200 V. If run under reducing conditions, 50 mM (DTT) was added to the sample, and 500 µl NuPAGE Antioxidant (Invitrogen) to the running buffer.

For Coomassie staining, the protein gels were washed in deionized water, stained with the Imperial Protein stain (Thermo Scientific) for 60 min at room temperature and then destained by washing several times in deionized water for at least 2 h.

Western blot analysis: The proteins were transferred onto a Nitrocellulose Hybond ECLs membrane (GE healthcare) by standard semi-dry blotting in 1 x NuPAGE Transfer buffer (Invitrogen), supplemented with 20 % (v/v) methanol, at 30 V (constant current) for 1-2 h, depending on protein size (180-220 mA per gel). The membrane was blocked for 1 h in blocking buffer. HuR was detected with mouse monoclonal anti-human HuR antibody raised against the N-terminus of HuR (19F12, IgG1, Molecular probes) at 1 µg/ml in blocking buffer for 16 h at 4 °C (protocol modified from (Meisner et al. 2007)). Ago2 and tubulin were detected by Ago2 (11A9, Ascension), and Tubulin (B-7, Santa Cruz), respectively.

Pierce Goat anti-mouse (for HuR and Tubulin) or anti-rat (for Ago2) IgG (H+L) Cross Adsorbed Secondary Antibody, HRP conjugate was used as a secondary antibody (1:5000 dilution in blocking buffer, 1 h incubation, at room temperature). The Precision Plus Protein WesternC standard (Biorad) was used and visualized by the addition of StrepTactin-HRP conjugate to the secondary antibody preparation at a final dilution of 1:25,000. Proteins were visualized on a Biorad XRS system.

Silver staining was performed with the SilverXpress Silver Staining Kit (Invitrogen), according to the manufacturer's protocol.

Bradford assay: Total protein concentration was determined using a commercially available Bradford assay (Biorad). According to the manufacturer's protocol, 5 μ l of protein was added to 495 μ l of PBS, before incubating the mixture for 5 min at room temperature with 100 μ l of the Dye reagent concentrate (Biorad). The absorbance at 595 nm was measured in triplicates in clear 96-well plates using the Spectramax Microplate reader. The protein concentration was determined based on a BSA (Pierce) calibration curve between 0 and 2000 ng/ μ l

RP-HPLC analysis: The concentration of HuR and HuR₁₂, D254A and D105A was determined by quantitative RP-HPLC based on a BSA calibration curve from 0 μ M to 5 μ M on an Agilent 110 ChemStation 1100 instrument. The machine is equipped with a UV and a fluorescence detector. Protein samples at concentrations from 100 nM to 10 μ M were injected onto a Poros[®] reversed phase column (C8, 4.6mm x 150mm, 5 μ m, 300 Å). The column was run at a constant flow of 0.5 ml/min with a gradient from Solvent A (5 % CH₃CN, 0.1 % TFA in water) to Solvent B (95 % CH₃CN, 0.1 % TFA) using the following program settings: 0 % B for 20 min, 5 % B for 5 min, gradient from 5 to 100 % B within 40 min, 100 % B for 5 min. UV absorption was detected at 210, 260 and 280 nm, protein fluorescence was monitored with an excitation of 280 nm and an emission of 340 nm. The protein was quantified in the Agilent Chemstation software based on the integration of peak areas for the BSA standard curve and HuR proteins. These values were transformed into molar protein concentrations using a linear equation derived from the standard curve, and corrected for the differences in 280 nm extinction coefficient between HuR/HuR₁₂ and BSA (HuR 25,900 M⁻¹ cm⁻¹, HuR₁₂ 8,940 M⁻¹ cm⁻¹, BSA 39,602 M⁻¹ cm⁻¹)

LC-MS/MS analysis: Recombinant HuR proteins were separated on a 4-12 % bis-tris NuPAGE protein gel. Each lane was cut horizontally into 24 pieces, which were digested with modified

porcine trypsin (Promega, Madison WI, USA) as described (Shevchenko et al. 1996) in a microtiter plate format (CB080, Thermo/Proxeon, Odense, DK). After overnight digestion at 37 °C, peptides were eluted into a second microtiter plate with 5 % (v/v) formic acid and dried before analysis by LC-MS.

For LC-MS/MS, the peptides mixtures were separated on a 15 cm x 75 µm ProteoPep 2 PicoFrit column (New Objectives), connected to an LTQ-Orbitrap Elite mass spectrometer (Thermo). Buffer A consisted of H₂O with 0.1 % formic acid and Buffer B of 100 % acetonitrile with 0.1 % formic acid. Peptides were separated using a 120 min gradient from 2 % B to 40 % B. Data acquisition was done using a “Top 15 method”, where every full MS scan was followed by 15 data-dependent scans on the 15 most intense ions from the parent scan. These 15 most abundant peptides were ignored by the detection algorithm for 30 s. The next 15 most abundant peptides were then identified etc. This ensures high sensitivity of the method. Full scans were performed in the Orbitrap at 120'000 resolution with target values of 1E6 ions and 200 ms injection time, while MS-MS scans were done in the ion trap with 1E4 ions and 200 ms. Database searches were performed with the Mascot Server using the human IPI database (version 3.87). Mass tolerances were set at 10 ppm for the full MS scans and at 0.8 Da for MS-MS. Search results were validated using Scaffold (Proteome Software) and protein identifications accepted when at least two unique peptides were detected with >95 % confidence (peptide FDR 1 %, protein FDR 0 %).

4.5.3. miRNA 5' labeling

5' labeling: 500 nM synthetic miRNA was labeled following a standard labeling protocol using T4 Polynucleotide Kinase (PNK, New England BioLabs) with 100 nM [γ -³²P]-ATP, 0.2 U/µl PNK in 1x PNK buffer for 60 min at 37 °C. The enzyme was inactivated for 20 min at 60 °C, and the unincorporated ATP was eliminated via NucAway spin columns (Ambion)

4.5.4. Preparation of miRNA-HuR targets by *in vitro* transcription

The DNA templates containing a T7 promoter were synthesized and amplified by overlap PCR (reaction setup in Table M2, sequences of chimeric RNA and the corresponding primers Table M3), and purified using a Qiaquick PCR reaction purification kit to remove salts and unincorporated nucleotides. For *in vitro* transcription, 40 ng template DNA was added to 1 x buffer, 30 mM NTPs, and the T7 enzyme mix in the *in vitro* transcription reaction (Megashortscript, Ambion). The reaction was performed for > 6 h at 37 °C, followed by a 20 min DNA digestion. The RNA product was purified by TRIzol® extraction or by ethanol precipitation followed by NucAway column purification (Ambion). The RNA quality and concentration was determined based on UV absorption spectra measured on a NanoDrop spectrophotometer, as well as based on TBE-urea PAGE.

A	Reagent	Concentration	Volume	Cycling parameter	Temperature	Time	Cycles
	Master mix Phusion	2x	25 µl	Initial denauration	98 °C	30 s	1
Fw primer	10 µM	10 µl	Denaturation	98 °C	10 s	30	
Rev primer	10 µM	10 µl	Annealing	60 °C	15 s		
H2O		ad 50 µl	Extension	72 °C	15 s		
			Final extension	72 °C	5 s	1	

B Megashortscript <i>in vitro</i> transcription		
Reaction buffer	10x	4 µl
NTPs	75 mM	16 µl
Enzyme mix		4 µl
Template, max	up to 40 ng/µl	ad 40 µl

Table M2. (A) PCR preparation of templates for *in vitro* transcription and Phusion® PCR cycling program (B) Megashortscript™ *in vitro* transcription

Short target sites miR-122 (5'-3')	
hs-CAT1-1e	GGAAAUGGCCAUGUCAUCACCCCU
hs-CAT1-perf	CAAACACCAUUGUCACACUCCA
Chimeric target sites for miR-122 (5'-3')	
ARE-1e (ARE 5')	ACCGUCUCCCUAUUUUUAUUUUAUUUGUUUGUUUGUUUUUAUUCAUUGGUCUAA CAUUAACUU GGAAAUGGCCAUGUCAUCACCCCU GCGGCUGUCC
1d-ARE	AAAUCAAUCC ACAGUCCAUGAAAUGUGACACUCCACC CAGAUUAAGUACCGUCUC CCU AUUUUUAUUUUAUUUGUUUGUUUGUUUUUAUUCAUUGGUCUA
1e-ARE (ARE 3')	ACAUUAACUU GGAAAUGGCCAUGUCAUCACCCCU GCGGCUGUCCACCGUCUCCC UAUUUUAUUUUAUUUGUUUGUUUGUUUUUAUUCAUUGGUCUA
1e-nonbinder	TAATACGACTCACTATAGGGACATTAACCTT GGAAATGGCCATGTCATCACCCCT GCG GCTGTCCACCGTCTCCCT TAGAGTCATCGCAATTGCACCTAGAGTCATCGCATTGGT CTA
1f-ARE	GGGGCCUGCG GCCAGCACCAUUUCACACACUCCU UGUAGAUGGGACCGUCUC CCU AUUUUUAUUUUAUUUGUUUGUUUGUUUUUAUUCAUUGGUCUA
perf-ARE	GGGGCCUGCG CAAACACCAUUGUCACACUCC AUGUAGAUGGGACCGUCUCCC UA UUUUAUUUUAUUUGUUUGUUUGUUUUUAUUCAUUGGUCUA
Primer pairs for synthesis of chimeric target sites for miR-122	
fw T7 ARE-1e	TAATACGACTCACTATAGGGACCGTCTCCCTATTTATTTATTTATTTGTTTGTGTTTT ATTCATTGGTCTAAATCAATCC
rev ARE-1e	GGACAGCCGCAGGGGTGATGACATGGCCATTCCAAGTAAATGTTAGACCAATGAAT AAAAC
fw T7-1d-ARE	TAATACGACTCACTATAGGGAAATCAATCCACAGTCCATGAAATTGTGACTCCACC AGATTAAGTACCGTCTCCC
rev 1d-ARE	TAGACCAATGAATAAACAACAAACAATAAATAAATAAATAGGGAGACGGTACTTA ATCTGGTGGAG
fw T7 1e-ARE	TAATACGACTCACTATAGGGACATTAACCTTGGAAATGGCCATGTCATCACCCCTGCG GCTGTCC
rev 1e-ARE	TAGACCAATGAATAAACAACAAACAATAAATAAATAAATAGGGAGACGGTGGACA GCCGCAGGGGTGATGACATG
fw T7 1f-ARE	TAATACGACTCACTATAGGGGGGGCTGCGCCAGCACCATTTACACACACTCCTT GTAGATG
rev 1f-ARE	TAGACCAATGAATAAACAACAAACAATAAATAAATAAATAGGGAGACGGTCCCAT CTACAAGGAGTGTGTGAAAT
fw T7 perf-ARE	TAATACGACTCACTATAGGGGGGGCTGCGCAAACACCATTGCACACTCCATGTAG ATGGGACCGTCTCCCTA
rev perf-ARE	TAGACCAATGAATAAACAACAAACAATAAATAAATAAATAGGGAGACGGTCCCAT CTACATGGAG
Short target sites miR-27a (5'-3')	
HSUR-1 miR-27a target	CUGGAACUUAUUAUCUGUGAU
miR-27a perf	GCGGAACUUAAGCCACUGUGAA
miR-27a HSUR target RNA (5'-3')	
HSUR	ACACUACUAUUUUAUUUUAUUUCUUA GUAAUGUUUA CUGGAACUUAUAUCUG UGAU AACCUAAACUAAAAGUCUAAACAACCCGUUACUUGCUGACC AAUUUUUGU AGGUACUGGGUGUAAAUUGAUGACCGGUACCA
Primer pairs for synthesis of miR-27a target RNA	
fw HSUR	TAATACGACTCACTATAGGGACACTACATATTTATTTATTTCTTAGTAATGTTTAC TGGAACTTAAATCTGTGATAACCTAAACTAAAAGTCTC
rev HSUR	TGGTACCGGTCATCATATTTACACCCAGTACCTACAAAAATTGGTCAGCAAGTAACG GGTTGTTTGAAGCTTTTAGTTTAGGTTATCACAG

Table M3. Sequences of primers for overlap-PCR driven synthesis of short and chimeric miR-122 and miR-27a target sites. HuR IL-1 β ARE binding site indicated in green. miRNA sites indicated in red.

4.5.5. HuR-RNA binding experiments

Recombinant human HuR protein was titrated in 11 steps against a constant concentration of 1 nM of 5'-P-(6-carboxytetramethylrhodamine) (TMR) fluorescently labeled RNA, which translates to approximately one molecule of labeled RNA in the confocal volume. Complex formation with

5' TMR RNA was monitored under equilibrium conditions by determination of the increase in fluorescence anisotropy with 2D-FIDA (Kask et al. 2000). The samples were incubated for at least 10 min at room temperature before measurement. Measurements were performed in 96-well glass bottom microtiter plates (Whatman) on an Evotec Clarina instrument (excitation path: HeNe 543 nm laser and polarization filter; 560 nm dichroic mirror, Emission path: 590/60 nm long pass filter and polarization filter; 50 μm pinhole). Fluorescence was recorded on single photon sensitive avalanche photo diodes. A 0.5 nM solution of TMR was used for the adjustment of the focus, optical fibers and pinhole, as well as for the calculation of the G-factor. 10 measurements of 10 s were performed per sample. Anisotropy was calculated according to the equation in Figure M3, panel (I). The dissociation constant (K_d) was determined by nonlinear curve fitting of the anisotropy data based on the equation in Figure M3, panel (II) using Grafit (version 7.0.2) (Meisner et al. 2004). The anisotropy data was additionally converted to fraction HuR-bound RNA according to the equation in Figure M3, panel (III)

$$(I) \quad r = \frac{q_{\parallel} - G^*q_{\perp}}{q_{\parallel} + 2G^*q_{\perp}}$$

$$(II) \quad K_d = \frac{[\text{RNA}_{\text{free}}][\text{HuR}_0] - [\text{RNA} \cdot \text{HuR}]}{[\text{RNA} \cdot \text{HuR}]}$$

$$(III) \quad \text{Fraction bound} = \frac{(r - r_{\text{min}})}{(r - r_{\text{min}}) + Q(r_{\text{max}} - r)}$$

$$(IV) \quad Q = \frac{q_{\text{totmin}}}{q_{\text{totmax}}}$$

$$(V) \quad q_{\text{tot}} = q_{\parallel} + 2q_{\perp}$$

Figure M3. (I) The anisotropy (r) was calculated from the molecular brightness for the parallel and perpendicular polarization (q_{\parallel} and q_{\perp}). (II) The dissociation constant (K_d) equation. RNA_0 : total concentration of RNA, HuR_0 total concentration of HuR, RNA_{free} free bound RNA, $\text{RNA} \cdot \text{HuR}$ HuR bound RNA. (III) The anisotropy data was converted to fraction bound. r_{min} : anisotropy of free RNA, r_{max} : anisotropy of HuR-RNA complex, r : anisotropy of the RNA–HuR complex equilibrium at the given HuR_0 and

RNA₀ concentrations, Q: quenching. (IV-V) The quenching factor is calculated by the ratio of qt_{ot} for free miRNA and qt_{ot} for HuR-miRNA complex.

4.5.6. [α -³²P]-ATP incorporation assay

HuR was thawed slowly on ice and buffer exchanged from a high-salt storage buffer to HuR reaction buffer by centrifugation on a NAP-10 column. The columns were pre-equilibrated with 5 column volumes of ice-cold buffer (GE Healthcare), and centrifuged to eliminate excess buffer (1 min, 1000 g), before adding 1ml of high-salt storage buffer HuR and centrifuging the column for 2 min at 1000 g to collect the protein. 10 μ M miRNA was mixed with 330 nM [α -³²P]-ATP (Perkin-Elmer) and added to HuR simultaneously in a 10 μ l reaction. The final concentrations were 1 μ M miRNA, 1 μ M HuR proteins, 33 nM [α -³²P]-ATP in HuR reaction buffer. The reaction was stopped after 1 h by the addition of a formamide-containing RNA Gel Loading Buffer II (Ambion). For gel analysis of the product, 5 μ l of sample was loaded onto a 10 cm Novex NuPAGE TBU gel (15 %) and separated at 180 V for 50 min in 1 x Ultra-pure TBE buffer (Invitrogen), suitable for detection of RNAs from ~5 nt to > 800 nt in length.

4.5.7. Tailing and trimming

HuR was thawed slowly on ice and buffer exchanged as described in 4.5.6. The 5' PNK-labeled miRNA (~50 nM) is reacted with 1 μ M HuR and 1 mM ATP (standard tailing and trimming reaction setup). The reaction is stopped at the given time points by addition of Proteinkinase A (60mU/ μ l reaction) and incubation for 5 min at 37 °C, New England BioLabs, 800 U/ ml, to degrade the proteins in the reaction and prevent gel artefacts derived from protein-miRNA mobility shifts, and subsequent addition of RNA Gel Loading Buffer II (Ambion). The reaction is then either applied on a 12-15 % TBE 6 M urea gel or stored at -20 °C.

For inhibitor testing, HuR was incubated with the compound/oligonucleotide (MS-444, IL-1 β ARE, invARE, Figure M4) for 30 min at room temperature prior to the reaction

The miRNA was, where applicable, pre-incubated with the corresponding target or chimeric construct (at following concentrations: miRNA 50 nM, target 2 μ M (Figure 4A) and 5 μ M (all

other experiments), sequences in Table M3). The chimeric targets were denatured at 60-90 °C for 2 min and, after a short incubation on ice, added to the miRNA for 15 min at room temperature prior to the addition of other reaction components.

For single nucleotide resolution in a range of 1- ~ 20 (50) nucleotides, the products were separated on a 20 cm (52 cm) 12 % (w/v) 6 M TBE-urea polyacrylamide gel.

Oligonucleotide	Sequence (5'-3')
IL-1 β ARE	TATTTATTTATTTATTTGTTTGTTTGTTTATT
invARE	AATAAAACAAACAAACAAATAAATAAATA

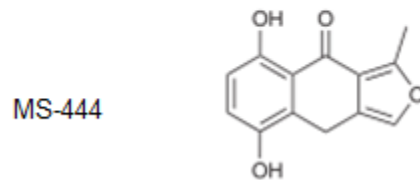


Figure M4. Upper panel: Sequence of IL-1 β ARE and invARE oligonucleotides, Lower panel: Chemical structure of the HuR inhibitor MS-444 (Tatsuta et al. 2004; Meisner et al. 2007)

Tailing and trimming of Ago2-loaded miRNA by HuR: 0.7 mg recombinant His6-TEV-Ago2 was captured on Ni-NTA agarose (100 μ l slurry, Qiagen), equilibrated with Ago binding buffer, washed with Ago wash buffer, and incubated with 100 pmol of 5'-³²P-labeled miR-122 for 1 h in a 1:1 diluted Ago binding buffer. The beads were washed with Ago wash buffer until no further radioactivity could be detected in the supernatant. The miRNA loaded Ago2 was eluted by TEV protease cleavage (Sigma, 2U/ μ l reaction) in 50 μ l TEV buffer, and added to HuR pre-incubated with chimeric construct.

4.5.8. Size exclusion chromatography

Previously affinity purified HuR₁₂ and HuR were separated on a Superdex 75 10 / 300 GL (GE Healthcare) on an Äkta Explorer system. Size calibration was performed using the Gel Filtration Calibration Kit (size standard, GE Healthcare). The column was equilibrated with 5 column volumes 20 mM Tris-HCl pH 8, 800 mM NaCl, 10 mM MgCl₂ and 5 mM DTT. 500 μ l of a 5-20 μ M HuR₁₂ preparation supplemented with 1 mM ATP, 10 mM MgCl₂ and 5 mM DTT was injected and

run at 0.7 ml/min, monitoring the absorbance at 280 nm and 260 nm. 500 μ l fractions were automatically collected, buffer exchanged into HuR buffer using spin columns and immediately used for the enzymatic reactions. Size exclusion chromatography of full length HuR was performed analogously.

4.5.9. HuR refolding

First, the HuR₁₂ (amino acids 2-189) peak was collected by reversedphase chromatography. 30 mg HuR₁₂ was applied onto a Vydac C4 column (Column, C4, 10 mm i.d. x 250 mm, 5 μ m bead size, 300 Å pore size), and eluted in a 0-70 % gradient of Buffer B at a flow of 4 ml/min (0.2 cm/min). The peak fraction was collected conservatively (as indicated in the chromatogram, Figure S3B) and lyophilized, recovering 22 mg of the protein. 7 mg of the lyophilized protein was dissolved and denatured in 6 M Urea, 25 mM Na₂HPO₄/NaH₂PO₄ pH, and applied directly onto the bed of a 10 ml FPLC cation exchange column packed with SP Sepharose Fast Flow. The refolded protein eluted at approximately 510 mM NaCl in a sharp peak. Multiple peak fractions as well as the preceding and following fractions were concentrated 7-fold and buffer exchanged into HuR reaction buffer for analysis in tailing and trimming assays.

4.5.10. Motif search

A positional nucleotide frequency analysis of miRNA substrates was performed by aligning the miRNA sequences from the 3' or the 5' end and analyzing the frequency distribution of nucleotides in positions 1-20 relative to the aligned end (sequences see Table M5). The analysis was performed either for HuR transferase substrate miRNA or for 500 randomly chosen miRNAs from miRbase.

GLAM2 analysis is a motif search algorithm which permits identification of subtle motifs while allowing for insertions and deletions within the motif. The analysis was performed on the same set of miRNAs, using the standard GLAM2 settings with the following changes: Minimum number of sequences in the alignment (10/20), Minimum number of aligned columns (20/20), 'Examine both strands' set to 'off'. The web logo of the highest scoring motif was used.

miRNA	Sequence 5'-3'	Score
miR-1	UGGAAUGUAAAGAAGUAUGUAU	6.6
miR-10*	CAAUUUCGUAUCUAGGGGAAUA	10.4
miR-106a	AAAAGUGCUUACAGUGCAGGUAG	80.1
miR-106b	UAAAGUGCUGACAGUGCAGAU	16.6
mir-1192	AAACAACAAACAGACCAAUUU	5.5
miR-122	UGGAGUGUGACAAUGGUGUUUG	100.0
miR-125a	UCCCUGAGACCCUUAACCUUGUA	-0.4
miR-125b	UCCCUGAGACCCUAACUUGUGA	5.9
miR-130b	CAGUGCAAUGAUGAAAGGGCAU	-5.8
miR-133*	GCUGGUAAAUGGAACCAAU	3.2
miR-140*	UACCACAGGGUAGAACCACGG	-4.1
miR-143	UGAGAUGAAGCACUGUAGCUC	-7.4
miR-145	GUCCAGUUUCCAGGAAUCCCU	-7.2
miR-148a	UCAGUGCACUACAGAACUUUGU	-3.3
miR-149	UCUGGCUCGUGUCUUCACUCCC	-6.3
miR-16	UAGCAGCACGUAAAUAUUGGCG	79.9
miR-192	CUGACCUAUGAAUUGACAGCC	-0.5
miR-196b	UAGGUAGUUUCCUGUUGUUGGG	118.1
miR--200c	UAAUACUGCCGGGUAUUGAUGGA	-3.2
miR-200c*	CGUCUUACCCAGCAGUGUUUGG	1.2
miR-208a	AUAAGACGAGCAAAAAGCUUGU	4.1
miR-208b	AUAAGACGAACAAAAGGUUUGU	6.0
miR-20a	UAAAGUGC UUAUAGUGCAGGUAG	83.4
miR-20b	CAAAGUGC UUAUAGUGCAGGUAG	63.8
miR-21	UAGCUUAUCAGACUGAUGUUGA	209.9
miR-21*	CAACAGCAGUCGAUGGGCUGUC	42.8
miR-220	CCACCACAGUGUCAGACACUU	42.3
miR-221	AGCUACA UUGUCUGCUGGGUUUC	0.0
miR-23a	AUCACAUUGCCAGGGAUUUC	13.3
miR--27a	UUCACAGUGGCUAAGUUCGCG	103.6
miR-291b-3p	AAAGUGCAUCCAUUUUGUUUGU	8.8
miR-29b	UAGCACCAUUUGAAAUCAGUGUU	36.4
miR-301a	CAGUGCAAUAGUAUUGUCAAAAGC	25.4
miR-301b	CAGUGCAAUGGUAUUGUCAAAAGC	9.5
miR-302a	UAAGUGC UUCAUGUUUUGGUGA	24.1
miR-302b	UAAGUGC UUCAUGUUUUGUAG	7.6
miR-302b*	ACUUUAACAUGGGAAUGCUUUCU	49.1
miR-337-5p	GAACGGCGUCAUGCAGGAGUU	86.2
miR-34a	UGGCAGUGUCUAGCUGGUUGU	24.9
miR-425	AAUGACACGAUCACUCCGUUGA	24.4
miR-429	UAAUACUGUCUGGUAUUGCCGU	28.9
miR-451	AAACCGUUACCAUACUGAGUU	5.0
miR-7	UGGAAGACUAGUGAUUUUGUUGU	50.7
miR-93	CAAAGUGCUGUUCGUGCAGGUAG	96.9

Table M5. Sequences of miRNA tested for in the HuR ATP incorporation assay, score according to % of [α - 32 P] –ATP incorporation. miR-122 = 100%

4.5.11. Ago2 Immunoprecipitation (IP)

50 μ l magnetic Dynabead protein G slurry (Invitrogen) was washed three times in 1 ml IP lysis buffer and incubated overnight with overhead rotation in presence of a large excess of purified 11A9 Ago2 antibody (15mg in 200 μ l IP buffer). HCT116 cells were grown in DMEM medium (Life technologies) supplemented with 10 % FCS (Bioconcept) and 2 mM L-Glutamine (Invitrogen). For

IPs, 5 million cells were trypsinized, washed three times with cold PBS (2x 10ml, 1x 1ml, with centrifugation at 1,000 g for 1 min at 4°C in between washes), and resuspended in 300 µl cold IP lysis buffer. After incubation on ice (10 min), the lysates were cleared (centrifugation at 10,000 g, 5 min, 4 °C). The antibody-loaded beads were washed and resuspended in 300 µl IP buffer and 240 µl cell lysate was added. The protein was captured onto the beads during a 16 h head over tail rotation at 4°C. The beads were washed 3 times with IP wash buffer, and the protein was eluted by incubating the beads for 10 min at 70 °C in either TCEP lysis solution (for direct RT-PCR analysis of associated RNA) or SDS loading buffer (for protein PAGE).

4.5.12. Fluorescence microscopy

Huh7 cells were grown in DMEM medium (Life technologies) supplemented with 10 % FCS (Bioconcept), 0.1mM NAE (Life technologies) and 2 mM L-Glutamine (Invitrogen). The cells (1×10^5 in 96-well glass bottom microtiter plates (Whatman), coated with 100 µg/ml fibronectine, 60 min, 37 °C) were transfected with 100 ng pSecTag2GFP, pSecTag2-HuR-GFP or pSecTag2-D105AD254A-GFP plasmids (Lipofectamine-2000, Invitrogen, according to the manufacturers protocol) . After 48 h the cell medium was changed to one of the following: (I) standard DMEM supplemented with 10 % FCS, 0.1mM NAE, 2 mM L-Glutamine and 0.05 % v/v DMSO (fed, DMSO), (II) DMEM without amino-acids (Genaxon Bioscience) supplemented with 10 % amino acid-depleted FCS (pre-dialyzed against 80 x volumes PBS pH 7.4 overnight at 4 °C, then in 60 x volumes for 3 h. membrane cutoff at 3500 Da), (III and IV) Same as I and II, with 50 µM MS-444 and 0.05 & v/v DMSO. After 6 h, the medium was aspirated and the cells were washed 3 times in PBS, fixed for 15 min in 4 % w/v paraformaldehyde, washed and stored in PBS. Live cell imaging was performed on an Operetta High Content Imaging System (PerkinElmer) or a Leica DMI6000B inverted Fluorescence Widefield Microscope.

4.5.13. CAT reporter experiments

Huh7 cells were grown in DMEM medium (Life technologies) supplemented with 10 % FCS (Bioconcept), 0.1 mM NAE (Life technologies) and 2 mM L-Glutamine (Invitrogen). The cells (at 80 % confluency, 32 million) were transfected with 1.1 µg RL-catA, RL-catB, and RL/FL (pRL-CMV

and pGL3 -FL) plasmids in combination with 5.5 µg pSecTag2GFP, pSecTag2-HuR-GFP or pSecTag2-D105AD254A-GFP (Lipofectamine-2000, Invitrogen, according to the manufacturer's protocol. After 48 h the cell medium was changed to one of the following: (I) standard DMEM supplemented with 10 % FCS, 0.1mM NAE, 2 mM L-Glutamine and 0.05 % v/v DMSO (fed, DMSO), (II) DMEM without amino-acids (Genaxon Bioscience) supplemented with 10 % amino acid-depleted FCS (pre-dialyzed against 80 x volumes PBS pH 7.4 overnight at 4 °C, then in 60 x volumes for 3 h. membrane cutoff at 3500 Da), (III and IV) Same as I and II, with 50 µM MS-444 and 0.05 & v/v DMSO.

Luciferase measurement: To determine Renilla and firefly luciferase levels, the cells were collected and treated according to the Dual-Luciferase® Reporter Assay (Promega) manufacturer's protocol.

4.5.14. RT-qPCR for miRNA and mRNA

For direct mRNA quantification from cells, 100,000 cells were lysed in 30 µl TCEP lysis solution for 5 min at room temperature with shaking. The lysate was diluted at least 1:10, and 2 µl were used for the RT-qPCR reaction. Alternatively, the RNA was isolated using standard TRIzol extraction (Life Technologies), or the mirVana RNA isolation kit (Life Technologies) according to the manufacturer's protocol. For the TRIzol extraction, cells are lysed directly in a culture dish by adding 1 ml TRIzol per 3.5cm diameter dish and incubated for 5 min. 0.2 ml Chloroform is added, mixed for 15 s, and the centrifuged for phase separation (15 min, 12,000g, 4 °C). The upper, aqueous phase is transferred and incubated with 0.5 ml isopropyl alcohol for 10 min to precipitate the RNA. To pellet the RNA, the solution is centrifuged (15 min, 12,000g, 4 °C), and the pellet is washed 3 x in 70% ethanol, dried and dissolved in H₂O.

A "1.5 step" RT-qPCR protocol, adapted from the modified stem-loop RT-qPCR assay described in (Pei et al. 2010) was used for miRNA quantification. In addition to samples in triplicates, a 11-point standard curve (chemically synthesized miR-122, concentrations from 2 ng to 0.2 fg in a solution containing poly(A) at a constant concentration of 10 ng/µl) was measured. Assay setup and cycling temperatures are shown in Table M6. Normalized Ct values were transformed into ng RNA according to a linear regression of the standard curve.

A		B	
RT mix (per reaction)		PCR mix (per reaction)	
	V(μ l)		V(μ l)
dNTPs (25 mM each)	0.1	dNTPs (25 μ M each)	0.1
10x PCR buffer	1	10x PCR buffer	0.5
MgCl ₂ (25 mM)	1	MgCl ₂ (25 mM)	0.5
rev primer (10 μ M)	0.1	fwd primer (10 μ M)	0.15
RT	0.1	rev primer (10 μ M)	0.15
H ₂ O	5.7	quencher (50 μ M)	0.075
total	8	Taq	0.1
2 μ l of sample added		H ₂ O	3.425
		total	5

Temperature profile reverse transcription		Temperature profile PCR	
5'	25 °C	10 min	95 °C 1x
5'	95 °C	3 s	95 °C 40x biphasic cycle
		30 s	50 °C Measuring point

Table M6. miRNA 1.5 step RT-PCR: Reverse transcription (A) and PCR (B) reaction setup and cycling program

For mRNA quantification, one-step RT-qPCR reactions were performed using 10-50 ng RNA, 1 mM dNTPs, 0.5 U Multiscribe reverse transcriptase (Applied Biosystems). Reverse transcription was performed for 10 min at 50 °C, PCR was activated for 15 min at 95 °C, and then the samples were cycled 40-50 times with a temperature cycle of 30 s at 94 °C and 30 s at 60 °C on a Light Cycler 480 system (Roche, Table M7). GAPDH, 18S and HuR was measured using the Assay-on-demand reagents from Applied Biosystems. (Hs99999905, Hs99999901, Hs00931450).

Reagent	Concentration	Volume (μ l)
RNase free water		1.9
QuantiTect Multiplex room temperature-PCR Master Mix	2 x	5
Assay-on-demand (5 μ M) for FAM	20 x	0.5
Assay-on-demand for VIC	20 x	0.5
QuantiTect Multiplex room temperature Mix	50 x	0.1
template DNA (5 pg / ml)		2
Total		10

Cycling step	Temperature	Time
Reverse transcription	50 °C	10 min
PCR initial activation step	95 °C	15 min
Denaturation	94°C	30 s
Annealing/extension	60°C*	30 s

Table M7. mRNA RT-PCR reaction setup and cycling program

4.5.15. Deep sequencing

1.25 million each, HCT116 cells were seeded to 60% confluency in DMEM medium supplemented with 10 % FCS and 2 mM L-glutamine (Invitrogen) on the previous day in 25 cm² flasks. HCT116 were treated with a mix of 3 siRNAs against the HuR mRNA, transfected with Lipofectamine 2000 at a final concentration of 50 nM. As a control, pGL3 siRNA was used at the same concentration (Table M8). After 5 h, the transfection complexes were removed, and the knockdown proceeded in DMEM, 10 % FCS and 2 mM L-glutamine. The siRNA transfection was repeated after 24 h and the cells were collected 48 h after the second transfection. Ago2 IP was performed from each lysate, and the RNA was isolated from total lysates and Ago2 IPs for RT-qPCR and deep sequencing analysis (TRIzol, miRvana). Knockdown and overexpression was verified by western blot.

siRNA	Guide strand (5'-3')	Passenger strand (5'-3')
HuR siRNA1	UUGGUCGCAAACUUCACUG	CAGUGAAGUUUGCAGCCAA
HuR siRNA2	UAAUUAUCUAUUCGUAACA	UGUACGGAAUAGAUAAUUA
HuR siRNA3	AAAUCAAUUUAAUUGGUCU	AGACCAUJAAAUUUGAUUU
pGL3 siRNA	UAUUUGUCAAUUCAGAGUGCUU	GCACUCUGAUUGACAAAUAUU

Table M8. siRNA Guide and passenger strand sequences for siRNAs against the HuR and pGL3 mRNA

A Truseq miRNA library was prepared from TRIzol (Life Technologies), or mirVana (Life Technologies) isolated total RNA and Ago IP samples. The RNA was ligated to 3' and 5' adaptors, and, to detect small RNAs from 18 to 60 nt, the appropriate gel regions were excised, reverse transcribed, amplified and sequenced (Illumina high-2000, according to the manufacturers protocol)

After mapping to the genome, the relevant miRNA isoforms used for the final analysis were selected based on the following criteria: had more than 10 counts in all replicates of both control (pGL3 knockdown) and treated conditions (HuR knockdown), displayed a less than 30 % variance between the 6 replicates analyzed (2 separate experiments, 3 replicates each), and, for a difference of more than 20 % between the control and the treated sample, the p-value was measured and only statistically significant differences were analyzed further. The data was then represented as the percent difference of treated/untreated sample.

4.6. Appendix I. Reaction buffers and solutions

S.O.C

2 % tryptone,
0.5 % yeast extract,
10 mM NaCl, 2.5 mM KCl
10 mM MgCl₂,
10 mM MgSO₄
20 mM glucose

HuR lysis/washing buffer

20 mM Tris-HCl (tris(hydroxymethyl)aminomethane,) pH 8.0
800 mM NaCl
1 mM EDTA
0.1mM PMSF
+/- 0.2 % Triton

MOPS running buffer

50 mM 3-(N-morpholino)propanesulfonic acid (MOPS)
50 mM Tris Base
0.1 % SDS
1 mM EDTA, pH 7.7

MES running buffer

50 mM 2-(N-morpholino)ethanesulfonic acid (MES)
50 mM Tris Base
1 % SDS,
1 mM EDTA, pH 7.3

Western blocking buffer

5 % (w/v) skim milk (Biorad)
TBST (Invitrogen)

HuR reaction buffer

PBS pH 7.2
5 mM MgCl₂
0.2 % Pluronic® F-127

Sf9 lysis buffer

50 mM Tris pH 7.8
1 M NaCl
5 mM MgCl₂
0.1 % Triton-X-100
0.5 mM TCEP
1x Complete EDTA-free protease inhibitor (Roche)

Sf9 buffer A pH 7.8

50 mM NaH₂PO₄
300 mM NaCl
20 mM Imidazole
0.5 mM TCEP

Sf9 buffer B pH 7.8

50 mM NaH₂PO₄
300 mM NaCl
250 mM Imidazole
0.5 mM TCEP

PNK buffer (NEB)

70 mM Tris-HCl
10 mM MgCl₂
5 mM DTT
pH 7.6

pCp buffer

50 mM HEPES, pH 7.5
15 mM MgCl₂
10 % DMSO

Ago binding buffer

50 mM NaH₂PO₄
300 mM NaCl
0.5 mM TCEP
pH 7.8

Ago wash buffer

50 mM NaH₂PO₄ pH 7.8
800 mM NaCl
0.5 mM TCEP

TEV buffer

50 mM TrisCl pH 8
10 mM EDTA
1 mM DTT

TCEP lysis solution

6 mM TCEP (tris(2-carboxyethyl)phosphine)
1 % Triton X-100
1 mM HCl, pH 2

IP lysis buffer

20 mM Tris-HCl pH 7.4
150 mM NaCl
0.5 % v/v NP-40
2 mM EDTA
+ freshly added
500 U/ ml RNAsin (Promega)
1 x Complete EDTA-free protease inhibitor (Roche)
0.5 mM DTT

IP buffer

20 M Tris-HCl pH 7.4
150 mM NaCl
2 mM EDTA
+ freshly added
500 U/ ml RNAsin (Promega)
1x Complete EDTA-free protease inhibitor (Roche)
0.5 mM DTT

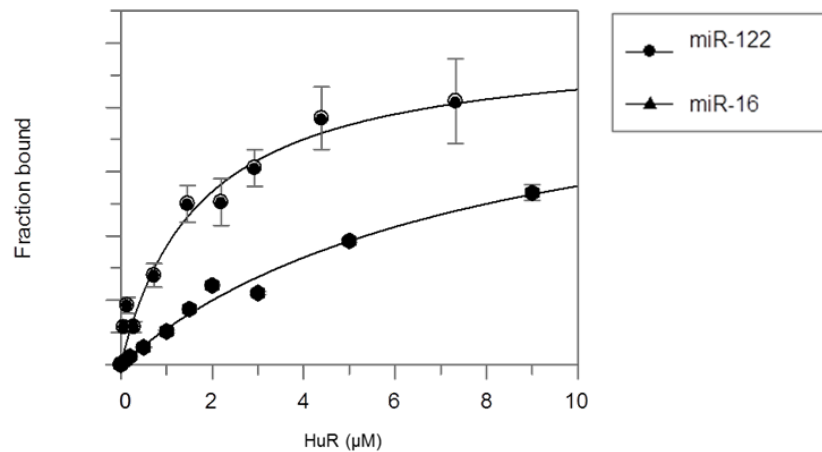
IP wash buffer

50 mM Tris-HCl pH 7.4
300 mM NaCl
0.05 % v/v NP-40
5 mM MgCl₂

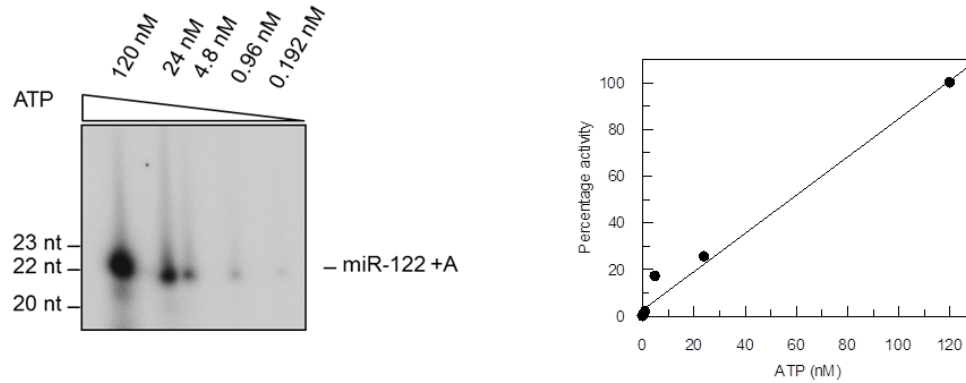
4.7. Supplementary figures

Supplementary Figure 1

A

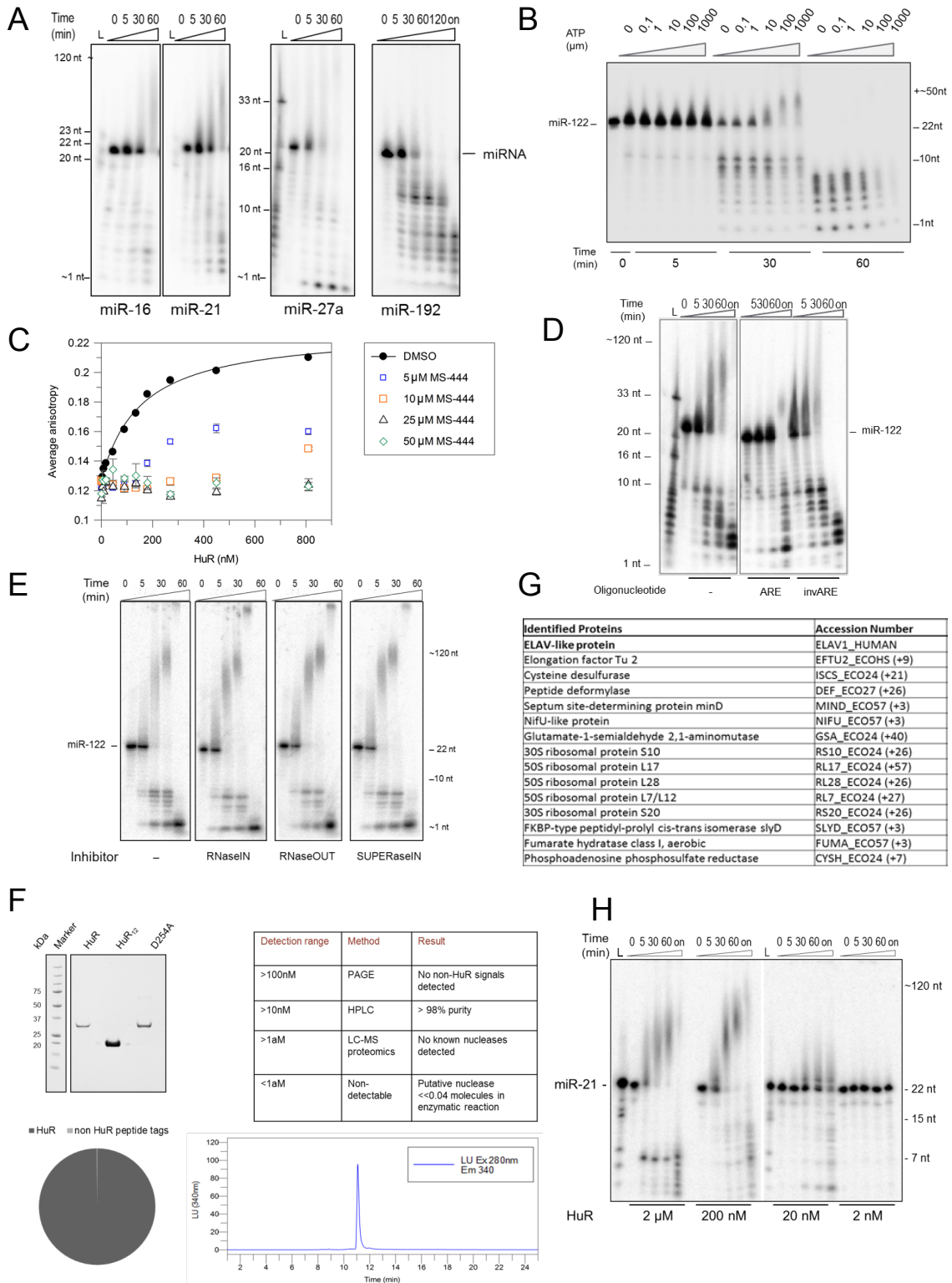


B



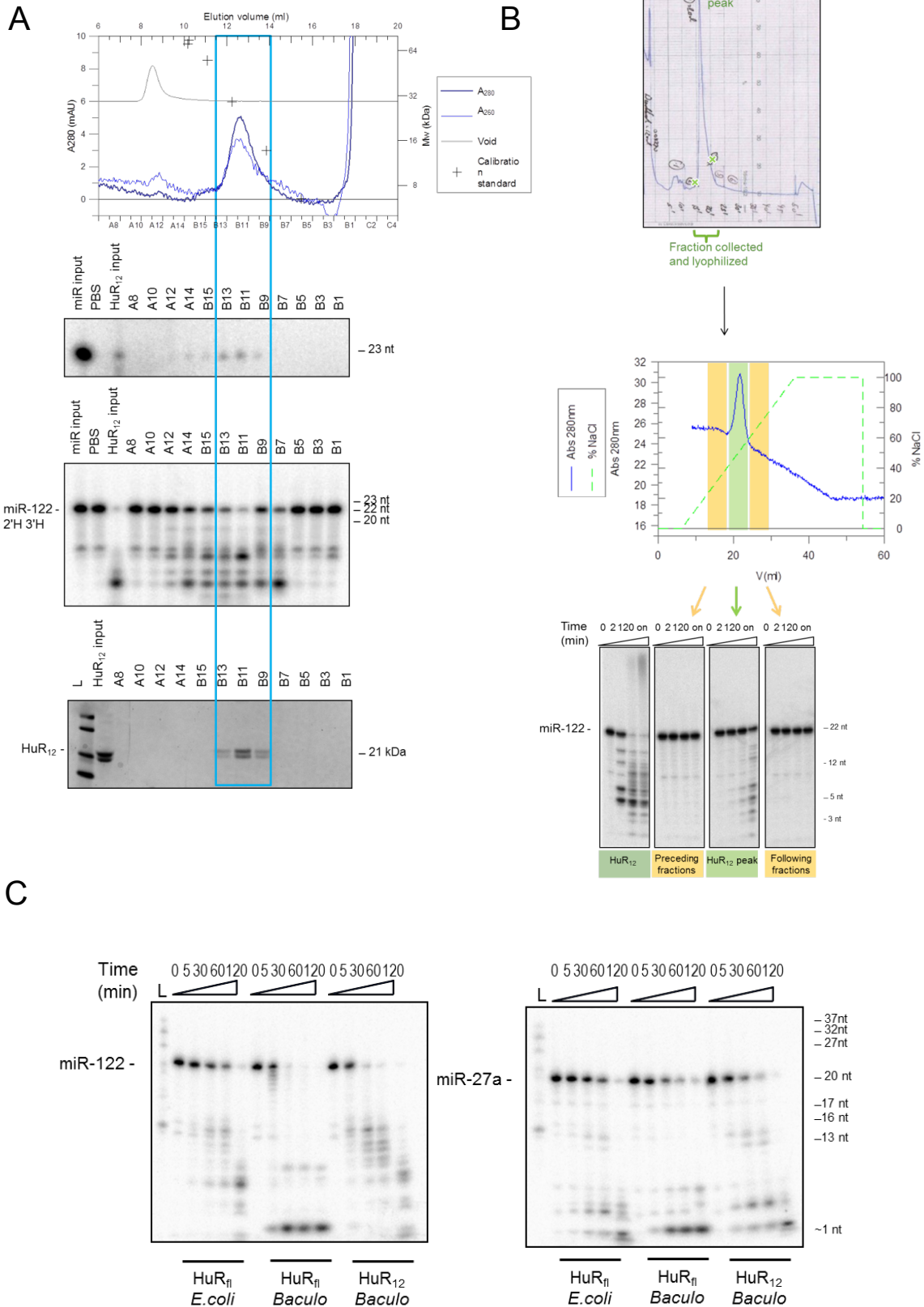
Supplementary Figure 1. (A) Binding of HuR₁₂ to 5'-TMR labeled miRNAs measured by 2D-FIDA anisotropy (Kask et al. 2000). 5 mM EDTA was used in the assay buffer to monitor the interaction under steady state conditions. HuR₁₂ affinities: miR-122: $K_d = 1.7 \pm 0.4 \mu\text{M}$; miR-16: $K_d = 8 \pm 2 \mu\text{M}$. (B) Left panel: Titration of [α-³²P]-ATP in miR-122 adenylation reactions with HuR (miRNA at 5 µM, HuR at 1.5 µM, MgCl₂ at 5 mM) monitored on a 10 cm 15 % TBE-urea PAGE with autoradiographic detection. Right panel: Densitometric quantification plotted as a function of ATP concentration.

Supplementary Figure 2



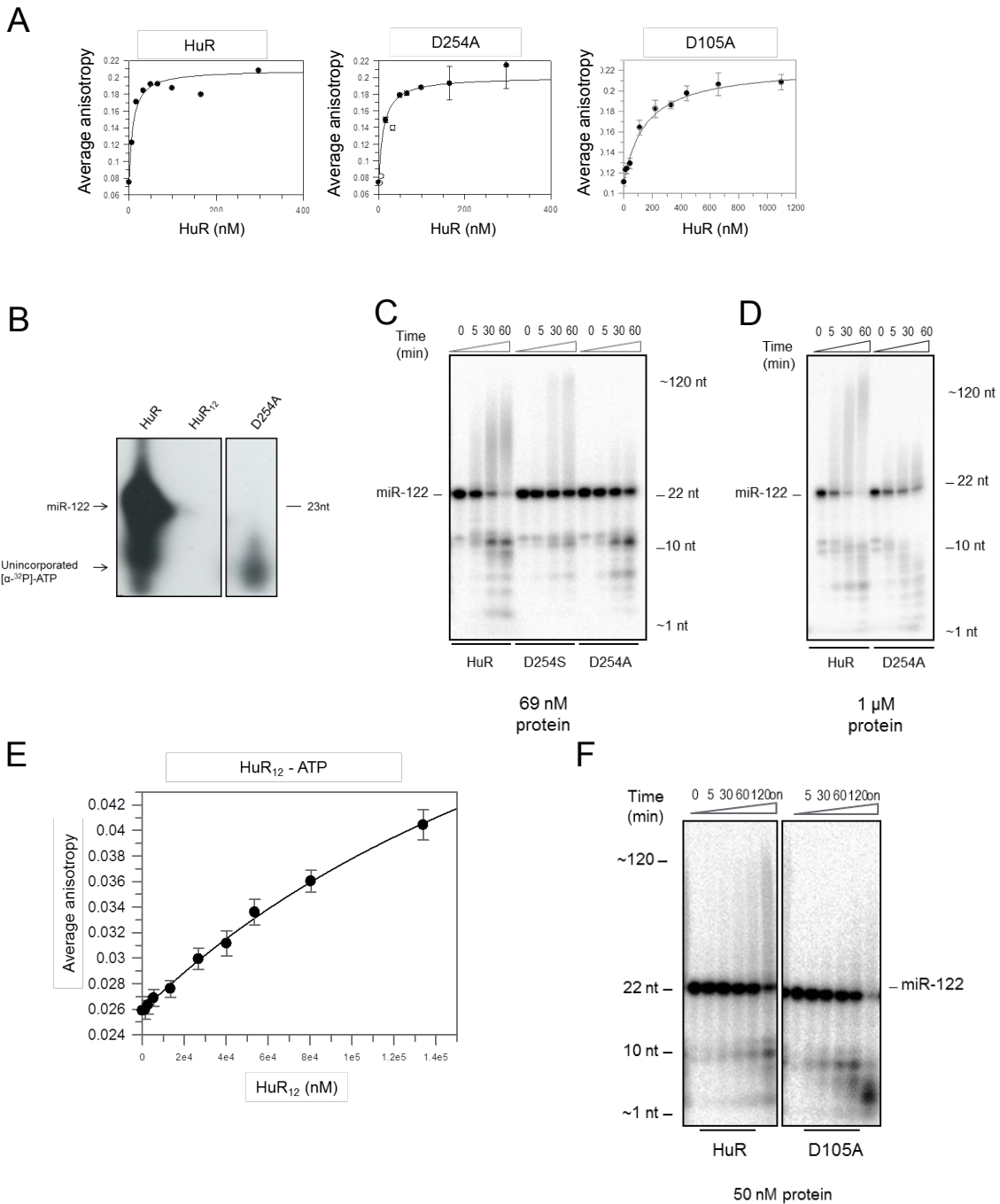
Supplementary Figure 2. (A) Time course of tailing and trimming of 5' ³²P-labeled miR-16, miR-21, miR-27a and miR-192 by HuR. Size determination using synthetic 5' ³²P-labeled RNA as indicated. (B) Tailing and trimming of radioactively labeled miR-122 by HuR with ATP titration. ATP was titrated in a standard tailing and trimming reaction from 100 nM to 1 mM. The reaction was monitored on a 20 cm 12% TBE-urea gel with autoradiographic detection. (C) Concentration dependent inhibition of HuR binding to 5'TMR labeled miR-21 by MS-444 as measured by 2D-FIDA-anisotropy (0.1% v/v) DMSO). (D) Tailing and trimming of 5' ³²P-labeled miR-122 in the absence or presence of the HuR cognate oligodesoxynucleotide IL-1 β ARE or an inverse complementary ARE (invARE, both at 10 mM, left panel) (E) Tailing and trimming of 5' ³²P-labeled miR-122 in the absence or presence of 100 U/ml RNase inhibitors RNaseIN, RNaseOUT or SUPERaseIN (right panel). (F) Determination of purity of recombinant HuR, HuR D254A and HuR₁₂. Upper left panel: Coomassie-blue stained SDS-PAGE of recombinant proteins. Size standard: Precision plus (Biorad) Upper right panel: HPLC chromatogram of recombinant HuR (fluorescent trace, excitation at 280 nm, emission at 340 nm). Lower left panel: Pie chart displaying the fraction of peptide tags detected by LC-MS/MS analysis of full length HuR mapping (gray) or not mapping (white) to the HuR sequence. Lower right panel: Summary of HuR protein analytics. The purity was determined from the RP-HPLC chromatograms based on peak height in 280 nm absorbance as well as 280 nm excitation / 340 nm emission protein fluorescence traces. To determine the maximum concentration of any putative, non-detectable (known) nucleases in molecules per reaction we assumed a ≤ 1 aM concentration (based on the established limit of detection of the LC/MS-MS analysis in the samples (typical HuR concentrations in the range of 1 μ M). With a maximum of 8 μ l HuR protein sample in a 10 μ l reaction this corresponds to a maximum of 1×10^{-18} [mol L⁻¹] \times 6.23×10^{23} [molecules mol⁻¹] \times 8×10^{-6} [L] \leq 5 molecules per reaction. For titrations of HuR concentration as shown in Figure S2H, activity was maintained up to at least 100-fold dilution, which would correspond to ≤ 0.05 molecules of putative non-detectable contaminants in the reaction. (G) Peptides detected in HuR preparations by LC-MS/MS, detected by the Top 15 method. All peptides detected in HuR, HuR₁₂ and D254A are listed. The recombinant proteins were separated on a reducing SDS-PAGE gel, and the whole lane was excised, treated and analyzed. No peptides mapping to known nucleases or nucleotide transferases could be detected at attomolar sensitivity (H) Titration of tailing and trimming of miR-21 by HuR.

Supplementary Figure 3



Supplementary Figure 3. (A) Co-fractionation of tailing and trimming activities with HuR₁₂ in size exclusion chromatography. Upper panel: Superdex-75 size-exclusion profiles are shown for Dextran (void, grey) and HuR₁₂ (dark blue: 280 nm absorbance, light blue: 260 nm absorbance). Retention volumes of the size standard are labeled in the chromatogram (black cross) with the corresponding molecular weight scale plotted on the right y-axis. 500 µl fractions were collected as indicated (fraction number bottom x-axis, elution volume top x-axis). Second panel from the top: Incorporation of [α -³²P]-ATP (33 nM) into miR-122 upon 30 minute reaction with HuR₁₂ input sample or indicated fractions. Third panel from the top: Trimming of 5' ³²P-labeled miR-122 (3' nucleotide with 2'H 3'H) by HuR₁₂ input and indicated fractions. Lower panel: Coomassie SDS-PAGE analysis of HuR₁₂ distribution in the indicated fractions. Size standard: Mark12 (Life technologies) (B) Tailing and trimming reaction after HuR₁₂ refolding. First panel from the top: HuR₁₂ preparative reverse-phase HPLC chromatogram. Collected HuR₁₂ peak fractions indicated with green crosses. Middle panel: Refolding of denatured HuR₁₂ via cation-exchange chromatography on a 10 cm x 1 cm column packed with SP Sepharose fast flow. The chromatogram at 280 nM absorbance (blue trace) and NaCl gradient (green dashed line) are shown. Third panel from the top: Time course of reaction of 5' ³²P-labeled miR-122 by pooled and concentrated fractions comprising either the HuR₁₂ peak, preceding or following fractions. HuR₁₂ input sample was used as reference. (C) Degradation patterns of 5' ³²P-labeled miR-122 and miR-27a in the absence of ATP generated by incubation with HuR₁₂ from *E.coli* and *Baculo* purifications and HuR₁₂ from *Baculo* purification

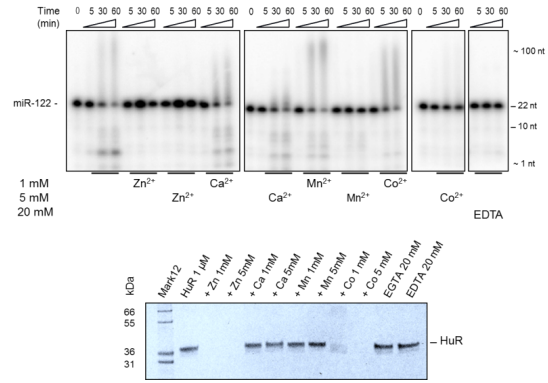
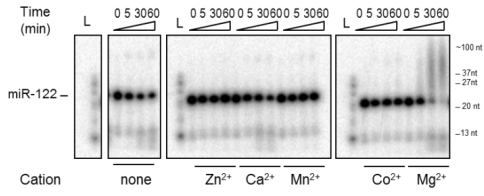
Supplementary Figure 4



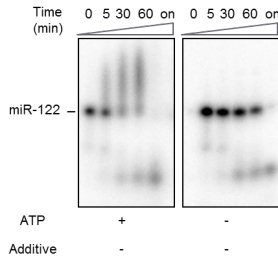
Supplementary Figure 4. (A) Binding of HuR, D254A and D105A to 5'-TMR oligodesoxynucleotide IL-1 β ARE was measured by 2D-FIDA anisotropy. Wild type HuR: $K_d = 8 \pm 2$ nM; HuR D254A: $K_d = 9.6 \pm 0.6$ nM; D105A: $K_d = 140 \pm 20$ nM. (B) [α - 32 P]-ATP incorporation into miR-122 by HuR, HuR $_{12}$ and HuR D254A mutant. (C) Comparison of tailing and trimming of 5'- 32 P-labeled miR-122 by HuR, D254S and D254A mutant (all proteins at 33 nM). (D) Comparison of tailing and trimming of 5'- 32 P-labeled miR-122 by HuR versus D254A (both proteins at 1 μ M). (E) Binding of HuR $_{12}$ to 5'-bodipy-FL labeled ATP was measured by 2D-FIDA anisotropy. $K_d = 230 \pm 40$ μ M (F) Comparison of tailing and trimming of 5'- 32 P-labeled miR-122 by HuR versus D105A (both proteins at 50 nM).

Supplementary Figure 5

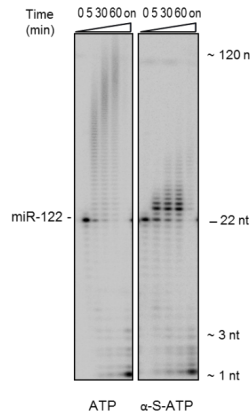
A



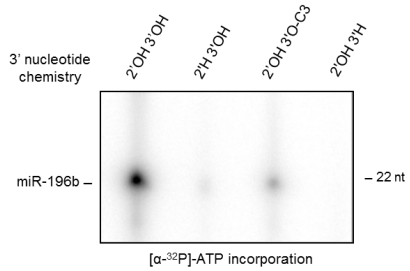
B



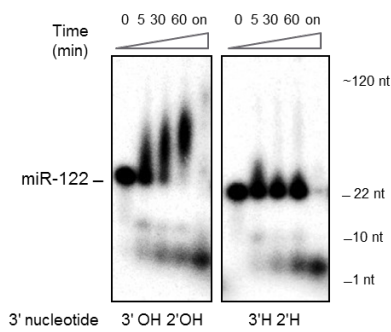
C



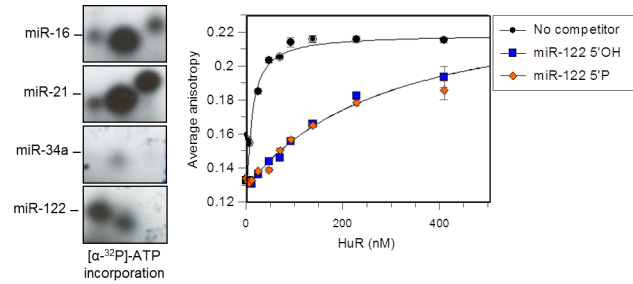
D



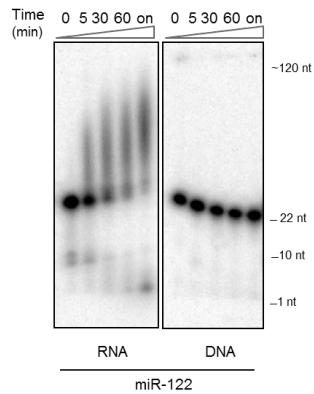
E



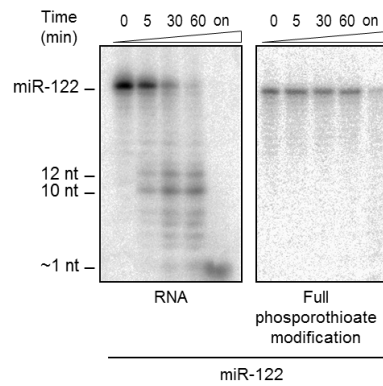
F



G

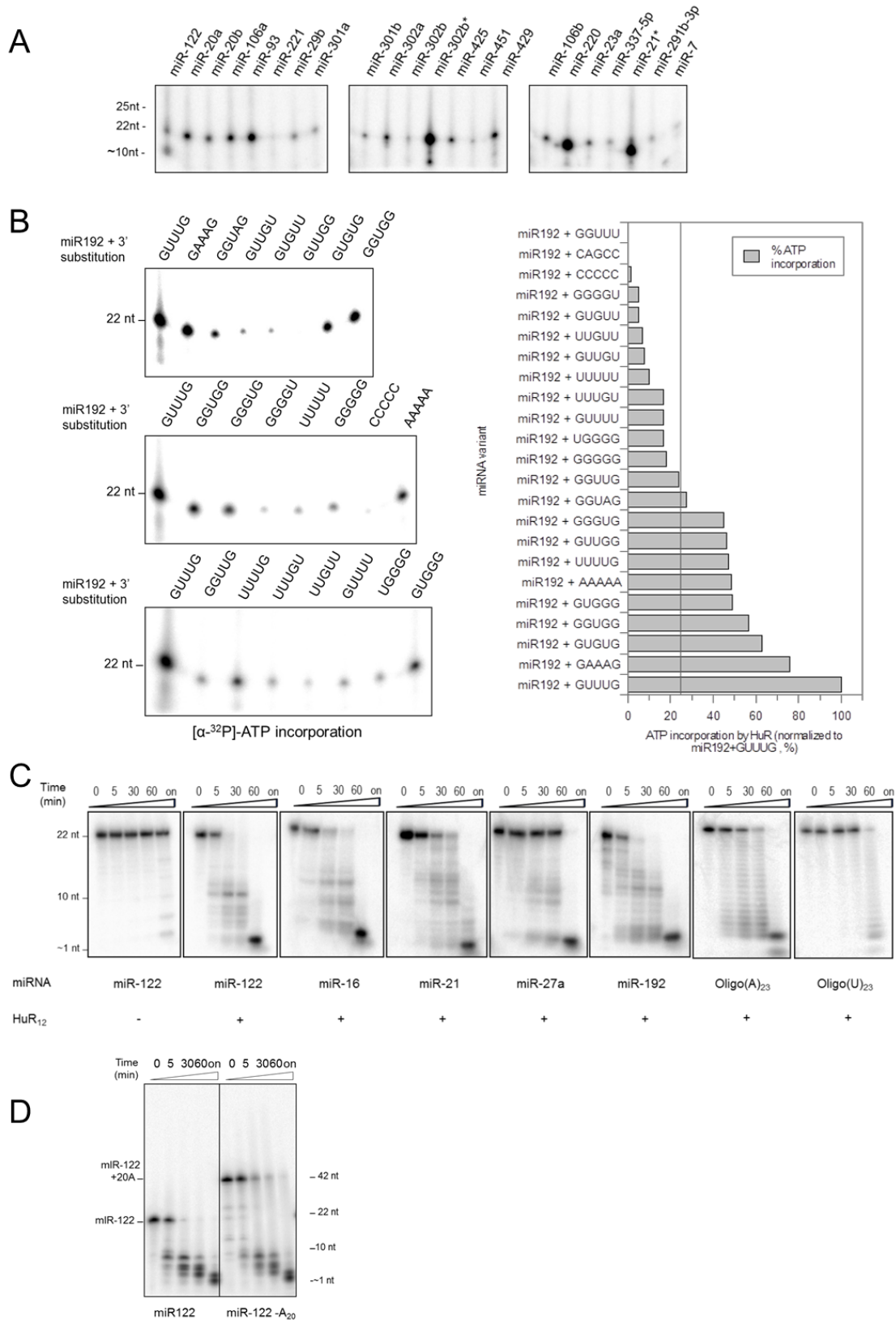


H



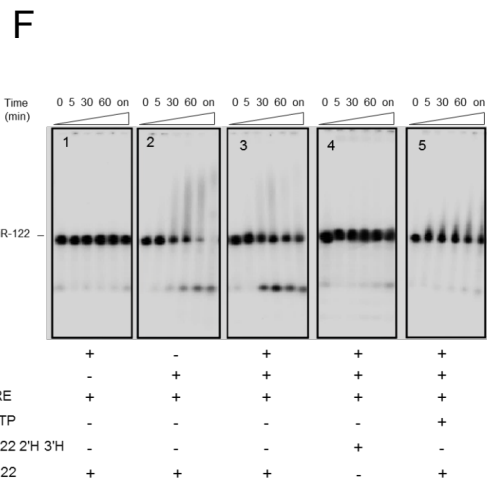
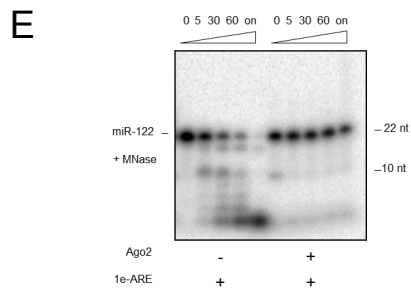
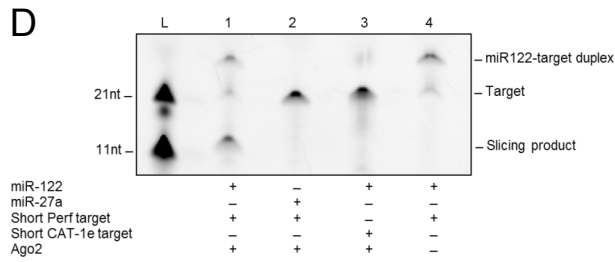
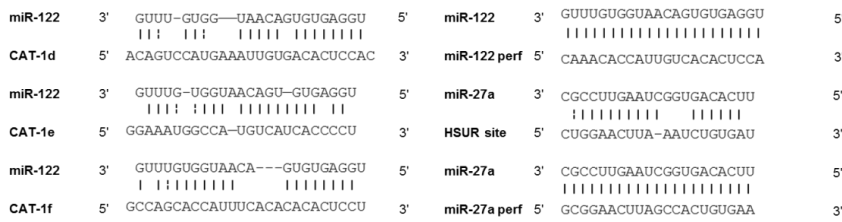
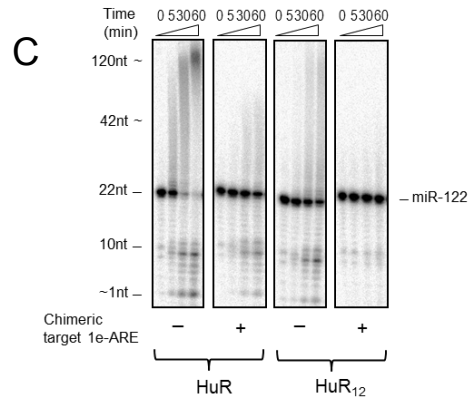
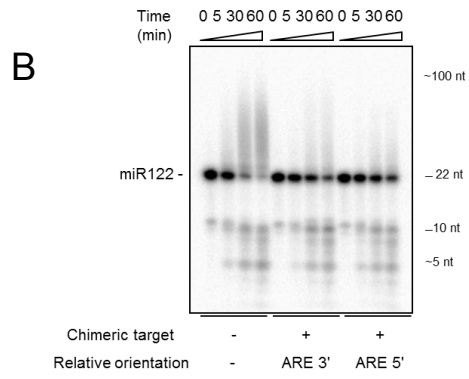
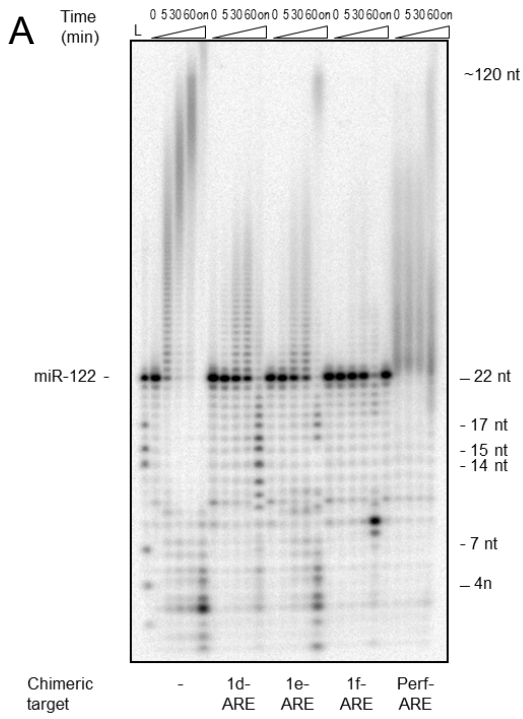
Supplementary Figure 5. (A) The effect of various divalent cations on HuR tailing, trimming and solubility. Left panel: Tailing and trimming of 5'-³²P-labeled miR-122 by HuR in the presence of divalent cations, as indicated. Right panels: Tailing and trimming of 5'-³²P-labeled miR-122 by HuR, and the respective PAGE analysis of protein solubility in the presence of 5 mM Mg²⁺, with or without addition of various divalent cations at 1 and 5 mM, as well EDTA at 20 mM, as indicated. (B) Tailing and trimming of 5'-³²P-labeled miR-122 by HuR in the presence or absence of ATP (1mM). (C) Tailing and trimming of 5'-³²P-labeled miR-122 by HuR in the presence of 1 mM ATP versus α -S-ATP (D) Incorporation of [α -³²P]-ATP into miR-196a by HuR with the following sequences and 3' ribose modifications: (2'OH 3'OH), (2'H 3'OH), (2'OH 3'O-C3), (2'OH 3'H). (E) HuR tailing and trimming of 5'-³²P-labeled miR-122 with 3' terminal ribose modifications (3'OH 2'OH), left or (3'H 2'H), right). (F) Left part: Incorporation of [α -³²P]-ATP by HuR into miR-16, miR-21, miR-34a and miR-122 with the following 5' nucleotide chemistries: 5'-hydroxyl (5'OH), 5'-phosphate (5'P) and 5'-tetramethylrhodamine (5'TMR). Right part: Comparison of HuR binding affinities for miRNAs with 5'-TMR, 5'-OH and 5'-P chemistry. The 5'-TMR labeled miR-122 at 1 nM was titrated with HuR in the absence (black circles) or presence of miR-122 5'OH (blue squares) or miR-122 5'P (orange diamonds) chemistry, at 1 μ M. The measured dissociation constant for the HuR-miR-122 interaction was K_d HuR miR-122 5'TMR = 8 +/- 1 nM. Through nonlinear 1:1 competition curve fitting we determined dissociation constants for the competitors at: K_d HuR-miR-122 3'OH = 40 +/- 2 nM and K_d HuR-miR-16 3'OH= 40 +/- 2 nM. (G) Tailing and trimming of miR-122 RNA versus DNA (H) Tailing and trimming of miR-122 RNA versus fully phosphorothioate modified miR-122 RNA.

Supplementary Figure 6



Supplementary Figure 6. (A) [α - 32 P]-ATP incorporation into 22 synthetic miRNAs by HuR. (B) Left panels: [α - 32 P]-ATP incorporation into synthetic miR-192 variants with different sequence substitutions of the five 3' terminal nucleotides for systematic variation of the GUUUG motif. Right panel: densitometric quantification of [α - 32 P]-ATP incorporation. (C) Nuclease assay: HuR₁₂ trimming time course of 5' 32 P-labeled miR-122, miR-16, miR-21, miR-27a miR-192 Oligo(A)₂₃, and Oligo(U)₂₃ in the absence of ATP. 20 cm 12% TBE-urea PAGE with autoradiographic detection (D) Trimming time course of miR-122 or a miR-122 variant with a synthetic 3' A₂₀ tail by HuR₁₂ in the absence of ATP.

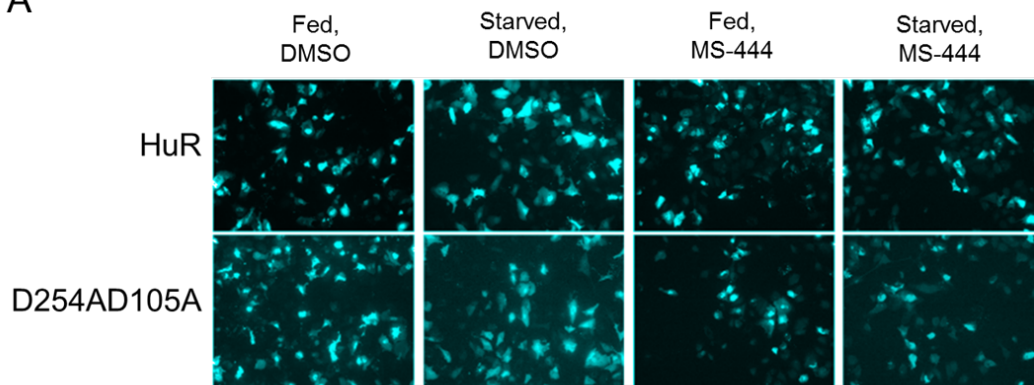
Supplementary Figure 7



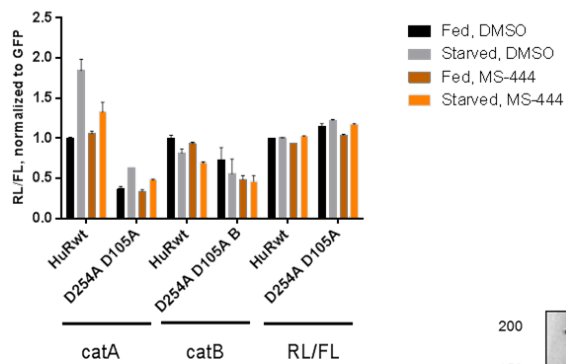
Supplementary Figure 7. (A) Tailing and trimming time course of 5'-³²P-labeled miR-122, either in free form or pre-hybridized to chimeric targets containing an HuR cognate ARE binding site and different natural miR-122 sites from the CAT-1 mRNA (CAT-1d, -1e, -1f), or a perfect complementary miR-122 site (perf), monitored on a high resolution TBE-urea PAGE with autoradiographic detection. Of note, signal trailing in the reaction with the perf-ARE (seen already at time point 0) is most likely due to tight binding of miRNA to imperfectly denatured target RNA during electrophoresis. Lower panel: Base pairing of miR-122 and miR-27a to perfect and natural binding sites (B) Tailing and trimming of 5'-³²P-labeled miR-122, either in free form or pre-hybridized to chimeric targets with the CAT-1e miR-122 target site positioned either upstream or downstream of the ARE HuR binding site (monitored on 10 cm 15% TBE-urea PAGE with autoradiographic detection). (C) Tailing and trimming of miR-122 either in free form or pre-hybridized to the chimeric 1e-ARE target by HuR and HuR₁₂, monitored on a 20 cm 12 % TBE-Urea PAGE with autoradiographic detection. (D) Slicing of 5'-TMR labeled target RNAs by recombinant Ago2 protein loaded *in vitro* with ssRNA, as indicated. Lane 1: miR-122 and a perfect miR-122 target. Lane 2: miR-27a and a perfect miR-122 target. Lane 3: miR-122 and a natural, bulged target. Lane 4: miR-122 and a perfect miR-122 target, no Ago2. (E) Time course of degradation of 5'-³²P-labeled miR-122, versus Ago-loaded 5'-³²P-labeled miR-122 (both pre-hybridized to the chimeric 1e-ARE target) by the *Staphylococcus aureus* micrococcal nuclease (MNase, NEB), monitored on a 10 cm 15 % TBE-urea PAGE with autoradiographic detection. (F) Turnover of Ago2 loaded 5'-³²P-labeled miR-122 in absence (panel 1) or presence of HuR (panel 3), and under conditions where tailing is inhibited by 3' desoxy modification of the 3' miRNA nucleotide (panel 4) or reaction with α-S-ATP (panel 5). All reactions were performed after pre-hybridization of miR-122 – Ago2 complexes to the 1e-ARE chimeric target (monitored on 10 cm 15 % TBE-urea PAGE with autoradiographic detection).

Supplementary Figure 8

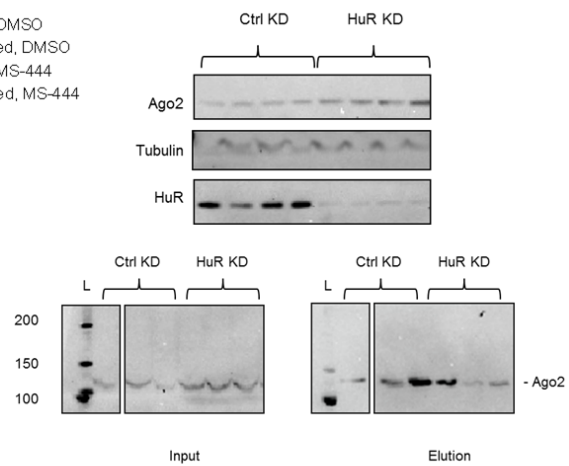
A



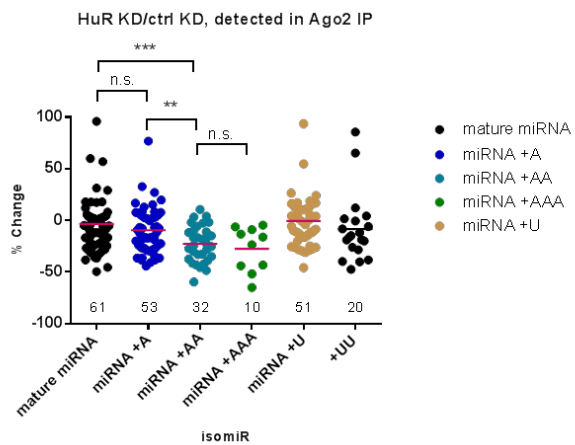
B



C



D



Supplementary Figure 8. (A) Live-cell fluorescent imaging of HuR and D105AD254A HuR double mutant localization in Huh7 cells under fed and amino-acid starved conditions in the absence or presence of MS-444 (50 μ M, all reactions at 0.1 % v/v DMSO). (B) Relief of miR-122 targeted Cat-1 reporters upon amino-acid starvation. Effect of MS-444 inhibition (6 h) with GFP, wild type HuR-GFP or HuR D105AD254A-GFP overexpression is shown on Renilla luciferase levels for catA, catB or a non-3'UTR control reporter. Renilla luciferase luminescence is shown normalized to firefly luciferase signal expressed from the same plasmid. (C) Upper panel: Western blot of Ago2, tubulin and HuR in HCT116 cells at 96 h after control (pGL3 siRNA, targeting Firefly luciferase (Stalder et al. 2013)) or HuR siRNA knockdown. 4 replicates are shown, and tubulin is shown as a loading control. Lower panels: Ago immune precipitations from HCT116 cells performed 72 h after HuR or control knockdown by siRNA. Three replicates are shown. Size standard: Protein plus western C (Biorad) (D) Deep sequencing analysis of mature miRNA and non-genomically encoded 3' extended isoforms in Ago2 immune precipitations from HCT116 cells upon HuR or control knockdown by siRNA (at 72 h post knockdown, western blot shown in Figure S8C). Relative change of mature miRNA levels with and without 3' terminal extensions upon HuR knockdown in the Ago-associated miRNA population. The total isoform number in each category is indicated. The data is an average of 2 separate experiments, with 4 biological replicates each

5. Discussion

5.1. Relation to initial data on HuR terminal transferase activity

HuR is composed of three RRM domains with a 45 amino acids long, flexible hinge between RRM2 and RRM3. Recently, we have shown that HuR has a 3'-terminal RNA adenosyl transferase activity (Meisner et al. 2009). However, its physiological substrates and biological function remained unknown to date. Here we show that HuR is a poly(A)polymerase, and that miRNAs act as substrates for this enzymatic activity. In addition, we have uncovered a novel, 3'→5' exonuclease activity associated with HuR that acts on miRNAs as well as oligo(A) substrates. Since HuR₁₂ is a fully functional enzyme, the data presented in this study map both catalytic sites to within the N-terminal 189 amino acids. Previously data however had shown that the HuR transferase activity involves a conserved DxD (residues 254-256) motif within RRM3, with D254 contributing to ATP binding (Meisner et al. 2009). While deficient in the transferase activity, none of the RRM3 point mutants including D254S, D256S, and D312S was catalytically dead (Meisner et al. 2009). In the current study, we mutated the D254 to A to circumvent potential hydrogen bonding activity of the serine mutations we had used initially. Although seemingly dead in the ATP incorporation assay, we still detected residual tailing by HuR D254A in the more sensitive tailing and trimming assay which uses 5'-radiolabeled miRNA substrate. This assay monitors the fate of the entire miRNA substrate, in contrast to the ATP incorporation, which represents the net result between the two counteracting activities. The residual tailing activity of D254A is consistent with a contribution of D254 to ATP binding rather than having an essential role in catalysis. Of note, the reduction in tailing activity for the D254A mutant was comparable to the weaker tailing activity also observed for HuR₁₂. Finally, the ATP affinity of HuR₁₂ was ca. 15-fold weaker than the affinity of the full length protein, similar to the reduced affinity previously observed for the D254S mutant (Meisner et al. 2009). Together these data show that both catalytic sites are contained within the N-terminal portion of HuR, with amino acids in RRM3 contributing to ATP binding.

5.2. The HuR-associated enzymatic activities

We have examined whether both poly(A)polymerase and exonuclease activities represent integral functions of HuR itself rather than being due to contaminating *E. coli* proteins copurifying with recombinant HuR. The following cumulative evidence summarizes our arguments so far: (I) the recombinant proteins migrated as single bands in SDS-PAGE following either coomassie or silver staining, and eluted as single peaks during RP-HPLC analysis; (II) in a LC-MS/MS analysis, no peptides mapping to known nucleases or polymerases were detected; (III) for both HuR and HuR₁₂, polymerase and nuclease activities co-eluted with respective protein bands during size exclusion chromatography; importantly, the activity peaks followed the shift in the elution volume according to the size difference between HuR and HuR₁₂; (IV) after isolating HuR₁₂ under denaturing conditions by preparative RP-HPLC chromatography and refolding of the denatured protein on a cation exchange column, the nuclease activity was recovered and cofractionated with the single peak after the successive chromatographies (V) both HuR activities were inhibited by MS-444, an HuR-targeting compound; (VI) likewise, they were inhibited *in trans* by an ARE deoxyoligonucleotide but not its inverse complementary variant. (VII) Moreover, the presence of the same HuR binding ARE sequence in a chimeric RNA target bearing also a miRNA binding site allowed HuR, but not micrococcal nuclease to turnover Ago-loaded miRNA, in a tailing-dependent manner. (VIII) HuR binds directly to ATP as demonstrated by direct visualization of HuR associating to ATP-beads (Meisner et al. 2009). Point mutants of HuR with reduced ATP binding affinity (D254S, D254A) paralleled a reduction in tailing activity. (IX) Finally, we could detect nuclease and transferase activities in proteins purified from a different system - Baculovirus-infected insect cells.

However, final evidence that these enzymatic activities are integral properties of HuR proteins, and not a copurifying contamination will be given only by generating nuclease-deficient mutants and thus mapping the catalytic site.

5.3. Characterization of transferase and nuclease preferences and specificities

The HuR poly(A)polymerase (tailing) is a Mg^{2+} dependent enzyme with a preference for single stranded RNA. A small screen of ~50 miRNAs has yielded a loosely defined GU-rich pentameric motif (G-G/U-U/G-A/U-G) in the 3' end of substrate miRNAs. Introducing GUUUG into the 3' end of a non-substrate miRNA was sufficient to render it a substrate; however, deleting this motif in substrate miRNA did not always abolish the activity. In addition, miRNA without the motif can act as a substrate for the poly(A)polymerase activity of HuR, indicating that a 3'terminal GU-rich pentamer is a sufficient, but not necessary feature of HuR substrates.

miRNAs that are poor transferase substrates are nevertheless turned over by the less selective exonuclease activity (trimming). The typical staling pattern that HuR generates in the course of miRNA degradation is completely missing from the reaction with oligo(A)₂₃, indicating that oligo/poly(A) is the preferred substrate for the HuR exonuclease. Oligo(A)₂₃ is only inefficiently tailed by HuR. Oligo(U)₂₃ is a poor substrate for trimming *in vitro*. A more systematic future study of substrate preferences (in particular for the transferase) as well as enzyme kinetics and processivity would require a more effective uncoupling of tailing and trimming activities, e.g. by selective inactivation of either catalytic activity by point mutations.

5.4. HuR tailing and trimming on a target

Although both tailing and trimming are most efficient on a free, single stranded miRNA *in vitro*, HuR can still tail and trim a miRNA hybridized to its target if bound to the same target RNA via an ARE sequence. These data suggest that the reaction is facilitated by bringing the two reactants into proximity on a target RNA, either for entropic reasons and/or due to conformational changes of HuR once it is ARE bound. Indeed, as based on CLIP data for HuR and Ago in mammalian cells, HuR and miRNA sites are enriched in the proximity to each other (Lebedeva et al. 2011; Mukherjee et al. 2011). Interestingly, the observation that addition of a short ARE oligonucleotide *in trans* significantly impairs both tailing and trimming even of free

miRNA suggests that HuR needs to dissociate from the ARE of the chimeric miRNA-ARE target to initiate processing of the pre-bound miRNA or miRISC.

5.5. Ago-miRNA complex stability and accessibility

The Ago-miRNA complex is highly stable *in vitro* (Martinez & Tuschl 2004), with dissociation rates in the range of $k_{\text{off}} \sim 10^{-5} \text{ sec}^{-1}$ (corresponding to half lives of > 20 hours, (De et al. 2013; Chatterjee & Grosshans 2009) and Meisner lab, unpublished data). The miRNA is enveloped by Ago proteins, which bind both ends of the miRNA (Ma et al. 2005; Boland et al. 2011). In cells, overexpression of Ago proteins was shown to stabilize miRNAs, whereas their depletion led to the decline of miRNA levels (Diederichs & Haber 2007; O'Carroll et al. 2007). However, under several conditions, Ago-loaded miRNAs can be accessed by modifying enzymes. In particular, Ameres et al have reported that in *D. melanogaster*, as well as in HeLa cells, an unknown polymerase/nuclease tailed and trimmed Ago-loaded miRNA bound to a highly complementary miRNA target site (Ameres et al. 2010). In *Drosophila*, the 3'→5' exonuclease Nibbler was suggested to trim the 3' terminal nucleotides of Ago-1-loaded miRNA to provide a better fit to the Ago PAZ domain (Han et al. 2011). In *C. elegans*, the unloading of miRNA from Ago was found to be a necessary prerequisite for Xrn-2 mediated degradation (Chatterjee & Grosshans 2009), whereas in mammalian cells it was revealed that unloading of guide RNA from Argonaute is promoted by the presence of highly complementary miRNA targets (De et al. 2013; Yoda et al. 2013).

5.6. HuR tails and trims Ago-loaded miRNA

Given that HuR can affect miRNA-mediated repression of mRNA (Bhattacharyya et al. 2006; Kim et al. 2009; Tominaga et al. 2011; Young et al. 2012; Epis et al. 2011), we tested whether HuR can access Ago-loaded miRNA, and whether the Ago-miRNA interaction can affect the interplay of miRNA and HuR on a mRNA. The 3' ends of Ago2-loaded miRNAs can reportedly be accessible to modifying enzymes (Juvvuna et al. 2012), therefore, one could imagine that the HuR transferase can access its substrate when loaded within Argonaute by detecting the preferred

GU-rich motif at the 3' end. Indeed, unlike micrococcal nuclease, HuR can access Ago-loaded miRNA and turn it over. Interestingly, the reaction was only possible when Ago and HuR were bound to the same RNA, and occurred in a tailing-dependent manner, as the miRNA 3'nucleotide 3'deoxy modification as well as the absence of ATP inhibited miRNA trimming, which is not the case for HuR acting on free miRNA. Consistent with this, adenylation and uridylation has been associated with the subsequent exonucleolytic attack on small RNA (Kim et al. 2010; Ameres et al. 2010; Kamminga et al. 2010; Yoda et al. 2013).

5.7. HuR₁₂ cannot process target-bound miRNA

Interestingly, although HuR₁₂ can tail and trim a free miRNA, albeit with diminished tailing efficiency, we see that its activity is strongly diminished on a target RNA. Given that HuR₁₂ displays weakened binding of both miRNA and ATP (70-fold and 15-fold, respectively), we speculate that the RRM3 could be involved in initial contact with miRNA and also contribute to ATP binding. Both of these reduced activities would contribute to ineffective processing by HuR₁₂ of a target-bound miRNA, where tailing is a prerequisite for trimming.

5.8. Contribution of HuR enzymatic activity to Ago displacement

In the human hepatoma Huh7 cell line, the miR-122-mediated repression of the CAT-1 mRNA is relieved by HuR upon amino-acid starvation and other stress conditions (Bhattacharyya et al. 2006). The derepression was dependent on RISC binding to target mRNA via miRNA base-pairing as the repression by Ago2 tethered to the mRNA cannot be antagonized by HuR (Kundu 2011). The displacement of the Ago2 protein from target RNA (Kundu et al. 2012), which accompanies the derepression, is therefore most probably caused by weakening of either mRNA-miRNA or Ago2-miRNA interactions. Given that we show that HuR can tail Ago2-loaded miRNA, we hypothesize that the extension of the miRNA out of the PAZ binding domain could weaken the interaction of Ago2 with the miRNA and thus help to displace it (Han et al. 2011; Juvvuna et al. 2012). In addition, the extended miRNA tail likely serves as a more ideal substrate and landing pad for the nuclease. Interestingly, given that HuR displays low tailing and preferential trimming

of oligo(A) substrates, tailing would generate a substrate that is ideal for trimming, leading to a handover from polymerase to nuclease activity. Of note, HuR likely has to release the ARE already prior to tailing since addition of ARE *in trans* inhibited both, tailing and trimming of free miRNA. It remains to be elucidated what the mechanism of handover of HuR from ARE to miRNA substrate is. Together, tailing and trimming may facilitate miRNA processing and Ago2 displacement from the target RNA. Consistent with this model, we observed derepression of the RL-catA mRNA reporter, which contains miR-122 and HuR sites in its 3'UTR, upon overexpression of HuR but not its D105A, D254A tailing deficient mutant. In addition, the derepression was prevented by treatment of cells with the HuR inhibitor MS-444.

5.9. HuR effect on miRNA bound to perfect target site

Kundu et al. reported that HuR can antagonize miRISC bound to a perfect complementary target, albeit with lower efficiency than that bound to a natural miRNA target site (Kundu et al. 2012). In addition, the to-date reported cases of tailing and trimming of miRNAs rely on the presence of a highly complementary miRNA site in target RNA (Ameres et al. 2010; Marcinowski et al. 2012). However, in the current study no tailing or trimming of a miRNA bound to a perfect complementary site could be detected even when HuR was associated with an ARE present *in cis*. However, as we have not yet tested the same situation in the presence of Ago, we cannot rule out the possibility that HuR might be capable to also process RISC loaded miRNA perfectly complementary to the target.

5.10. Proximity of HuR and miRNA binding sites and competitive versus cooperative effects

A few studies have suggested that HuR antagonizes miRNA due to competition for mRNA binding (Mukherjee et al. 2011). In most of these studies, the binding sites for both factors were however non-overlapping, ruling out direct competition for binding as the mechanism of derepression, consistent with the findings that when the HuR and miRNA sites are found in proximity to one another, they typically do not overlap (Lebedeva et al. 2011; Mukherjee et al.

2011). In the case of the miR-122-repressed CAT-1 mRNA, miRNA and HuR binding sites were even over 200 nt apart. Sites in Top2A, NCL and *stim1* mRNAs were likewise distant (Srikantan et al. 2011; Tominaga et al. 2011; Zhuang et al. 2013). In such situations, the reported oligomerization property of HuR could facilitate the de-repression (Kundu et al. 2012; Kasashima et al. 2002; Dean et al. 2001). However, there are also reports that HuR and miRNAs can work in a cooperative manner, with HuR promoting miRNA access to the mRNA. Interestingly, in most such hitherto described cases, HuR and miRNA sites were in proximity (Kim et al. 2009; Glorian et al. 2011), and therefore it has been proposed that HuR binding introduces changes to the local secondary structure, promoting miRNA binding, as was shown in the case of PUM and p27 mRNA (Kedde et al. 2010; Srikantan et al. 2012). Therefore, thus far no common positional or sequence properties can be derived from these few examples, which could predict whether HuR will act in a competitive or a cooperative manner. It will therefore be interesting to identify factors that determine whether an Ago-loaded miRNA will or will not be turned over by HuR *in vivo*.

Mukherjee et al have analyzed the behavior of HuR and miRNA targets upon HuR and miRNA depletion (Mukherjee et al. 2011). The authors differentiated between overlapping target sites positioned less than 10 nt apart from each other, non-overlapping sites (> 10 nt distance), as well as target mRNAs with only miRNA sites, only HuR sites, or neither. Upon HuR knockdown, the downregulation of targets containing overlapping sites and non-overlapping sites was comparable. These results indicate that the levels of both sets of mRNAs are being fine-tuned by both HuR and miRNAs, irrespective of their distance. While it is possible that the mRNAs with overlapping sites were regulated by competitive interaction of HuR and miRNA for binding, such a mechanism is highly unlikely for the non-overlapping sites.

5.11. HuR knockdown modulates levels of miRNAs and iso-miRs with 3' non-templated A additions

We also show that HuR has a direct effect on miRNA levels. This is consistent with the observations made previously by monitoring the increase of miRNA levels upon HuR knockdown (Young et al. 2012) and knock-out (Chang et al. 2013). Conversely, another study (Lebedeva et al. 2011) detected only minor effect of HuR knockdown on total miRNA levels; however, this

study was performed in non-stressed HeLa cells, where HuR is predominantly nuclear. Of note, Bhattacharaya et al. did not detect a decrease of miR-122 levels accompanying the HuR-mediated relief of CAT-1 mRNA repression upon amino acid starvation (Bhattacharyya et al. 2006). One possible explanation might be that increased miRNA turnover upon stress is being actively compensated for by an increase in miRNA biogenesis, which would result in comparable steady state levels.

We verified the effect of HuR on miRNA levels in a deep sequencing experiment, using HCT116 cells in which HuR is constitutively localized in nucleus as well as cytoplasm even under non-stress conditions. We found that HuR knockdown leads to a modest upregulation of several mature miRNAs (up to 2-fold). Interestingly however, when looking at miRNA isoforms with 3' non-templated A additions, we found a downregulation of these miRNA isoforms and extent of downregulation increased with the number of A-additions. This trend was confirmed for 9 out of 10 individually analyzed miRNA, supporting that miRNA A-tailing in HCT116 cells is indeed, at least in part, dependent on HuR. Importantly, no such effect was observed for miRNA isoforms with 3' non-templated U or other non-A residue additions.

5.12. Mechanistic model for enzymatic turnover of RISC-loaded miRNAs by HuR on the 3'UTR

Based on our data, we propose a model wherein HuR can antagonize the function of miRNAs associated with Ago2 by their enzymatic turnover. To access and degrade the miRNA buried within the complex with Argonaute protein, HuR employs an elaborate multiple step mechanism when bound *in cis* to the same target RNA through an HuR-specific ARE. Very likely accompanied by a release of the ARE, HuR first catalyzes addition of a poly(A) tail to the miRNA 3' end. Thereby it generates a "landing pad" for another hitherto unknown catalytic activity associated with the protein, a 3'→5' exonuclease. Upon the handover from transferase to nuclease activity the protein catalyzes exonucleolytic degradation of the tailed miRNA. The complete turnover of the miRNA body implies that in the process, the miRNA substrate is released from Argonaute. While further mechanistic and structural detail of this sophisticated process remains to be elucidated, this model provides a first mechanistic explanation of how HuR antagonizes miRNA repression.

5.13. Nuclease diversity

HuR is composed of three RRM domains. While the RRM is one of the most widespread and ancient RNA binding domains, present in ~1 % of human proteins, and while RRM-like PALM domain folds are part of many polymerases (see next chapter), the connection between RRM domains and nucleases has not been yet made in the literature. However, nucleases are, as previously discussed (see Introduction), a heterogeneous group encompassing many different protein folds and catalytic center organizations. Members of one family of nucleases (the PD-(D/E)XK superfamily) share a structural core composed of four β -sheets flanked by two α -helices, similar to RRM domains which adopt a $\beta_1\alpha_1\beta_2\beta_3\alpha_2\beta_4$ topology forming a four-stranded β -sheet packed against two α -helices. The first members of the PD-(D/E)XK superfamily were initially identified as type II restriction enzymes (endonucleases), but now include exonucleases, transposases and ssDNA nicking enzymes (reviewed in (Kosinski et al. 2005)). The active sites vary, and can be composed of different combinations of 2-3 acidic residues (D and E, occasionally replaced by N and Q) and lysine (which can be substituted for an acidic residue). The side chains may be located in different parts of the primary sequence, only maintaining their position in the three-dimensional organization of the molecule. The authors summarize: "That ... suggests that more strongly diverged members still await discovery".

5.14. Catalytic activity – a novel function of the RRM domain?

A number of polymerases contain PALM domains with RRM-like folds (Anantharaman et al. 2010). In tRNA(His) guanylyltransferase (Thg1) for example, the catalytic site is thought to be composed of three acidic residues situated in the linker regions at the end on the first β -sheet and in the hairpin region between sheets 2 and 3. Although HuR possesses several surface exposed acidic residues located outside secondary structures, the distribution of these residues does not conform to this arrangement. In contrast, HuR transferase activity was impaired upon exchange of D105, an amino acid located between RRM1 and 2, to alanine. An additional amino acid, E101 is found in the immediate proximity of D105 in the crystal structure of HuR, and could conceivably, in combination with the N-terminal peptide which was not part of the

crystallization construct but contains 5 additional acidic amino acid residues, constitute a catalytic center.

In general, for free miRNA substrates we consistently observed that whenever transferase activity was reduced (eg for tailing mutants D105A or D254A, in absence of ATP or for poor tailing substrates) this resulted in an increase in exonucleolytic processing, suggesting that in absence of a confined conformational arrangement on a mutual target, the two reactions compete with each. One possibility for such a competition would be that the substrate binds in two different modes positioning the 3' end either in one or the other catalytic center. However, as an alternative explanation the transferase and exonuclease activities might be an opposing function of the same catalytic center. A precedent for such a two-way enzymatic activity is given by Polynucleotide Phosphorylase (PNPase), a component of the bacterial degradosome, which uses the same poly(A)-dependent degradation strategy. PNPase can act both as a 3' poly(A)polymerase and a 3'→5' exonuclease (Mohanty & Kushner 2000) using one catalytic center. This is enabled by employing a phosphorolytic rather than a hydrolytic nuclease mechanism – which is the only energetic possibility for a fully reversible reaction since the energy of the cleaved phosphodiester bond is conserved in nucleoside-diphosphates as leaving groups. Interestingly, the HuR₁₂ crystal structure reveals a sulfate ion tightly bound in the region where the N-term and D105 come close together, which is furthermore in vicinity of the 3' end of the bound RNA. However, more work remains to be done and future efforts must be focused on the elucidation of the catalytic residues in HuR by mutational analysis.

5.15. Summary and outlook

The tailing- and trimming-dependent antagonization of Ago-loaded miRNA mediated by HuR represents a possible mechanism of how HuR, together with RISC, can co-regulate mutual target mRNAs. Possibly, it acts synergistically with the reported oligomerization of HuR on target RNA, providing mechanistic means to antagonize the repressive function of miRNA bound to the same mRNA even far away from the HuR binding region. However, the proposed mechanism needs more testing to uncover the exact biological context and miRNAs which act as HuR substrates *in vivo*. Especially, the context in which HuR acts competitively or cooperatively with a miRNA on a message will be interesting to elucidate. In addition, the HuR enzymatic activities need to be

investigated in more detail, with a focus on identification and characterization of the catalytic centers. Finally, the in depth mechanism of this sophisticated molecular process, including contact of miRNA deeply buried within Argonaute, handover from ARE to miRNA substrate, transition from tailing to trimming, and unloading of the miRNA from Argonaute remain to be studied in depth with biophysical, biochemical, and structural biological methods.

6. References

- Abdelmohsen, K. et al., 2008. miR-519 reduces cell proliferation by lowering RNA-binding protein HuR levels. *Proc.Natl.Acad.Sci.U.S.A.*, 105(51), pp.20297–20302.
- Abdelmohsen, K. et al., 2008. Posttranscriptional gene regulation by RNA-binding proteins during oxidative stress: implications for cellular senescence. *Biological chemistry*, 389(3), pp.243–55. Available at: <http://www.ncbi.nlm.nih.gov/pubmed/18177264> [Accessed January 25, 2014].
- Abelson, J., Trotta, C.R. & Li, H., 1998. tRNA splicing. *The Journal of biological chemistry*, 273(21), pp.12685–8. Available at: <http://www.ncbi.nlm.nih.gov/pubmed/9582290> [Accessed November 4, 2013].
- Amarasinghe, G.K. et al., 2000. NMR structure of the HIV-1 nucleocapsid protein bound to stem-loop SL2 of the psi-RNA packaging signal. Implications for genome recognition. *Journal of molecular biology*, 301(2), pp.491–511. Available at: <http://www.ncbi.nlm.nih.gov/pubmed/10926523> [Accessed October 30, 2013].
- Ameres, S.L. et al., 2010. Target RNA-directed trimming and tailing of small silencing RNAs. *Science (New York, N.Y.)*, 328(5985), pp.1534–9. Available at: <http://www.pubmedcentral.nih.gov/articlerender.fcgi?artid=2902985&tool=pmcentrez&rendertype=abstract> [Accessed October 18, 2013].
- Ameres, S.L. & Fukunaga, R., 2010. Riding in silence: a little snowboarding, a lot of small RNAs. *Silence*, 1(1), p.8. Available at: <http://www.pubmedcentral.nih.gov/articlerender.fcgi?artid=2851661&tool=pmcentrez&rendertype=abstract> [Accessed October 21, 2013].
- Anantharaman, V., Iyer, L.M. & Aravind, L., 2010. Presence of a classical RRM-fold palm domain in Thg1-type 3'-5' nucleic acid polymerases and the origin of the GGDEF and CRISPR polymerase domains. *Biology direct*, 5(1), p.43. Available at: <http://www.biology-direct.com/content/5/1/43> [Accessed November 4, 2013].
- Ashraf, S.I. & Kunes, S., 2006. A trace of silence: memory and microRNA at the synapse. *Current opinion in neurobiology*, 16(5), pp.535–9. Available at: <http://www.ncbi.nlm.nih.gov/pubmed/16962314> [Accessed January 23, 2014].
- Atasoy, U. et al., 1999. ELAV protein HuA (HuR) can redistribute between nucleus and cytoplasm and is upregulated during serum stimulation and T cell activation. *Journal of Cell Science*, 111(21), pp.3145–3156. Available at: <http://jcs.biologists.org/cgi/content/abstract/111/21/3145>.
- Avraham, R. et al., 2010. EGF decreases the abundance of microRNAs that restrain oncogenic transcription factors. *Science signaling*, 3(124), p.ra43. Available at: <http://www.ncbi.nlm.nih.gov/pubmed/20516477> [Accessed January 26, 2014].

- Baccarini, A. et al., 2011. Kinetic analysis reveals the fate of a microRNA following target regulation in mammalian cells. *Current biology : CB*, 21(5), pp.369–76. Available at: <http://www.pubmedcentral.nih.gov/articlerender.fcgi?artid=3088433&tool=pmcentrez&rendertype=abstract> [Accessed October 23, 2013].
- Baek, D. et al., 2008. The impact of microRNAs on protein output. *Nature*, 455(7209), pp.64–71. Available at: <http://www.pubmedcentral.nih.gov/articlerender.fcgi?artid=2745094&tool=pmcentrez&rendertype=abstract> [Accessed October 17, 2013].
- Bail, S. et al., 2010. Differential regulation of microRNA stability. *RNA (New York, N.Y.)*, 16(5), pp.1032–9. Available at: <http://www.pubmedcentral.nih.gov/articlerender.fcgi?artid=2856875&tool=pmcentrez&rendertype=abstract> [Accessed November 1, 2013].
- Bailey, T.L., 2011. DREME: motif discovery in transcription factor ChIP-seq data. *Bioinformatics (Oxford, England)*, 27(12), pp.1653–9. Available at: <http://www.pubmedcentral.nih.gov/articlerender.fcgi?artid=3106199&tool=pmcentrez&rendertype=abstract> [Accessed January 27, 2014].
- Bailey, T.L. & Elkan, C., 1994. Fitting a mixture model by expectation maximization to discover motifs in biopolymers. *Proceedings / ... International Conference on Intelligent Systems for Molecular Biology ; ISMB. International Conference on Intelligent Systems for Molecular Biology*, 2, pp.28–36. Available at: <http://www.ncbi.nlm.nih.gov/pubmed/7584402> [Accessed January 21, 2014].
- Bakheet, T. et al., 2001. ARED: human AU-rich element-containing mRNA database reveals an unexpectedly diverse functional repertoire of encoded proteins. *Nucleic Acids Res.*, 29(1), pp.246–254.
- Bakheet, T., Williams, B.R. & Khabar, K.S., 2003. ARED 2.0: an update of AU-rich element mRNA database. *Nucleic Acids Res.*, 31(1), pp.421–423.
- Bakheet, T., Williams, B.R. & Khabar, K.S., 2006. ARED 3.0: the large and diverse AU-rich transcriptome. *Nucleic Acids Res.*, 34(Database issue), pp.D111–D114.
- Barreau, C., Paillard, L. & Osborne, H.B., 2005. AU-rich elements and associated factors: are there unifying principles? *Nucleic Acids Res.*, 33(22), pp.7138–7150. Available at: <http://www.pubmedcentral.nih.gov/articlerender.fcgi?artid=1325018&tool=pmcentrez&rendertype=abstract> [Accessed October 17, 2013].
- Beckel-Mitchener, A.C. et al., 2002. Poly(A) Tail Length-dependent Stabilization of GAP-43 mRNA by the RNA-binding Protein HuD. *Journal of Biological Chemistry*, 277(31), pp.27996–28002. Available at: <http://www.jbc.org/cgi/content/abstract/277/31/27996>.
- Behm-Ansmant, I. et al., 2006. mRNA degradation by miRNAs and GW182 requires both CCR4:NOT deadenylase and DCP1:DCP2 decapping complexes. *Genes & development*,

20(14), pp.1885–98. Available at:
<http://www.pubmedcentral.nih.gov/articlerender.fcgi?artid=1522082&tool=pmcentrez&rendertype=abstract> [Accessed October 21, 2013].

Bhattacharyya, S. et al., 2006. Relief of microRNA-mediated translational repression in human cells subjected to stress. *Cell*, 125(6), pp.1111–1124. Available at:
<http://www.ncbi.nlm.nih.gov/pubmed/16777601> [Accessed October 17, 2013].

Boland, A. et al., 2011. Crystal structure of the MID-PIWI lobe of a eukaryotic Argonaute protein. *Proceedings of the National Academy of Sciences of the United States of America*, 108(26), pp.10466–71. Available at:
<http://www.pubmedcentral.nih.gov/articlerender.fcgi?artid=3127882&tool=pmcentrez&rendertype=abstract> [Accessed October 21, 2013].

Bregues, M., Teixeira, D. & Parker, R., 2005. Movement of eukaryotic mRNAs between polysomes and cytoplasmic processing bodies. *Science (New York, N.Y.)*, 310(5747), pp.486–9. Available at:
<http://www.pubmedcentral.nih.gov/articlerender.fcgi?artid=1863069&tool=pmcentrez&rendertype=abstract> [Accessed October 18, 2013].

Brennan, C.M., Gallouzi, I.-E. & Steitz, J.A., 2000. Protein Ligands to HuR Modulate Its Interaction with Target mRNAs In Vivo. *The Journal of Cell Biology*, 151(1), pp.1–13. Available at:
<http://www.jcb.org/cgi/content/full/151/1/1>.

Brennecke, J. et al., 2005. Principles of microRNA-target recognition. *PLoS biology*, 3(3), p.e85. Available at:
<http://www.pubmedcentral.nih.gov/articlerender.fcgi?artid=1043860&tool=pmcentrez&rendertype=abstract> [Accessed October 21, 2013].

Brodersen, P. & Voinnet, O., 2009. Revisiting the principles of microRNA target recognition and mode of action. *Nature reviews. Molecular cell biology*, 10(2), pp.141–8. Available at:
<http://www.ncbi.nlm.nih.gov/pubmed/19145236> [Accessed October 21, 2013].

Budde-Steffen, C. et al., 1988. Expression of an antigen in small cell lung carcinoma lines detected by antibodies from patients with paraneoplastic dorsal root ganglionopathy. *Cancer Res.*, 48(2), pp.430–434.

Bühler, M. et al., 2008. TRAMP-mediated RNA surveillance prevents spurious entry of RNAs into the *Schizosaccharomyces pombe* siRNA pathway. *Nature structural & molecular biology*, 15(10), pp.1015–23. Available at:
<http://www.pubmedcentral.nih.gov/articlerender.fcgi?artid=3240669&tool=pmcentrez&rendertype=abstract> [Accessed November 6, 2013].

Burroughs, a M. et al., 2010. A comprehensive survey of 3' animal miRNA modification events and a possible role for 3' adenylation in modulating miRNA targeting effectiveness. *Genome Res.*, 20(10), pp.1398–1410. Available at:

<http://www.pubmedcentral.nih.gov/articlerender.fcgi?artid=2945189&tool=pmcentrez&rendertype=abstract> [Accessed October 17, 2013].

- Cai, X., Hagedorn, C.H. & Cullen, B.R., 2004. Human microRNAs are processed from capped, polyadenylated transcripts that can also function as mRNAs. *RNA*, 10(12), pp.1957–1966.
- Campos, A.R., Grossman, D. & White, K., 1985. Mutant alleles at the locus *elav* in *Drosophila melanogaster* lead to nervous system defects. A developmental-genetic analysis. *J.Neurogenet.*, 2(3), pp.197–218.
- Caput, D. et al., 1986. Identification of a common nucleotide sequence in the 3'-untranslated region of mRNA molecules specifying inflammatory mediators. *Proceedings of the National Academy of Sciences of the United States of America*, 83(6), pp.1670–4. Available at: <http://www.pubmedcentral.nih.gov/articlerender.fcgi?artid=323145&tool=pmcentrez&rendertype=abstract> [Accessed February 1, 2014].
- Carballo, E., Lai, W.S. & Blackshear, P.J., 2000. Evidence that tristetraprolin is a physiological regulator of granulocyte-macrophage colony-stimulating factor messenger RNA deadenylation and stability. *Blood*, 95(6), pp.1891–1899.
- Cazalla, D. & Steitz, J. a, 2010. Down-regulation of a host microRNA by a viral noncoding RNA. *Cold Spring Harbor symposia on quantitative biology*, 75, pp.321–4. Available at: <http://www.ncbi.nlm.nih.gov/pubmed/21139068> [Accessed October 17, 2013].
- Cerutti, H. & Ibrahim, F., 2010. Turnover of mature miRNAs and siRNAs in plants and algae. *Advances in experimental medicine and biology*, 700, pp.124–39. Available at: <http://www.ncbi.nlm.nih.gov/pubmed/21627035> [Accessed November 6, 2013].
- Chang, J. et al., 2004. miR-122, a Mammalian Liver-Specific microRNA, is Processed from hcr mRNA and May Downregulate the High Affinity Cationic Amino Acid Transporter CAT-1. *RNA biology*, 1(2), pp.106–13. Available at: <http://www.ncbi.nlm.nih.gov/pubmed/17179747> [Accessed December 11, 2013].
- Chang, N. et al., 2010. HuR uses AUF1 as a cofactor to promote p16INK4 mRNA decay. *Molecular and Cellular Biology*, 30(15), pp.3875–3886.
- Chang, S.H. et al., 2013. Antagonistic function of the RNA-binding protein HuR and miR-200b in post-transcriptional regulation of vascular endothelial growth factor-A expression and angiogenesis. *Journal of Biological Chemistry*, 288(7), pp.4908–4921. Available at: <http://www.ncbi.nlm.nih.gov/pubmed/23223443> [Accessed November 1, 2013].
- Chatterjee, S. et al., 2011. Target-mediated protection of endogenous microRNAs in *C. elegans*. *Developmental cell*, 20(3), pp.388–96. Available at: [http://www.cell.com/developmental-cell/fulltext/S1534-5807\(11\)00077-3](http://www.cell.com/developmental-cell/fulltext/S1534-5807(11)00077-3) [Accessed January 23, 2014].

- Chatterjee, S. & Grosshans, H., 2009. Active turnover modulates mature microRNA activity in *Caenorhabditis elegans*. *Nature*, 461(7263), pp.546–9. Available at: <http://www.ncbi.nlm.nih.gov/pubmed/19734881> [Accessed October 21, 2013].
- Chen, C.-Y.A. et al., 2009. Ago-TNRC6 triggers microRNA-mediated decay by promoting two deadenylation steps. *Nature structural & molecular biology*, 16(11), pp.1160–6. Available at: <http://www.pubmedcentral.nih.gov/articlerender.fcgi?artid=2921184&tool=pmcentrez&rendertype=abstract> [Accessed October 21, 2013].
- Chen, C.Y. & Shyu, A.B., 1996. AU-rich elements: characterization and importance in mRNA degradation. *Trends Biochem Sci*, 20(11), pp.465–470.
- Chendrimada, T.P. et al., 2005. TRBP recruits the Dicer complex to Ago2 for microRNA processing and gene silencing. *Nature*, 436(7051), pp.740–744.
- Cherry, J. et al., 2006. HuR, an RNA-binding protein, involved in the control of cellular differentiation. *In Vivo.*, 20(1), pp.17–23.
- Chu, C.-Y. & Rana, T.M., 2007. Small RNAs: regulators and guardians of the genome. *Journal of cellular physiology*, 213(2), pp.412–9. Available at: <http://www.ncbi.nlm.nih.gov/pubmed/17674365> [Accessed November 4, 2013].
- Cléry, A., Blatter, M. & Allain, F.H.-T., 2008. RNA recognition motifs: boring? Not quite. *Current opinion in structural biology*, 18(3), pp.290–8. Available at: <http://www.ncbi.nlm.nih.gov/pubmed/18515081> [Accessed October 31, 2013].
- Cléry, A. & H.-T. Allain, F., 2012. From Structure to Function of RNA Binding Domains. In *RNA binding protein*.
- Cok, S.J., Acton, S.J. & Morrison, A.R., 2003. The proximal region of the 3'-untranslated region of cyclooxygenase-2 is recognized by a multimeric protein complex containing HuR, TIA-1, TIAR, and the heterogeneous nuclear ribonucleoprotein U. *Journal of Biological Chemistry*, 278(38), pp.36157–36162.
- Coller, J. & Parker, R., 2005. General translational repression by activators of mRNA decapping. *Cell*, 122(6), pp.875–86. Available at: <http://www.pubmedcentral.nih.gov/articlerender.fcgi?artid=1853273&tool=pmcentrez&rendertype=abstract> [Accessed October 21, 2013].
- Condon, C., 2007. Maturation and degradation of RNA in bacteria. *Current opinion in microbiology*, 10(3), pp.271–8. Available at: <http://www.ncbi.nlm.nih.gov/pubmed/17560162> [Accessed November 6, 2013].
- Cook, H.L., Mischo, H.E. & Steitz, J.A., 2004. The Herpesvirus saimiri small nuclear RNAs recruit AU-rich element-binding proteins but do not alter host AU-rich element-containing mRNA levels in virally transformed T cells. *Mol. Cell Biol.*, 24(10), pp.4522–4533.

- Cowan, J. a, 2002. Structural and catalytic chemistry of magnesium-dependent enzymes. *Biometals : an international journal on the role of metal ions in biology, biochemistry, and medicine*, 15(3), pp.225–35. Available at: <http://www.ncbi.nlm.nih.gov/pubmed/12206389> [Accessed November 4, 2013].
- Dalmau, J. et al., 1991. Detection of the anti-Hu antibody in specific regions of the nervous system and tumor from patients with paraneoplastic encephalomyelitis/sensory neuronopathy. *Neurology*, 41(11), pp.1757–1764.
- Dalmau, J. et al., 1990. Detection of the anti-Hu antibody in the serum of patients with small cell lung cancer--a quantitative western blot analysis. *Ann.Neurol.*, 27(5), pp.544–552.
- Das, S.K. et al., 2010. Human polynucleotide phosphorylase selectively and preferentially degrades microRNA-221 in human melanoma cells. *Proceedings of the National Academy of Sciences of the United States of America*, 107(26), pp.11948–53. Available at: <http://www.pubmedcentral.nih.gov/articlerender.fcgi?artid=2900648&tool=pmcentrez&rendertype=abstract> [Accessed November 1, 2013].
- De, N. et al., 2013. Highly complementary target RNAs promote release of guide RNAs from human Argonaute2. *Molecular cell*, 50(3), pp.344–55. Available at: <http://www.ncbi.nlm.nih.gov/pubmed/23664376> [Accessed October 31, 2013].
- Dean, J.L.E. et al., 2001. The 3'-Untranslated region of Tumor Necrosis Factor Alpha mRNA Is a Target of the mRNA-Stabilizing Factor HuR. *Molecular and Cellular Biology*, 21(3), pp.721–730.
- Dellavalle, R.P., Petersen, R. & Lindquist, S., 1994. Preferential deadenylation of Hsp70 mRNA plays a key role in regulating Hsp70 expression in *Drosophila melanogaster*. *Mol.Cell Biol.*, 14(6), pp.3646–3659.
- Derech-Haim, S. et al., 2012. Ribonuclease activity of p53 in cytoplasm in response to various stress signals. *Cell cycle (Georgetown, Tex.)*, 11(7), pp.1400–13. Available at: <http://www.ncbi.nlm.nih.gov/pubmed/22421154> [Accessed January 26, 2014].
- Deutscher, M.P., Marshall, G.T. & Cudny, H., 1988. RNase PH: an *Escherichia coli* phosphate-dependent nuclease distinct from polynucleotide phosphorylase. *Proceedings of the National Academy of Sciences of the United States of America*, 85(13), pp.4710–4. Available at: <http://www.pubmedcentral.nih.gov/articlerender.fcgi?artid=280505&tool=pmcentrez&rendertype=abstract> [Accessed November 4, 2013].
- Devaux, A., Colegrove-Otero, L.J. & Standart, N., 2006. *Xenopus* ElrB, but not ElrA, binds RNA as an oligomer: possible role of the linker. *FEBS Lett.*, 580(20), pp.4947–4952.
- Didiano, D. & Hobert, O., 2006. Perfect seed pairing is not a generally reliable predictor for miRNA-target interactions. *Nature structural & molecular biology*, 13(9), pp.849–51.

Available at: <http://www.ncbi.nlm.nih.gov/pubmed/16921378> [Accessed October 21, 2013].

- Diederichs, S. & Haber, D.A., 2007. Dual role for argonautes in microRNA processing and posttranscriptional regulation of microRNA expression. *Cell*, 131(6), pp.1097–108. Available at: <http://www.ncbi.nlm.nih.gov/pubmed/18083100> [Accessed November 5, 2013].
- Doench, J.G. & Sharp, P.A., 2004. Specificity of microRNA target selection in translational repression. *Genes & development*, 18(5), pp.504–11. Available at: <http://www.pubmedcentral.nih.gov/articlerender.fcgi?artid=374233&tool=pmcentrez&rendertype=abstract> [Accessed October 17, 2013].
- Dormoy-Raclet, V. et al., 2013. HuR and miR-1192 regulate myogenesis by modulating the translation of HMGB1 mRNA. *Nature communications*, 4, p.2388. Available at: <http://www.ncbi.nlm.nih.gov/pubmed/24005720> [Accessed December 3, 2013].
- Epis, M.R. et al., 2011. The RNA-binding protein HuR opposes the repression of ERBB-2 gene expression by microRNA miR-331-3p in prostate cancer cells. *Journal of Biological Chemistry*, 286(48), pp.41442–41454.
- Epis, M.R. et al., 2011. The RNA-binding protein HuR opposes the repression of ERBB-2 gene expression by microRNA miR-331-3p in prostate cancer cells. *Journal of Biological Chemistry*, 286(48), pp.41442–41454. Available at: <http://www.pubmedcentral.nih.gov/articlerender.fcgi?artid=3308856&tool=pmcentrez&rendertype=abstract> [Accessed January 28, 2014].
- Eulalio, A., Huntzinger, E. & Izaurralde, E., 2008. GW182 interaction with Argonaute is essential for miRNA-mediated translational repression and mRNA decay. *Nature structural & molecular biology*, 15(4), pp.346–53. Available at: <http://www.ncbi.nlm.nih.gov/pubmed/18345015> [Accessed November 15, 2013].
- Fan, X.C. & Steitz, J.A., 1998. HNS, a nuclear-cytoplasmic shuttling sequence in HuR. *Proc.Natl.Acad.Sci.USA*, 95, pp.15293–15298.
- Fan, X.C. & Steitz, J.A., 2001. Overexpression of HuR, a nuclear-cytoplasmic shuttling protein, increases the in vivo stability of ARE-containing mRNAs. *The EMBO Journal*, 17(12), pp.3448–3460.
- Fialcowitz-White, E.J. et al., 2007. Specific protein domains mediate cooperative assembly of HuR oligomers on AU-rich mRNA-destabilizing sequences. *Journal of Biological Chemistry*, 282(29), pp.20948–20959.
- Fischer, U. et al., Rev-mediated nuclear export of RNA is dominant over nuclear retention and is coupled to the Ran-GTPase cycle. *Nucleic Acids Res.*, 27(21), pp.4128–4134.

- Ford, L.P. et al., 1999. ELAV proteins stabilize deadenylated intermediates in a novel in vitro mRNA deadenylation/degradation system. *Genes Dev.*, 13(2), pp.188–201.
- Friedhoff, P. et al., 1999. A similar active site for non-specific and specific endonucleases. *Nature structural biology*, 6(2), pp.112–3. Available at: <http://www.ncbi.nlm.nih.gov/pubmed/10048918> [Accessed November 4, 2013].
- Friedman, R.C. et al., 2009. Most mammalian mRNAs are conserved targets of microRNAs. *Genome research*, 19(1), pp.92–105. Available at: <http://www.pubmedcentral.nih.gov/articlerender.fcgi?artid=2612969&tool=pmcentrez&rendertype=abstract> [Accessed October 17, 2013].
- Frith, M.C. et al., 2008. Discovering sequence motifs with arbitrary insertions and deletions. *PLoS computational biology*, 4(4), p.e1000071. Available at: <http://www.pubmedcentral.nih.gov/articlerender.fcgi?artid=2323616&tool=pmcentrez&rendertype=abstract> [Accessed November 20, 2013].
- Fukuda, T. et al., 2007. DEAD-box RNA helicase subunits of the Drosha complex are required for processing of rRNA and a subset of microRNAs. *Nature cell biology*, 9(5), pp.604–11. Available at: <http://www.ncbi.nlm.nih.gov/pubmed/17435748> [Accessed October 18, 2013].
- Gallouzi, I.E., Brennan, C.M. & Steitz, J.A., 2001. Protein ligands mediate the CRM1-dependent export of HuR in response to heat shock. *RNA (New York, N.Y.)*, 7(9), pp.1348–61. Available at: <http://www.pubmedcentral.nih.gov/articlerender.fcgi?artid=1370177&tool=pmcentrez&rendertype=abstract> [Accessed December 2, 2013].
- Gallouzi, I.E. & Wilusz, J., 2013. A DIStinctively novel exoribonuclease that really likes U. *The EMBO journal*, 32(13), pp.1799–801. Available at: <http://www.ncbi.nlm.nih.gov/pubmed/23756464> [Accessed October 17, 2013].
- Gherzi, R. et al., 2004. A KH Domain RNA Binding Protein, KSRP, Promotes ARE-Directed mRNA Turnover by Recruiting the Degradation Machinery. *Mol.Cell*, 14(5), pp.571–583.
- Glorian, V. et al., 2011. HuR-dependent loading of miRNA RISC to the mRNA encoding the Ras-related small GTPase RhoB controls its translation during UV-induced apoptosis. *Cell Death.Differ.*, 18(11), pp.1692–1701.
- Good, P.J., 1995. A conserved family of elav-like genes in vertebrates. *Proc.Natl.Acad.Sci.USA*, 92, pp.4557–4561.
- Grindley, N.D.F., Whiteson, K.L. & Rice, P.A., 2006. Mechanisms of site-specific recombination. *Annual review of biochemistry*, 75, pp.567–605. Available at: <http://www.ncbi.nlm.nih.gov/pubmed/16756503> [Accessed November 4, 2013].

- Grishin, N. V., 2001. KH domain: one motif, two folds. *Nucleic Acids Res.*, 29(3), pp.638–643. Available at: <http://www.pubmedcentral.nih.gov/articlerender.fcgi?artid=30387&tool=pmcentrez&rendertype=abstract> [Accessed November 5, 2013].
- Guil, S. & Cáceres, J.F., 2007. The multifunctional RNA-binding protein hnRNP A1 is required for processing of miR-18a. *Nature structural & molecular biology*, 14(7), pp.591–6. Available at: <http://www.ncbi.nlm.nih.gov/pubmed/17558416> [Accessed October 18, 2013].
- Guo, H. et al., 2010. Mammalian microRNAs predominantly act to decrease target mRNA levels. *Nature*, 466(7308), pp.835–40. Available at: <http://www.pubmedcentral.nih.gov/articlerender.fcgi?artid=2990499&tool=pmcentrez&rendertype=abstract> [Accessed October 18, 2013].
- Guo, X., Wu, Y. & Hartley, R.S., 2009. MicroRNA-125a represses cell growth by targeting HuR in breast cancer. *RNA.Biol.*, 6(5), pp.575–583.
- Guttinger, S. et al., 2004. From The Cover: Transportin2 functions as importin and mediates nuclear import of HuR. *Proc.Natl.Acad.Sci.U.S.A*, 101(9), pp.2918–2923.
- Von der Haar, T., Ball, P.D. & McCarthy, J.E., 2000. Stabilization of eukaryotic initiation factor 4E binding to the mRNA 5'-Cap by domains of eIF4G. *Journal of Biological Chemistry*, 275(39), pp.30551–30555.
- Haase, A.D. et al., 2005. TRBP, a regulator of cellular PKR and HIV-1 virus expression, interacts with Dicer and functions in RNA silencing. *EMBO reports*, 6(10), pp.961–7. Available at: <http://www.pubmedcentral.nih.gov/articlerender.fcgi?artid=1369185&tool=pmcentrez&rendertype=abstract> [Accessed October 21, 2013].
- Hagan, J.P., Piskounova, E. & Gregory, R.I., 2009. Lin28 recruits the TUTase Zcchc11 to inhibit let-7 maturation in mouse embryonic stem cells. *Nature structural & molecular biology*, 16(10), pp.1021–5. Available at: <http://dx.doi.org/10.1038/nsmb.1676> [Accessed November 5, 2013].
- Han, B.W. et al., 2011. The 3'-to-5' exoribonuclease Nibbler shapes the 3' ends of microRNAs bound to *Drosophila* Argonaute1. *Curr.Biol.*, 21(22), pp.1878–1887. Available at: <http://www.pubmedcentral.nih.gov/articlerender.fcgi?artid=3236499&tool=pmcentrez&rendertype=abstract> [Accessed October 17, 2013].
- Helwak, A. et al., 2013. Mapping the human miRNA interactome by CLASH reveals frequent noncanonical binding. *Cell*, 153(3), pp.654–65. Available at: <http://www.pubmedcentral.nih.gov/articlerender.fcgi?artid=3650559&tool=pmcentrez&rendertype=abstract> [Accessed October 21, 2013].
- Hendrickson, D.G. et al., 2009. Concordant regulation of translation and mRNA abundance for hundreds of targets of a human microRNA. *PLoS biology*, 7(11), p.e1000238. Available at:

<http://www.pubmedcentral.nih.gov/articlerender.fcgi?artid=2766070&tool=pmcentrez&rendertype=abstract> [Accessed October 21, 2013].

Heo, I. et al., 2009. TUT4 in concert with Lin28 suppresses microRNA biogenesis through pre-microRNA uridylation. *Cell*, 138(4), pp.696–708. Available at: <http://www.ncbi.nlm.nih.gov/pubmed/19703396> [Accessed October 18, 2013].

Houseley, J., LaCava, J. & Tollervey, D., 2006. RNA-quality control by the exosome. *Nature reviews. Molecular cell biology*, 7(7), pp.529–39. Available at: <http://www.ncbi.nlm.nih.gov/pubmed/16829983> [Accessed November 6, 2013].

Hsia, K.-C., Li, C.-L. & Yuan, H.S., 2005. Structural and functional insight into sugar-nonspecific nucleases in host defense. *Current opinion in structural biology*, 15(1), pp.126–34. Available at: <http://www.ncbi.nlm.nih.gov/pubmed/15718143> [Accessed November 4, 2013].

Hwang, H.-W., Wentzel, E.A. & Mendell, J.T., 2007. A hexanucleotide element directs microRNA nuclear import. *Science (New York, N.Y.)*, 315(5808), pp.97–100. Available at: <http://www.sciencemag.org/content/315/5808/97.long> [Accessed October 31, 2013].

Ibrahim, F. et al., 2010. Uridylation of mature miRNAs and siRNAs by the MUT68 nucleotidyltransferase promotes their degradation in *Chlamydomonas*. *Proceedings of the National Academy of Sciences of the United States of America*, 107(8), pp.3906–11. Available at: <http://www.pubmedcentral.nih.gov/articlerender.fcgi?artid=2840426&tool=pmcentrez&rendertype=abstract> [Accessed November 6, 2013].

Iost, I. & Dreyfus, M., 2006. DEAD-box RNA helicases in *Escherichia coli*. *Nucleic acids research*, 34(15), pp.4189–97. Available at: <http://www.pubmedcentral.nih.gov/articlerender.fcgi?artid=1616957&tool=pmcentrez&rendertype=abstract> [Accessed November 6, 2013].

Jacob, F. & Monod, J., 1961. Genetic regulatory mechanisms in the synthesis of proteins. *J.Mol.Biol.*, 3, pp.318–356.

Jafarifar, F. et al., 2011. Repression of VEGFA by CA-rich element-binding microRNAs is modulated by hnRNP L. *The EMBO journal*, 30(7), pp.1324–34. Available at: <http://www.pubmedcentral.nih.gov/articlerender.fcgi?artid=3094116&tool=pmcentrez&rendertype=abstract> [Accessed January 26, 2014].

Jing, Q. et al., 2005. Involvement of microRNA in AU-rich element-mediated mRNA instability. *Cell.*, 120(5), pp.623–634. Available at: <http://www.ncbi.nlm.nih.gov/pubmed/15766526> [Accessed October 17, 2013].

Jones, M.R. et al., 2009. Zcchc11-dependent uridylation of microRNA directs cytokine expression. *Nat.Cell Biol.*, 11(9), pp.1157–1163.

- Jones-Rhoades, M.W., Bartel, D.P. & Bartel, B., 2006. MicroRNAs and their regulatory roles in plants. *Annual review of plant biology*, 57, pp.19–53. Available at: <http://www.ncbi.nlm.nih.gov/pubmed/16669754> [Accessed October 21, 2013].
- Juvvuna, P.K. et al., 2012. Argonaute identity defines the length of mature mammalian microRNAs. *Nucleic acids research*, 40(14), pp.6808–20. Available at: <http://www.pubmedcentral.nih.gov/articlerender.fcgi?artid=3413106&tool=pmcentrez&rendertype=abstract> [Accessed November 6, 2013].
- Kai, Z.S. & Pasquinelli, A.E., 2010. MicroRNA assassins : factors that regulate the disappearance of miRNAs. *Nature Structural & Molecular Biology*, 17(1), pp.5–10. Available at: <http://www.ncbi.nlm.nih.gov/pubmed/20051982> [Accessed November 6, 2013].
- Kammaing, L.M. et al., 2010. Hen1 is required for oocyte development and piRNA stability in zebrafish. *The EMBO journal*, 29(21), pp.3688–700. Available at: <http://www.pubmedcentral.nih.gov/articlerender.fcgi?artid=2982757&tool=pmcentrez&rendertype=abstract> [Accessed January 22, 2014].
- Kao, H.-I. & Bambara, R.A., 2003. The protein components and mechanism of eukaryotic Okazaki fragment maturation. *Critical reviews in biochemistry and molecular biology*, 38(5), pp.433–52. Available at: <http://www.ncbi.nlm.nih.gov/pubmed/14693726> [Accessed November 4, 2013].
- Kasashima, K. et al., 2002. Complex formation of the neuron-specific ELAV-like Hu RNA-binding proteins. *Nucleic Acids Res.*, 30(20), pp.4519–4526. Available at: <http://nar.oupjournals.org/cgi/content/abstract/30/20/4519>.
- Kask, P. et al., 2000. Two-dimensional fluorescence intensity distribution analysis: theory and applications. *Biophysical journal*, 78(4), pp.1703–13. Available at: <http://www.pubmedcentral.nih.gov/articlerender.fcgi?artid=1300767&tool=pmcentrez&rendertype=abstract> [Accessed February 17, 2014].
- Katoh, T. et al., 2009. Selective stabilization of mammalian microRNAs by 3' adenylation mediated by the cytoplasmic poly(A) polymerase GLD-2. *Genes Dev.*, 23(4), pp.433–438. Available at: <http://www.pubmedcentral.nih.gov/articlerender.fcgi?artid=2648654&tool=pmcentrez&rendertype=abstract> [Accessed October 17, 2013].
- Kedde, M. et al., 2010. A Pumilio-induced RNA structure switch in p27-3' UTR controls miR-221 and miR-222 accessibility. *Nature cell biology*, 12(10), pp.1014–20. Available at: <http://www.ncbi.nlm.nih.gov/pubmed/20818387> [Accessed January 21, 2014].
- Kedde, M., 2008. Interplay between microRNAs and RNA-binding proteins determines developmental processes. *Development, Germ Cell*, (April), pp.899–903.

- Kedde, M. et al., 2007. RNA-binding protein Dnd1 inhibits microRNA access to target mRNA. *Cell*, 131(7), pp.1273–86. Available at: <http://www.ncbi.nlm.nih.gov/pubmed/18155131> [Accessed January 21, 2014].
- Kedde, M. & Agami, R., 2008. Interplay between microRNAs and RNA-binding proteins determines developmental processes. *Cell Cycle*, 7(7), pp.899–903.
- Kedersha, N. & Anderson, P., 2002. Stress granules: sites of mRNA triage that regulate mRNA stability and translatability. *Biochem.Soc.Trans.*, 30(Pt 6), pp.963–969.
- Ketting, R.F. et al., 2001. Dicer functions in RNA interference and in synthesis of small RNA involved in developmental timing in *C. elegans*. *Genes Dev.*, 15(20), pp.2654–2659. Available at: <http://www.pubmedcentral.nih.gov/articlerender.fcgi?artid=312808&tool=pmcentrez&rendertype=abstract> [Accessed October 18, 2013].
- Khan, A.A. et al., 2009. Transfection of small RNAs globally perturbs gene regulation by endogenous microRNAs. *Nature biotechnology*, 27(6), pp.549–55. Available at: <http://www.pubmedcentral.nih.gov/articlerender.fcgi?artid=2782465&tool=pmcentrez&rendertype=abstract> [Accessed November 5, 2013].
- Khvorova, A., Reynolds, A. & Jayasena, S.D., 2003. Functional siRNAs and miRNAs exhibit strand bias. *Cell*, 115(2), pp.209–216.
- Kim, H.H. et al., 2009. HuR recruits let-7/RISC to repress c-Myc expression. *Genes Dev.*, 23(15), pp.1743–1748.
- Kim, Y.-K., Heo, I. & Kim, V.N., 2010. Modifications of small RNAs and their associated proteins. *Cell*, 143(5), pp.703–9. Available at: <http://www.ncbi.nlm.nih.gov/pubmed/21111232> [Accessed October 17, 2013].
- Kojima, K. et al., 2010. MiR-34a attenuates paclitaxel-resistance of hormone-refractory prostate cancer PC3 cells through direct and indirect mechanisms. *Prostate*, 70(14), pp.1501–1512.
- Koonin, E. V & Ilyina, T. V, 1993. Computer-assisted dissection of rolling circle DNA replication. *Bio Systems*, 30(1-3), pp.241–68. Available at: <http://www.ncbi.nlm.nih.gov/pubmed/8374079> [Accessed November 4, 2013].
- Kosinski, J., Feder, M. & Bujnicki, J.M., 2005. The PD-(D/E)XK superfamily revisited: identification of new members among proteins involved in DNA metabolism and functional predictions for domains of (hitherto) unknown function. *BMC bioinformatics*, 6, p.172. Available at: <http://www.pubmedcentral.nih.gov/articlerender.fcgi?artid=1189080&tool=pmcentrez&rendertype=abstract> [Accessed November 4, 2013].
- Krol, J. et al., 2010. Characterizing light-regulated retinal microRNAs reveals rapid turnover as a common property of neuronal microRNAs. *Cell*, 141(4), pp.618–31. Available at: <http://www.ncbi.nlm.nih.gov/pubmed/20478254> [Accessed October 21, 2013].

- Kühlmann, U.C. et al., 1999. Structural parsimony in endonuclease active sites: should the number of homing endonuclease families be redefined? *FEBS letters*, 463(1-2), pp.1–2. Available at: <http://www.ncbi.nlm.nih.gov/pubmed/10601625> [Accessed November 4, 2013].
- Kullmann, M. et al., 2002. ELAV/Hu proteins inhibit p27 translation via an IRES element in the p27 5'UTR. *Genes Dev.*, 16(23), pp.3087–3099. Available at: <http://www.pubmedcentral.nih.gov/articlerender.fcgi?artid=187493&tool=pmcentrez&rendertype=abstract> [Accessed November 6, 2013].
- Kundu, P. et al., 2012. HuR protein attenuates miRNA-mediated repression by promoting miRISC dissociation from the target RNA. *Nucleic Acids Res.*, 40(11), pp.5088–5100.
- Kundu, P., 2011. *Role of RNA Binding Protein HuR in antagonizing the microRNA-mediated Repression*. University of Basel.
- Lafon, I. et al., 1998. Developmental expression of AUF1 and HuR, two c-myc mRNA binding proteins. *Oncogene*, 16(26), pp.3413–3421.
- Lagnado, C.A., Brown, C.Y. & Goodall, G.J., 1994. AUUUA is not sufficient to promote poly(A) shortening and degradation of an mRNA: the functional sequence within AU-rich elements may be UUAUUUA(U/A)(U/A). *Mol.Cell Biol.*, 14(12), pp.7984–7995.
- Lagos-Quintana, M. et al., 2001. Identification of novel genes coding for small expressed RNAs. *Science*, 294(5543), pp.853–858.
- Lai, E.C., 2002. Micro RNAs are complementary to 3' UTR sequence motifs that mediate negative post-transcriptional regulation. *Nature genetics*, 30(4), pp.363–4. Available at: <http://www.ncbi.nlm.nih.gov/pubmed/11896390> [Accessed October 21, 2013].
- Landgraf, P. et al., 2007. A mammalian microRNA expression atlas based on small RNA library sequencing. *Cell*, 129(7), pp.1401–14. Available at: <http://www.pubmedcentral.nih.gov/articlerender.fcgi?artid=2681231&tool=pmcentrez&rendertype=abstract> [Accessed November 6, 2013].
- Lebedeva, S. et al., 2011. Transcriptome-wide Analysis of Regulatory Interactions of the RNA-Binding Protein HuR. *Mol.Cell*, 43(3), pp.340–352.
- Lee, R.C., Feinbaum, R.L. & Ambros, V., 1994. The *C. elegans* heterochronic gene *lin-4* encodes small RNAs with antisense complementarity to *lin-14*. *Cell*, 75(5), pp.843–854.
- Lee, S. et al., 2013. Article Selective Degradation of Host MicroRNAs by an Intergenic HCMV Noncoding RNA Accelerates Virus Production. *Cell Host and Microbe*, 13(6), pp.678–690. Available at: <http://dx.doi.org/10.1016/j.chom.2013.05.007>.
- Lee, Y. et al., 2002. MicroRNA maturation: stepwise processing and subcellular localization. *EMBO J.*, 21(17), pp.4663–4670.

- Lee, Y. et al., 2003. The nuclear RNase III Drosha initiates microRNA processing. *Nature*, 425(6956), pp.415–419. Available at: <http://www.ncbi.nlm.nih.gov/pubmed/14508493> [Accessed October 18, 2013].
- Lehrbach, N.J. et al., 2009. LIN-28 and the poly(U) polymerase PUP-2 regulate let-7 microRNA processing in *Caenorhabditis elegans*. *Nature structural & molecular biology*, 16(10), pp.1016–20. Available at: <http://www.pubmedcentral.nih.gov/articlerender.fcgi?artid=2988485&tool=pmcentrez&rendertype=abstract> [Accessed November 6, 2013].
- Lewis, B.P. et al., 2003. Prediction of mammalian microRNA targets. *Cell*, 115(7), pp.787–98. Available at: <http://www.ncbi.nlm.nih.gov/pubmed/14697198> [Accessed October 18, 2013].
- Lewis, T. et al., 1998. Mapping of a Minimal AU-rich Sequence Required for Lipopolysaccharide-induced Binding of a 55kDa Protein on Tumor Necrosis Factor- α mRNA. *The Journal of Biological Chemistry*, 273(22), pp.13781–13786.
- Li, J. et al., 2005. Methylation protects miRNAs and siRNAs from a 3'-end uridylation activity in *Arabidopsis*. *Current biology : CB*, 15(16), pp.1501–7. Available at: <http://www.ncbi.nlm.nih.gov/pubmed/16111943> [Accessed November 6, 2013].
- Lim, L.P. et al., 2005. Microarray analysis shows that some microRNAs downregulate large numbers of target mRNAs. *Nature*, 433(7027), pp.769–73. Available at: <http://www.ncbi.nlm.nih.gov/pubmed/15685193> [Accessed October 21, 2013].
- Liu, J. et al., 1995. Paraneoplastic encephalomyelitis antigens bind to the AU-rich elements of mRNA. *Neurology*, 45(3 Pt 1), pp.544–550.
- Lopez de Silanes, I., Paz, Q.M. & Esteller, M., 2007. Aberrant regulation of messenger RNA 3'-untranslated region in human cancer. *Cell Oncol.*, 29(1), pp.1–17.
- Lu, S., Sun, Y.-H.H. & Chiang, V.L., 2009. Adenylation of plant miRNAs. *Nucleic Acids Res.*, 37(6), pp.1878–1885. Available at: <http://www.pubmedcentral.nih.gov/articlerender.fcgi?artid=2665221&tool=pmcentrez&rendertype=abstract> [Accessed October 17, 2013].
- Ma, J.-B. et al., 2005. Structural basis for 5'-end-specific recognition of guide RNA by the *A. fulgidus* Piwi protein. *Nature*, 434(7033), pp.666–70. Available at: <http://www.ncbi.nlm.nih.gov/pubmed/15800629> [Accessed October 18, 2013].
- Ma, W.-J., Chung, S. & Furneaux, H., 1997. The ELAV-like proteins bind to AU-rich elements and to the poly(A) tail of mRNA. *Nucleic Acids Research*, 25(18), pp.3564–3569.
- MacRae, I.J. et al., 2008. In vitro reconstitution of the human RISC-loading complex. *Proc.Natl.Acad.Sci.U.S.A.*, 105(2), pp.512–517.

- MacRae, I.J., Zhou, K. & Doudna, J.A., 2007. Structural determinants of RNA recognition and cleavage by Dicer. *Nature structural & molecular biology*, 14(10), pp.934–40. Available at: <http://www.ncbi.nlm.nih.gov/pubmed/17873886> [Accessed October 30, 2013].
- Maguire, M.E. & Cowan, J.A., 2002. Magnesium chemistry and biochemistry. *Biometals : an international journal on the role of metal ions in biology, biochemistry, and medicine*, 15(3), pp.203–10. Available at: <http://www.ncbi.nlm.nih.gov/pubmed/12206387> [Accessed November 4, 2013].
- Maniataki, E. & Mourelatos, Z., 2005. A human, ATP-independent, RISC assembly machine fueled by pre-miRNA. *Genes Dev.*, 19(24), pp.2979–2990. Available at: <http://genesdev.cshlp.org/content/19/24/2979.short> [Accessed October 18, 2013].
- Manival, X. et al., 2001. RNA-binding strategies common to cold-shock domain- and RNA recognition motif-containing proteins. *Nucleic Acids Res.*, 29(11), pp.2223–2233.
- Marcinowski, L. et al., 2012. Degradation of cellular mir-27 by a novel, highly abundant viral transcript is important for efficient virus replication in vivo. *PLoS pathogens*, 8(2), p.e1002510. Available at: <http://www.pubmedcentral.nih.gov/articlerender.fcgi?artid=3276556&tool=pmcentrez&rendertype=abstract> [Accessed November 1, 2013].
- Maris, C., Dominguez, C. & Allain, F.H.-T., 2005. The RNA recognition motif, a plastic RNA-binding platform to regulate post-transcriptional gene expression. *FEBS J.*, 272(9), pp.2118–2131. Available at: <http://www.ncbi.nlm.nih.gov/pubmed/15853797> [Accessed November 3, 2013].
- Martinez, J. & Tuschl, T., 2004. RISC is a 5' phosphomonoester-producing RNA endonuclease. *Genes & development*, 18(9), pp.975–80. Available at: <http://www.pubmedcentral.nih.gov/articlerender.fcgi?artid=406288&tool=pmcentrez&rendertype=abstract> [Accessed November 6, 2013].
- Meijlink, F. et al., 1985. Removal of a 67-base-pair sequence in the noncoding region of protooncogene fos converts it to a transforming gene. *Proc.Natl.Acad.Sci.U.S.A.*, 82(15), pp.4987–4991.
- Meisner, N.-C. et al., 2004. mRNA Openers and Closers : Modulating AU- Rich Element- Controlled mRNA Stability by a Molecular Switch in mRNA Secondary Structure. , pp.1432–1447.
- Meisner, N.-C. & Filipowicz, W., 2010. Properties of the regulatory RNA-binding protein HuR and its role in controlling miRNA repression. *Advances in experimental medicine and biology*, 700, pp.106–23. Available at: <http://www.ncbi.nlm.nih.gov/pubmed/21627034> [Accessed October 21, 2013].
- Meisner, N.C. et al., 2007. Identification and mechanistic characterization of low-molecular-weight inhibitors for HuR. *Nat.Chem.Biol.*, 3(8), pp.508–515.

- Meisner, N.C. et al., 2004. mRNA openers and closers: modulating AU-rich element-controlled mRNA stability by a molecular switch in mRNA secondary structure. *Chembiochem.*, 5(10), pp.1432–1447.
- Meisner, N.C., 2005. mRNA stability regulation as a drug target. Part A: mRNA stability X-screening. Part B: Molecular mechanisms in posttranscriptional regulation resolved by quantitative biology. , p.-.
- Meisner, N.C. et al., 2009. Terminal adenosyl transferase activity of posttranscriptional regulator HuR revealed by confocal on-bead screening. *J.Mol.Biol.*, 386(2), pp.435–450. Available at: <http://dx.doi.org/10.1016/j.jmb.2008.12.020>.
- Meisner, N.C. et al., The chemical hunt for the identification of drugable targets. *Curr.Opin.Chem.Biol.*, 8(4), pp.424–431.
- Meyer, S., Temme, C. & Wahle, E., 2004. Messenger RNA turnover in eukaryotes: pathways and enzymes. *Critical reviews in biochemistry and molecular biology*, 39(4), pp.197–216. Available at: <http://www.ncbi.nlm.nih.gov/pubmed/15596551> [Accessed October 17, 2013].
- Miki, T.S. et al., 2014. Engineering of a conditional allele reveals multiple roles of XRN2 in *Caenorhabditis elegans* development and substrate specificity in microRNA turnover. *Nucleic acids research*, (15), pp.1–12. Available at: <http://nar.oxfordjournals.org/content/early/2014/01/20/nar.gkt1418.long> [Accessed January 24, 2014].
- Millard, S.S. et al., 2000. A U-rich element in the 5' untranslated region is necessary for the translation of p27 mRNA. *Molecular and cellular biology*, 20(16), pp.5947–59. Available at: <http://www.pubmedcentral.nih.gov/articlerender.fcgi?artid=86072&tool=pmcentrez&rendertype=abstract> [Accessed November 6, 2013].
- Mohanty, B.K. & Kushner, S.R., 2000. Polynucleotide phosphorylase functions both as a 3' right-arrow 5' exonuclease and a poly(A) polymerase in *Escherichia coli*. *Proceedings of the National Academy of Sciences of the United States of America*, 97(22), pp.11966–71. Available at: <http://www.pnas.org/content/97/22/11966> [Accessed November 4, 2013].
- Monzingo, A.F. et al., 2007. The structure of the minimal relaxase domain of MobA at 2.1 Å resolution. *Journal of molecular biology*, 366(1), pp.165–78. Available at: <http://www.pubmedcentral.nih.gov/articlerender.fcgi?artid=1894915&tool=pmcentrez&rendertype=abstract> [Accessed November 4, 2013].
- Moore, M.J. & Proudfoot, N.J., 2009. Pre-mRNA processing reaches back to transcription and ahead to translation. *Cell*, 136(4), pp.688–700. Available at: <http://www.ncbi.nlm.nih.gov/pubmed/19239889> [Accessed November 4, 2013].
- Muddashetty, R.S. et al., 2011. Reversible inhibition of PSD-95 mRNA translation by miR-125a, FMRP phosphorylation, and mGluR signaling. *Molecular cell*, 42(5), pp.673–88. Available at:

<http://www.pubmedcentral.nih.gov/articlerender.fcgi?artid=3115785&tool=pmcentrez&rendertype=abstract> [Accessed October 21, 2013].

Mukherjee, N. et al., 2011. Integrative Regulatory Mapping Indicates that the RNA-Binding Protein HuR Couples Pre-mRNA Processing and mRNA Stability. *Molecular cell*, 43(3), pp.327–339. Available at:
<http://www.pubmedcentral.nih.gov/articlerender.fcgi?artid=3220597&tool=pmcentrez&rendertype=abstract> [Accessed January 23, 2014].

Murthy, S., Kamine, J. & Desrosiers, R.C., 1986. Viral-encoded small RNAs in herpes virus saimiri induced tumors. *The EMBO journal*, 5(7), pp.1625–32. Available at:
<http://www.pubmedcentral.nih.gov/articlerender.fcgi?artid=1166988&tool=pmcentrez&rendertype=abstract> [Accessed January 27, 2014].

Myer, V.E., Fan, X.C. & Steitz, J.A., 1997. Identification of HuR as a protein implicated in AUUUA-mediated mRNA decay. *The EMBO Journal*, 16(8), pp.2130–2139.

Nowotny, M. & Yang, W., 2009. Structural and functional modules in RNA interference. *Current opinion in structural biology*, 19(3), pp.286–93. Available at:
<http://www.pubmedcentral.nih.gov/articlerender.fcgi?artid=2721689&tool=pmcentrez&rendertype=abstract> [Accessed November 2, 2013].

O'Carroll, D. et al., 2007. A Slicer-independent role for Argonaute 2 in hematopoiesis and the microRNA pathway. *Genes & development*, 21(16), pp.1999–2004. Available at:
<http://www.pubmedcentral.nih.gov/articlerender.fcgi?artid=1948855&tool=pmcentrez&rendertype=abstract> [Accessed November 5, 2013].

Parker, R. & Song, H., 2004. The enzymes and control of eukaryotic mRNA turnover. *Nat.Struct.Mol.Biol.*, 11(2), pp.121–127. Available at:
<http://www.ncbi.nlm.nih.gov/pubmed/14749774> [Accessed October 17, 2013].

Pasquinelli, A.E. et al., 2000. Conservation of the sequence and temporal expression of let-7 heterochronic regulatory RNA. *Nature*, 408(6808), pp.86–89.

Patel, A.A. & Steitz, J.A., 2003. Splicing double: insights from the second spliceosome. *Nature reviews. Molecular cell biology*, 4(12), pp.960–70. Available at:
<http://www.ncbi.nlm.nih.gov/pubmed/14685174> [Accessed November 4, 2013].

Pauley, K.M. et al., 2006. Formation of GW bodies is a consequence of microRNA genesis. *EMBO reports*, 7(9), pp.904–10. Available at:
<http://www.pubmedcentral.nih.gov/articlerender.fcgi?artid=1559661&tool=pmcentrez&rendertype=abstract> [Accessed January 23, 2014].

Pei, Y. et al., 2010. Quantitative evaluation of siRNA delivery in vivo. *RNA (New York, N.Y.)*, 16(12), pp.2553–63. Available at:
<http://www.pubmedcentral.nih.gov/articlerender.fcgi?artid=2995415&tool=pmcentrez&rendertype=abstract> [Accessed January 29, 2014].

- Pesole, G. et al., 2000. The untranslated regions of eukaryotic mRNAs: Structure, function, evolution and bioinformatic tools for their analysis. *Briefings in Bioinformatics*, 1(3), pp.236–249.
- Pillai, R.S., Artus, C.G. & Filipowicz, W., 2004. Tethering of human Ago proteins to mRNA mimics the miRNA-mediated repression of protein synthesis. *RNA (New York, N.Y.)*, 10(10), pp.1518–25. Available at: <http://www.pubmedcentral.nih.gov/articlerender.fcgi?artid=1370638&tool=pmcentrez&rendertype=abstract> [Accessed October 21, 2013].
- Pillai, R.S., Bhattacharyya, S. & Filipowicz, W., 2007. Repression of protein synthesis by miRNAs: how many mechanisms? *Trends in cell biology*, 17(3), pp.118–26. Available at: <http://www.ncbi.nlm.nih.gov/pubmed/17197185> [Accessed October 17, 2013].
- Piskounova, E. et al., 2011. Lin28A and Lin28B Inhibit let-7 MicroRNA Biogenesis by Distinct Mechanisms. *Cell*, 147(5), pp.1066–1079. Available at: <http://dx.doi.org/10.1016/j.cell.2011.10.039>.
- Portnoy, V. et al., 2005. RNA polyadenylation in Archaea: not observed in Haloferax while the exosome polynucleotidylates RNA in Sulfolobus. *EMBO reports*, 6(12), pp.1188–93. Available at: <http://www.pubmedcentral.nih.gov/articlerender.fcgi?artid=1369208&tool=pmcentrez&rendertype=abstract> [Accessed January 22, 2014].
- Rajasethupathy, P. et al., 2009. Characterization of small RNAs in Aplysia reveals a role for miR-124 in constraining synaptic plasticity through CREB. *Neuron*, 63(6), pp.803–17. Available at: <http://www.pubmedcentral.nih.gov/articlerender.fcgi?artid=2875683&tool=pmcentrez&rendertype=abstract> [Accessed January 23, 2014].
- Rajewsky, N., 2006. microRNA target predictions in animals. *Nature genetics*, 38 Suppl, pp.S8–13. Available at: <http://www.ncbi.nlm.nih.gov/pubmed/16736023> [Accessed October 18, 2013].
- Rangarajan, E.S. & Shankar, V., 2001. Sugar non-specific endonucleases. *FEMS microbiology reviews*, 25(5), pp.583–613. Available at: <http://www.ncbi.nlm.nih.gov/pubmed/11742693> [Accessed November 4, 2013].
- Rebane, A., Aab, A. & Steitz, J.A., 2004. Transportins 1 and 2 are redundant nuclear import factors for hnRNP A1 and HuR. *RNA*, 10(4), pp.590–599.
- Régnier, P. & Hajnsdorf, E., 2009. Poly(A)-assisted RNA decay and modulators of RNA stability. *Progress in molecular biology and translational science*, 85(08), pp.137–85. Available at: <http://www.sciencedirect.com/science/article/pii/S0079660308008040> [Accessed November 4, 2013].

- Reha-Krantz, L.J., 2010. DNA polymerase proofreading: Multiple roles maintain genome stability. *Biochimica et biophysica acta*, 1804(5), pp.1049–63. Available at: <http://www.ncbi.nlm.nih.gov/pubmed/19545649> [Accessed November 4, 2013].
- Reinhart, B.J. et al., 2000. The 21-nucleotide let-7 RNA regulates developmental timing in *Caenorhabditis elegans*. *Nature*, 403(6772), pp.901–906.
- Rissland, O.S., Hong, S.-J. & Bartel1, D.P., 2011. MicroRNA destabilization enables dynamic regulation of the miR-16 family in response to cell-cycle changes. *Molecular cell*, 43(6), pp.993–1004. Available at: <http://www.pubmedcentral.nih.gov/articlerender.fcgi?artid=3202612&tool=pmcentrez&rendertype=abstract> [Accessed October 18, 2013].
- Von Roretz, C. & Gallouzi, I.-E., 2008. Decoding ARE-mediated decay: is microRNA part of the equation? *J. Cell Biol.*, 181(2), pp.189–194.
- Rüegger, S. & Großhans, H., 2012. MicroRNA turnover: when, how, and why. *Trends in Biochemical Sciences*, 37(10), pp.436–446. Available at: <http://www.ncbi.nlm.nih.gov/pubmed/22921610> [Accessed November 1, 2013].
- Ruggiero, T. et al., 2009. LPS induces KH-type splicing regulatory protein-dependent processing of microRNA-155 precursors in macrophages. *FASEB journal : official publication of the Federation of American Societies for Experimental Biology*, 23(9), pp.2898–908. Available at: <http://www.ncbi.nlm.nih.gov/pubmed/19423639> [Accessed October 21, 2013].
- Schoeffler, A.J. & Berger, J.M., 2008. DNA topoisomerases: harnessing and constraining energy to govern chromosome topology. *Quarterly reviews of biophysics*, 41(1), pp.41–101. Available at: <http://www.ncbi.nlm.nih.gov/pubmed/18755053> [Accessed January 25, 2014].
- Schratt, G.M. et al., 2006. A brain-specific microRNA regulates dendritic spine development. *Nature*, 439(7074), pp.283–9. Available at: <http://www.ncbi.nlm.nih.gov/pubmed/16421561> [Accessed October 21, 2013].
- Schwarz, D.S. et al., 2003. Asymmetry in the assembly of the RNAi enzyme complex. *Cell*, 115(2), pp.199–208.
- Selbach, M. et al., 2008. Widespread changes in protein synthesis induced by microRNAs. *Nature*, 455(7209), pp.58–63. Available at: <http://www.ncbi.nlm.nih.gov/pubmed/18668040> [Accessed October 18, 2013].
- Sethi, P. & Lukiw, W.J., 2009. Micro-RNA abundance and stability in human brain: specific alterations in Alzheimer's disease temporal lobe neocortex. *Neuroscience letters*, 459(2), pp.100–4. Available at: <http://www.ncbi.nlm.nih.gov/pubmed/19406203> [Accessed January 22, 2014].

- Shaw, G. & Kamen, R., 1986. A conserved AU sequence from the 3' untranslated region of GM-CSF mRNA mediates selective mRNA degradation. *Cell*, 46(5), pp.659–667.
- Shen, B. et al., 2005. Multiple but dissectible functions of FEN-1 nucleases in nucleic acid processing, genome stability and diseases. *BioEssays : news and reviews in molecular, cellular and developmental biology*, 27(7), pp.717–29. Available at: <http://www.ncbi.nlm.nih.gov/pubmed/15954100> [Accessed November 4, 2013].
- Shevchenko, A. et al., 1996. A strategy for identifying gel-separated proteins in sequence databases by MS alone. *Biochemical Society transactions*, 24(3), pp.893–6. Available at: <http://www.ncbi.nlm.nih.gov/pubmed/8878870> [Accessed January 19, 2014].
- Shyu, A.B., Greenberg, M.E. & Belasco, J.G., 1989. The c-fos transcript is targeted for rapid decay by two distinct mRNA degradation pathways. *Genes Dev.*, 3(1), pp.60–72.
- De Silanes, I.L. et al., 2004. Identification of a target RNA motif for RNA-binding protein HuR. *Proc.Natl.Acad.Sci.U.S.A.*, 101(9), pp.2987–2992.
- Slomovic, S. et al., 2008. Polynucleotide phosphorylase and the archaeal exosome as poly(A)-polymerases. *Biochimica et biophysica acta*, 1779(4), pp.247–55. Available at: <http://www.ncbi.nlm.nih.gov/pubmed/18177749> [Accessed January 22, 2014].
- Soller, M. & White, K., 2005. ELAV multimerizes on conserved AU4-6 motifs important for ewg splicing regulation. *Mol.Cell Biol.*, 25(17), pp.7580–7591.
- Song, J.-J. et al., 2003. The crystal structure of the Argonaute2 PAZ domain reveals an RNA binding motif in RNAi effector complexes. *Nature structural biology*, 10(12), pp.1026–32. Available at: <http://www.ncbi.nlm.nih.gov/pubmed/14625589> [Accessed October 18, 2013].
- Srikantan, S. et al., 2011. Translational control of TOP2A influences doxorubicin efficacy. *Mol.Cell Biol.*, 31(18), pp.3790–3801. Available at: <http://www.pubmedcentral.nih.gov/articlerender.fcgi?artid=3165726&tool=pmcentrez&rendertype=abstract> [Accessed November 6, 2013].
- Srikantan, S., Tominaga, K. & Gorospe, M., 2012. Functional interplay between RNA-binding protein HuR and microRNAs. *Curr.Protein Pept.Sci.*, 13(4), pp.372–379.
- Stalder, L. et al., 2013. The rough endoplasmic reticulum is a central nucleation site of siRNA-mediated RNA silencing. *The EMBO journal*, 32(8), pp.1115–27. Available at: <http://www.pubmedcentral.nih.gov/articlerender.fcgi?artid=3630355&tool=pmcentrez&rendertype=abstract>.
- Stefl, R., Skrisovska, L. & Allain, F.H.-T., 2005. RNA sequence- and shape-dependent recognition by proteins in the ribonucleoprotein particle. *EMBO reports*, 6(1), pp.33–8. Available at: <http://www.pubmedcentral.nih.gov/articlerender.fcgi?artid=1299235&tool=pmcentrez&rendertype=abstract> [Accessed November 5, 2013].

- Sureban, S.M. et al., 2007. Functional antagonism between RNA binding proteins HuR and CUGBP2 determines the fate of COX-2 mRNA translation. *Gastroenterology*, 132(3), pp.1055–65. Available at: <http://www.ncbi.nlm.nih.gov/pubmed/17383427> [Accessed November 6, 2013].
- Szankasi, P. & Smith, G.R., 1996. Requirement of *S. pombe* exonuclease II, a homologue of *S. cerevisiae* Sep1, for normal mitotic growth and viability. *Current genetics*, 30(4), pp.284–93. Available at: <http://www.ncbi.nlm.nih.gov/pubmed/8781170> [Accessed November 4, 2013].
- Tabara, H. et al., 1999. The rde-1 gene, RNA interference, and transposon silencing in *C. elegans*. *Cell*, 99(2), pp.123–32. Available at: <http://www.ncbi.nlm.nih.gov/pubmed/10535731> [Accessed October 18, 2013].
- Tatsuta, K., Nakanishi, S. & Takahashi, I., 2004. Preparation of MS-444 derivatives as immunosuppressive and anti-itching agents L. (Kyowa Hakko Kogyo Co. Japan), ed. , 98-JP265(9832750), p.28–.
- Thomas, M.F. et al., 2012. Eri1 regulates microRNA homeostasis and mouse lymphocyte development and antiviral function. *Blood*, 120(1), pp.130–42. Available at: <http://bloodjournal.hematologylibrary.org/content/120/1/130.long> [Accessed November 1, 2013].
- Toba, G. & White, K., 2008. The third RNA recognition motif of *Drosophila* ELAV protein has a role in multimerization. *Nucleic Acids Res.*, 36(4), pp.1390–1399.
- Tominaga, K. et al., 2011. Competitive regulation of nucleolin expression by HuR and miR-494. *Mol.Cell Biol.*, 31(20), pp.4219–4231.
- Trabucchi, M. et al., 2009. The RNA-binding protein KSRP promotes the biogenesis of a subset of microRNAs. *Nature*, 459(7249), pp.1010–4. Available at: <http://www.pubmedcentral.nih.gov/articlerender.fcgi?artid=2768332&tool=pmcentrez&rendertype=abstract> [Accessed October 20, 2013].
- Tucker, M. et al., 2002. Ccr4p is the catalytic subunit of a Ccr4p/Pop2p/Notp mRNA deadenylase complex in *Saccharomyces cerevisiae*. *EMBO J.*, 21(6), pp.1427–1436.
- Valverde, R., Edwards, L. & Regan, L., 2008. Structure and function of KH domains. *The FEBS journal*, 275(11), pp.2712–26. Available at: <http://www.ncbi.nlm.nih.gov/pubmed/18422648> [Accessed November 5, 2013].
- Venter, J.C. et al., 2001. The sequence of the human genome. *Science*, 291(5507), pp.1304–1351.
- Viswanathan, S.R., Daley, G.Q. & Gregory, R.I., 2008. Selective blockade of microRNA processing by Lin28. *Science*, 320(5872), pp.97–100.

- Wang, H. et al., 2013. The structure of the ARE-binding domains of Hu antigen R (HuR) undergoes conformational changes during RNA binding. *Acta crystallographica. Section D, Biological crystallography*, 69(Pt 3), pp.373–80. Available at: <http://www.ncbi.nlm.nih.gov/pubmed/23519412> [Accessed November 5, 2013].
- Wang, W. et al., 2000. HuR regulates p21 mRNA Stabilization by UV Light. *Molecular and Cellular Biology*, 20(3), pp.760–769.
- Wang, X. & Tanaka Hall, T.M., 2001. Structural basis for recognition of AU-rich element RNA by the HuD protein. *Nature Structural Biology*, 8(2), pp.141–145.
- Wang, Y. et al., 2009. Nucleation, propagation and cleavage of target RNAs in Ago silencing complexes. *Nature*, 461(7265), pp.754–61. Available at: <http://www.pubmedcentral.nih.gov/articlerender.fcgi?artid=2880917&tool=pmcentrez&rendertype=abstract> [Accessed October 18, 2013].
- Wee, L.M. et al., 2012. Argonaute divides its RNA guide into domains with distinct functions and RNA-binding properties. *Cell*, 151(5), pp.1055–67. Available at: <http://www.pubmedcentral.nih.gov/articlerender.fcgi?artid=3595543&tool=pmcentrez&rendertype=abstract> [Accessed October 18, 2013].
- Westmark, C.J., Bartleson, V.B. & Malter, J.S., 2005. RhoB mRNA is stabilized by HuR after UV light. *Oncogene*, ., p.-.
- Wightman, B., Ha, I. & Ruvkun, G., 1994. Posttranscriptional regulation of the heterochronic gene *lin-14* by *lin-4* mediates temporal pattern formation in *C. elegans*. *Cell*, 75(5), pp.855–862.
- Wilusz, C.J. et al., 2001. THE CAP-TO-TAIL GUIDE TO mRNA TURNOVER. , 2(April).
- Winter, J. et al., 2009. Many roads to maturity: microRNA biogenesis pathways and their regulation. *Nat.Cell Biol.*, 11(3), pp.228–234.
- Wolfe, S.A., Nekludova, L. & Pabo, C.O., 2000. DNA recognition by Cys2His2 zinc finger proteins. *Annual review of biophysics and biomolecular structure*, 29, pp.183–212. Available at: <http://www.ncbi.nlm.nih.gov/pubmed/10940247> [Accessed November 5, 2013].
- Wyman, S.K. et al., 2011. Post-transcriptional generation of miRNA variants by multiple nucleotidyl transferases contributes to miRNA transcriptome complexity. *Genome research*, 21(9), pp.1450–61. Available at: <http://www.pubmedcentral.nih.gov/articlerender.fcgi?artid=3166830&tool=pmcentrez&rendertype=abstract> [Accessed October 17, 2013].
- Xie, J. et al., 2012. Long-term, efficient inhibition of microRNA function in mice using rAAV vectors. *Nature methods*, 9(4), pp.403–9. Available at: <http://dx.doi.org/10.1038/nmeth.1903> [Accessed October 21, 2013].

- Xu, F. et al., 2010. Loss of repression of HuR translation by miR-16 may be responsible for the elevation of HuR in human breast carcinoma. *J. Cell Biochem.*, 111(3), pp.727–734.
- Yamagata, K. et al., 2009. Maturation of microRNA is hormonally regulated by a nuclear receptor. *Molecular cell*, 36(2), pp.340–7. Available at: <http://www.ncbi.nlm.nih.gov/pubmed/19854141> [Accessed October 21, 2013].
- Yaman, I. et al., 2002. Nutritional control of mRNA stability is mediated by a conserved AU-rich element that binds the cytoplasmic shuttling protein HuR. *Journal of Biological Chemistry*, 277(44), pp.41539–41546.
- Yan, J. et al., 2012. Effective small RNA destruction by the expression of a short tandem target mimic in Arabidopsis. *The Plant cell*, 24(2), pp.415–27. Available at: <http://www.pubmedcentral.nih.gov/articlerender.fcgi?artid=3315224&tool=pmcentrez&rendertype=abstract> [Accessed October 21, 2013].
- Yang, W., 2008. An equivalent metal ion in one- and two-metal-ion catalysis. *Nature structural & molecular biology*, 15(11), pp.1228–31. Available at: <http://www.pubmedcentral.nih.gov/articlerender.fcgi?artid=2597392&tool=pmcentrez&rendertype=abstract> [Accessed November 4, 2013].
- Yang, W., 2011. Nucleases: diversity of structure, function and mechanism. *Quarterly reviews of biophysics*, 44(1), pp.1–93. Available at: <http://www.ncbi.nlm.nih.gov/pubmed/20854710> [Accessed November 3, 2013].
- Yang, W., Lee, J.Y. & Nowotny, M., 2006. Making and breaking nucleic acids: two-Mg²⁺-ion catalysis and substrate specificity. *Molecular cell*, 22(1), pp.5–13. Available at: <http://www.ncbi.nlm.nih.gov/pubmed/16600865> [Accessed November 4, 2013].
- Yates, L. a, Norbury, C.J. & Gilbert, R.J.C., 2013. The long and short of microRNA. *Cell*, 153(3), pp.516–9. Available at: <http://www.ncbi.nlm.nih.gov/pubmed/23622238> [Accessed October 17, 2013].
- Yi, R. et al., 2003. Exportin-5 mediates the nuclear export of pre-microRNAs and short hairpin RNAs. *Genes Dev.*, 17(24), pp.3011–3016. Available at: <http://www.pubmedcentral.nih.gov/articlerender.fcgi?artid=305252&tool=pmcentrez&rendertype=abstract> [Accessed January 25, 2014].
- Yoda, M. et al., 2013. Poly(A)-specific ribonuclease mediates 3'-end trimming of Argonaute2-cleaved precursor microRNAs. *Cell reports*, 5(3), pp.715–26. Available at: <http://www.pubmedcentral.nih.gov/articlerender.fcgi?artid=3856240&tool=pmcentrez&rendertype=abstract> [Accessed January 28, 2014].
- Young, L.E. et al., 2012. The mRNA stability factor HuR inhibits microRNA-16 targeting of COX-2. *Mol. Cancer Res.*, 10(1), pp.167–180. Available at: <http://www.pubmedcentral.nih.gov/articlerender.fcgi?artid=3262080&tool=pmcentrez&rendertype=abstract> [Accessed October 17, 2013].

- Yu, Z. & Hecht, N.B., 2008. The DNA/RNA-binding protein, translin, binds microRNA122a and increases its in vivo stability. *Journal of andrology*, 29(5), pp.572–9. Available at: <http://www.ncbi.nlm.nih.gov/pubmed/18567644> [Accessed October 21, 2013].
- Zdanowicz, A. et al., 2009. Drosophila miR2 primarily targets the m7GpppN cap structure for translational repression. *Molecular cell*, 35(6), pp.881–8. Available at: <http://www.ncbi.nlm.nih.gov/pubmed/19782035> [Accessed December 8, 2013].
- Zhang, Z. et al., 2011. Uracils at nucleotide position 9-11 are required for the rapid turnover of miR-29 family. *Nucleic acids research*, 39(10), pp.4387–95. Available at: <http://www.pubmedcentral.nih.gov/articlerender.fcgi?artid=3105410&tool=pmcentrez&rendertype=abstract> [Accessed January 26, 2014].
- Zhuang, R. et al., 2013. miR-195 competes with HuR to modulate stim1 mRNA stability and regulate cell migration. *Nucleic Acids Res.*, 41(16), pp.7905–7919.

7. Curriculum vitae

Lena Sokol

Klybeckstrasse 7, 4057 Basel, Switzerland
+41794403221 +41764210809, anel.sokol@gmail.com



Born: 09.08.1983 in Dubrovnik, Croatia

Education and work experience

19th Feb 2014

PhD defense

Dec 2009 – Feb 2014

Doctoral studies in cell biology at NIBR /FMI institute in Basel in the group of Dr. Nicole Meisner-Kober, co-supervised by Prof. Witold Filipowicz

Thesis topic: Selective trimming and tailing of Ago-loaded miRNA by the AU-rich element binding protein HuR

Jun 2009 – Dec 2009

Trainee at Novartis at the lab of Nicole Meisner-Kober

Oct 2002 – Nov 2009

Master studies at the University of Vienna, Austria

Master thesis topic: Selective and accurate translation by protein depleted ribosomes formed in the presence of kasugamycin *in vivo*

Work experience as student **tutor** and student **supervisor**

Major in **molecular biology**

Minors in: Immunology/microbiology, molecular medicine and cell biology

1998 – 2002

Natural Science High school: Jovan Jovanovic Zmaj, Novi Sad, Serbia

Awards

First poster prize at the RNA Society meeting 2012: **Nature Structural & Molecular Biology (NSMB) Poster Awards**

Second prize for presentation at the PhD student workshop at the Sixth Microsymposium on Small RNAs, Vienna, Austria

Skills

Practical skills

Microbiology

Handling various bacteria
Classical cloning approaches, Quikchange
Planning and execution, analysis
In vitro transcription/translation

Biochemistry

Protein expression and purification using a variety of tags and systems (His, FLAG, Intein system)
Protein refolding

Molecular biology

Recombinant enzymatic reactions
Immunoprecipitation
Ligand binding assays
RT-qPCR, probe design, analysis (mRNA, miRNA)
Northern blot (mRNA and miRNA)
Western blot
Expertise in PAGE analysis by RNA PAA-Urea sequencing quality gels
2D electrophoresis
RNA labeling, biotin, radioactive
Radioactivity incorporation assays
In vitro transcription and translation
Primer extension

Cell biology

Transfection with (si)RNA/DNA
Luciferase assays
Survival assays
Toxicity assays
Overexpression systems (Tet OFF)

Analytical chemistry

HPLC
Thin layer chromatography analysis

Biophysics

RNA-RNA/protein anisotropy based binding assays

Computer skills

Grafit	Curve fitting, K_d calculation, IC_{50} calculation
Prism	
Quantity one, image lab	Device specific image analysis, quantification
Vector NTI	Cloning planning, oligo design
Adobe illustrator	Publication preparation
Mendeley	Citation management

Language skills

Croatian/Serbian	Mother language
English	IELTS grade 8 expert user
German	Proficient user
French	Beginner

Publications

In preparation: Tailing-dependent trimming of RISC-associated miRNAs by the HuR protein
Sokol L, Ripin N, Filipowicz W, Meisner-Kober NC.

The rough endoplasmic reticulum is a central nucleation site of siRNA-mediated RNA silencing.

Stalder L, Heusermann W, Sokol L, Trojer D, Wirz J, Hean J, Fritzsche A, Aeschmann F, Pfanzagl V, Basselet P, Weiler J, Hintersteiner M, Morrissey DV, Meisner-Kober NC.
EMBO J. 2013 Apr 17;32(8):1115-27

The mRNA stability factor HuR inhibits microRNA-16 targeting of COX-2.

Young LE, Moore AE, Sokol L, Meisner-Kober N, Dixon DA
Mol Cancer Res. 2012 Jan;10(1):167-80.

RNA stability alterations mediated by HuR are necessary to sustain the fast growth of glioma cells.

Bolognani F, Gallani AI, Sokol L, Baskin DS, Meisner-Kober N.
J Neurooncol. 2012 Feb;106(3):531-42.

Further education

Radioactivity work certificate SUVA (Strahlenschutzkurs)
Target to therapy course (Novartis – analyzing the process from target validation to clinical testing of new drugs)
RNPnet structural biology summer school (NMR, Crystalization, Electron microscopy etc.)
Course on Experimental Cancer Research: Clinic and Molecular Biology